EARTHQUAKE RISK MITIGATION: HAZARD IDENTIFICATION AND RESOURCE ALLOCATION

A Dissertation

Presented to the Faculty of the Graduate School

of Cornell University

In Partial Fulfillment of the Requirements for the Degree of

Doctor of Philosophy

by

Pantea Vaziri

January 2009

EARTHQUAKE RISK MITIGATION: HAZARD IDENTIFICATION AND RESOURCE ALLOCATION

Pantea Vaziri, Ph. D.

Cornell University 2009

The purpose of this dissertation is to provide the means for contingency planners for regional earthquake risk mitigation to systematically determine how much to spend on mitigation versus post-event reconstruction and to prioritize alternative mitigation and reconstruction options.

This dissertation is organized into three chapters. The focus of chapter one is the development of a method to estimate earthquake hazard for use in regional loss estimation. The method includes formulation of a linear program that selects a small subset of earthquake scenarios from a library of such events and estimates hazard-consistent annual occurrence probabilities so that their combined effect on the region of interest approximates that described by *r*-year return period for all possible events. The method is reproducible, computationally tractable, and results in earthquake scenarios, which are easily understood. We apply it to the identification of earthquake scenarios for Tehran, Iran.

The second chapter develops an optimization model to help highly seismically active developing countries decide: (1) How much should be spent on pre-earthquake mitigation versus waiting until after an event and paying for reconstruction or simply not rebuilding damaged buildings?; (2) Which buildings should be mitigated and how?; and (3) Which buildings should be reconstructed and how? It extends previously developed optimization models to consider the particular issues that arise in such countries. First, the model allows for the possibility that some damaged buildings

will not be reconstructed immediately and keeps track of any lost building inventory. Second, it allows the set of possible mitigation alternatives to be both the upgrade of a particular structural type or a change in the structural type. Third, the model relaxes the assumption that all buildings should be reconstructed to their pre-earthquake condition. Finally, it includes as one objective minimizing the chance of an extremely high death toll in any one earthquake as well as minimizing the average annual death toll across earthquakes. This chapter incorporates the results from the first chapter into a case study analysis for Tehran, Iran

The focus of the third chapter is the introduction of equity into this type of analysis.

BIOGRAPHICAL SKETCH

Pantea Vaziri was born August 15, 1978 in Tehran, Iran. She received her B.S. in Civil Engineering from Imam Khomeini International University (Qazvin, Iran) in 2001, followed by her M.Eng. in Systems Analysis and Economics for Public Decision Making from The Johns Hopkins University (Baltimore, MD) in 2002. In the Fall of 2002 she joined Cornell University to pursue her Ph.D. in Civil and Environmental Engineering.

To my father for instilling in me the value of education

To my mother who epitomizes the spirit of living

ACKNOWLEDGMENTS

First and foremost, I want to thank my advisor Professor Linda K. Nozick for her extensive help and guidance in completion of this work. Above all, I would like to thank her for her support and for giving me the chance to learn from this endeavor the life lessons that will be my source of strength in the years to come.

I would like to thank Dr. Rachel Davidson for her close collaboration and help in every step of this work. The quality of this research wouldn't simply be the same without her invaluable contributions. I also wish to thank Professor Richard E. Schuler and Dr. Mahmood Hosseini for offering me advice and insight through out my research.

I would like to thank my friends and colleagues Carmen G. Rawls and Yashoda Dadkar, for their love and support. I can not imagine my years at Cornell without them. I wish to thank my friend Ali Mahmoudoff for his support and honest feedbacks which always compelled me to challenge my limits. I also wish to thank my counselor of 3 years Dr. Mahnaz Mousavi for her extraordinary support and professional help.

I can not thank my family enough for all their encouragements and support. I wish to thank my parents for instilling in me the principles which carried me through this journey. I wish to thank my sister Kabeh for being a candid mentor and a compassionate friend through out my academic career. I thank my sister Katayoun for giving me perspective, inspiration, and courage.

I also thank my feline members of family Juge and Pishi. I wish you knew how much joy and balance you bring to my life. Finally, I want to thank my friend Pradeep for all his exceptional love, support, and trustworthiness.

This material is based upon work supported by the National Science Foundation under Grant No. CMS-0555738 and Grant No. CMS-0408577. This funding is gratefully acknowledged but it implies no endorsement of findings.

TABLE OF CONTENTS

LIST OF FIGURES

LIST OF TABLES

CHAPTER1 IDENTIFICATION OF HAZARD-CONSISTENT PROBABILISTIC EARTHQUAKE SCENARIOS FOR REGIONAL LOSS ESTIMATION

1.1 INTRODUCTION

This paper describes a regional earthquake hazard assessment method for use in loss estimation. It was developed especially for situations in which the desired output is probability of exceedence vs. loss curves for every site in a region (or r-year return period maps), computational demands are of concern, and the spatial coherence of individual earthquake scenarios is desirable. Computation may be of particular concern: (1) when computationally intensive analyses are conducted following the hazard analysis, as when one estimates damage to lifeline network for each possible earthquake scenario, then estimates service restoration times for each damage scenario (e.g., in Çağnan et al. 2006), or (2) when loss estimation must be repeated many times, as when evaluating the relative benefits of many mitigation alternatives (e.g., in Dodo et al. 2005). Retaining coherent individual earthquake scenarios can be desirable because they are easy for stakeholders to understand (e.g., Anderson 1997) and they capture the spatial correlation of ground motion across a region.

The method presented herein is a new formulation of the hazard-consistent probabilistic scenario approach introduced by Chang et al. (2000). It similarly involves selecting a relatively small subset of all possible earthquakes and adjusting their annual occurrence probabilities so that each of the reduced set of events represents all events “like that one” in terms of the frequency and distribution of ground motion it causes, and together the reduced set of events represents the total regional seismic hazard. However, the method introduced in this paper is novel in three key ways. For the first time, it uses a constrained optimization formulation to estimate the adjusted hazard-consistent occurrence probabilities for the reduced set of events. Unlike previous versions of the hazard-consistent probabilistic scenario method, this

formulation guarantees the minimum possible error between the regional hazard as estimated by the reduced set and by a full probabilistic seismic hazard analysis. It also allows the optimization to determine which events should be included rather than forcing the user to identify the reduced set of events *a priori*, without a full understanding of the implications of the choice in terms of accuracy and computation. Finally, it clarifies the magnitude and distribution of errors so that the user can make informed decisions about the tradeoff between computational savings and introduction of errors. In a case study for Tehran, Iran, with 8 earthquakes, the method provides unbiased results with errors that are small enough for most practical uses. The method is described and illustrated for earthquakes, but it can easily be adapted for hurricanes and other hazards.

Available earthquake hazard assessment methods are compared in the next section. The new formulation and a case study application for Tehran, Iran are then described. The paper concludes with a summary of the method's strengths and limitations.

1.2 Earthquake Hazard Assessment for Use in Regional Loss Estimation

This section summarizes available earthquake hazard assessment methods in terms of their potential to be used in regional loss estimation: (1) individual scenarios, (2) probabilistic seismic hazard assessment (PSHA), (3) deaggregated PSHA, (4) Monte Carlo simulation, and (5) hazard-consistent probabilistic scenarios (HCPS). Except for the first, they all incorporate the effects of all possible events and their occurrence probabilities and result in *r*-year return period maps of loss for a region (as opposed to a single site). Crowley and Bommer (2006) provides a helpful overview of the first four of these methods.

1.2.1 Individual Scenarios

In what is often called the deterministic approach, one particular scenario event is specified and losses are estimated conditional on occurrence of that scenario. Magnitude, location, and perhaps other parameters typically define a scenario. Ground motion is estimated using the median or median plus one standard deviation point in the attenuation relation. Scenario ground motion and loss maps provide a coherent story of what might happen in a particular future earthquake, and thus can be invaluable for communication with stakeholders. Compared to PSHA, focusing on one or a few individual earthquake scenarios allows estimation of more ground motion characteristics that can be important in seismic design, such as duration or full acceleration time histories. However, for many decisions, such as insurance portfolio planning or regional mitigation resource allocation, it is important to consider all possible future earthquakes because what is an optimal decision under the occurrence of one earthquake might be completely ineffective if a different earthquake occurs. In those cases, loss exceedence curves or *r*-year return period maps can be useful.

1.2.2 Probabilistic Seismic Hazard Analysis

In probabilistic seismic hazard analysis (PSHA), the effects of all possible earthquakes with different sizes, occurring at different locations with different probabilities of occurrence are integrated to determine the probability of exceeding different levels of ground motion (e.g., peak ground acceleration) at a site of interest during a specified period of time (e.g., Reiter 1990). For a single site, the hazard curve derived from PSHA can be convolved with exposure and vulnerability information to obtain a loss exceedence curve (see Bazzurro and Luco 2005 for the formulation). When considering multiple sites, however, the situation is complicated because correlation among ground motions at the different sites must be considered. FEMA 366 applies the single-site PSHA approach to every site in a region independently

without considering spatial correlation in the ground motion (FEMA 2001). Crowley and Bommer (2006) compare that approach to simulation for a case study in Turkey, demonstrating how this application of PSHA works for a single site, but overestimates the loss exceedence curve when applied to multiple sites. As they explain, the PSHA method effectively treats all ground motion variability as inter-event (earthquake-to-earthquake) variability, whereas most of it is actually intra-event (spatial) variability. In other words, it assumes that ground motions at different sites are perfectly correlated. The ground motion associated with a particular exceedence probability at one site, and the ground motion associated with the same exceedence probability at another site do not necessarily occur together; PSHA-based loss estimation assumes they do. It is theoretically possible to extend the PSHA formulation to estimate losses while accounting for spatial correlation, but it is difficult in practice. Rhoades and McVerry (2001) extend PSHA to estimate the joint ground motion hazard at multiple sites. Wesson and Perkins (2001) provide a method to estimate the mean and variance (although not the entire distribution) of losses to a portfolio.

1.2.3 Deaggregated PSHA

Recognizing the benefits of scenario earthquakes, a great deal of research has focused on identifying one or a few design earthquakes that are compatible in some sense with a certain hazard level (e.g., Ishikawa and Kameda 1988, McGuire 1995, Bazzurro and Cornell 1999). (These design earthquakes are sometimes called "hazard-consistent," but with a different meaning than that used in this paper.) These efforts have aimed to identify a single or few design earthquakes that can provide a detailed representation of ground motion for seismic design. They have not been intended for use in estimating regional losses. Nevertheless, as Crowley and Bommer (2006) describe, it is theoretically possible to use deaggregated scenarios in regional earthquake loss estimation although it would require a large computational effort

because all contributing scenarios must be considered. Campbell and Seligson (2003), described below, can be considered a type of deaggregation approach.

1.2.4 Monte Carlo Simulation

Monte Carlo simulation (also called the walkthrough or event-based method) provides an alternate method for regional loss estimation that retains the ability to identify the contributions of specific earthquake events to the regional risk. It involves simulating the occurrence of many earthquakes in the region of interest (on the order of tens of thousands); estimating the losses caused by each earthquake; and using the resulting database of losses to calculate the loss-exceedence curves. Simulation has recently become more common (e.g., Crowley and Bommer 2006, Bazzurro and Luco 2005, Ebel and Kafka 1999, Werner et al. 2006, and He 2006). There are many variations in the details of how each earthquake, its characteristics, and the resulting ground motion are simulated. For example, earthquakes may be simulated based on a historical earthquake catalogue; or by simulating location, magnitude, and other characteristics to create synthetic earthquakes. (It is interesting to note that simulation has long been the dominant approach for hurricanes since hurricane scenarios are not easily defined by just a couple parameters like magnitude and location, and therefore, a PSHA-based approach cannot be used for hurricane loss estimation.)

This approach has the advantages of being straightforward conceptually; representing the spatial correlation among sites; and allowing explicit incorporation of temporal changes in hazard, exposure, vulnerability, or economic parameters (Jain and Davidson 2007, Taylor et al. 2001). Nevertheless, the simulation method can be computationally intensive, which may be problematic if the analysis must be repeated many times or if many analyses build on the initial hazard assessment. Werner et al. (2006) discusses post-sampling variance reduction techniques that can reduce the number of simulations required by a factor of three or more.

1.2.5 Hazard-Consistent Probabilistic Scenarios

The hazard-consistent probabilistic scenario (HCPS) approach estimates losses the same way the simulation method does, but it offers a different way to identify the set of earthquakes that are simulated and their mean annual occurrence probabilities. A relatively small subset of all possible earthquakes is identified (on the order of tens), and the annual occurrence probability of each is adjusted so that each of the subset of events represents all events "like that one" in terms of the frequency and distribution of ground motion it causes, and together the subset of events with their adjusted hazard-consistent occurrence probabilities represent the total regional hazard.

Chang et al. (2000) first developed this approach and applied it in Southern California. Without explaining how exactly, they identified a set of 47 earthquakes. To estimate the hazard-consistent occurrence probability for each scenario, they tried to match the regional ground shaking produced by the reduced set of 47 earthquakes to that produced by a PSHA conducted with the full set of all possible earthquakes. Specifically, they matched several points on the hazard curve at a single location (Los Angeles city hall), and the 475-year ground motion at the centroids of 16 particular census tracts. Hazard-consistent occurrence probabilities were adjusted iteratively and manually until the match was considered to be within "reasonable bounds."

Campbell and Seligson (2003) provides a more objective, reproducible version of the HCPS method. They assume the reduced set of earthquakes is comprised of only maximum credible events (MCEs) with moment magnitude of at least 6.5. An application for Los Angeles included 17 scenarios. To estimate the adjusted hazard-consistent occurrence probabilities for those reduced set earthquakes, they match system-wide average ground motion values (averaged over all grid points in the system of interest) one hazard bin at a time, where each bin k is an interval on a hazard (annual probability of exceedence vs. ground motion) curve. The average system-wide

hazard associated with bin *k* as given by a full PSHA is distributed among the MCEs that contribute significantly to it, in proportion to their contributions. That provides an annual occurrence probability for the MCE for each bin. The mean ground motion associated with each MCE and grid point is then adjusted so that the system-wide average value equals the average of the ground motion values in each bin *k*. This adjustment accounts for the fact that each scenario may not have been contributing to the bin *k* at its mean value (K. Campbell, personal communication, 2007). The result of this analysis is, for each bin *k*, a set of MCEs, each described by its soil-amplified ground motion map and its annual frequency. The set of scenarios may be different for each bin, which may be less intuitively appealing than one set of earthquakes, each with a single annual frequency. This method could also be considered a type of deaggregation method in which the deaggregation is done by earthquake, rather than separately by magnitude, distance, and epsilon as in the other methods mentioned in the Deaggregated PSHA section.

Unlike the other HCPS methods (including the one presented in this paper), Campbell and Seligson (2003) in effect approximate the hazard curve as a step function, then match it perfectly. The effect of reducing the number of bins (and computation) on the resulting error is not clear. Further, because the match is based on a system-wide average, it is not clear how uniform the resulting errors are across the study region.

In Lee et al. (2005), from an initial set of earthquakes based on all regional faults, the reduced set was determined such that they all caused at least a threshold level of ground motion in the study region and there were not multiple events with similar magnitudes and high correlation in ground motion they caused. For an analysis of a water supply system in Los Angeles, this process resulted in a set of 59 scenarios. An unconstrained optimization was conducted to estimate the hazard-consistent

occurrence probabilities for each of those 59 earthquakes (J. Lee, personal communication, 2006). An error function was defined to represent the difference, at a set of 56 distributed grid points, between the regional hazard estimated by the reduced set of events and that represented by the full PSHA. The error function was defined as the sum of errors when uncertainty in the ground motion prediction equation was and was not considered. For the former component, 5 points on the hazard curve were matched (for 10- to 2475-year return periods); for the latter, 19 points were. The errors calculated in each case were normalized so that they were weighted equally in the optimization. In all cases, the error for a particular grid point was defined as $[\ln(P_r/P_f)]^2$, where P_r and P_f are the annual exceedence probabilities for the reduced set and the full set of events, respectively (J. Lee, personal communication, 2006). The P_r are the values estimated by the optimization. The logarithm was used so that the points in the high exceedence probability range of the hazard curve did not have undue influence. The errors for the case without ground motion uncertainty were included because the users anticipated using only the mean attenuation relations when applying the reduced set of events. The optimization was solved using the variable metric method, which does not guarantee a global minimum.

The HCPS approach has the advantages of including the contributions of earthquakes on all regional faults and preserving the coherence of particular scenarios (as compared to PSHA), while reducing the computational demands significantly compared to using a full historical or synthetic earthquake set. Spatial correlation is not explicitly addressed in any of the hazard-consistent probabilistic scenario methods (including the one in this paper). However, their ability to capture spatial correlation can be assumed to be somewhere between PSHA, which incorrectly assumes perfect correlation, and Monte Carlo simulation which, to the extent that it includes all possible earthquakes, does capture spatial correlation. Since the HCPS method is like

a simulation with a smaller set of carefully chosen earthquakes, they implicitly, partially capture spatial correlation. To some extent, including more earthquakes in the final reduced set is likely to lead to a better representation of the true spatial correlation, but the exact relationship between number of events and match to the true spatial correlation is unknown. Thus, a tradeoff exists between fully capturing spatial correlation but at a high computational cost with a full Monte Carlo simulation, and partially capturing spatial correlation with a lower computational cost with a HCPS method. The most appropriate choice of method will depend on the intended use. Further, all of these methods determine the reduced set of earthquakes and their associated hazard-consistent occurrence probabilities based on matching according to a single ground motion parameter (e.g., PGA), so the extent to which the reduced set accurately represents other ground motion parameters or collateral hazards like liquefaction, for example, remains unknown.

Unlike the method presented in this paper, (1) none of these three hazard-consistent probabilistic scenario methods guarantees the minimum possible error between the regional hazard as estimated by the reduced set and by a full probabilistic seismic hazard analysis, (2) all require the user to identify the reduced set of events *a priori*, without a full understanding of the implications of the choice in terms of accuracy and computation, and (3) none explores the effect of modeling decisions on the resulting error or the implications of the resulting error for subsequent loss estimation or other analyses.

1.3 METHOD

1.3.1 Overall Method

The method we developed for characterizing earthquake hazard for use in regional loss estimation includes three main steps: (1) Identify a set of candidate earthquakes, (2) select a reduced set of earthquakes from the candidate set, and (3) determine

hazard-consistent annual occurrence probabilities for each earthquake in the reduced set. In the first step, the goal is to identify a candidate set of earthquakes such that each is physically realistic, and together they cover the study region and the full range of possible ground shaking intensity, so that a subset of them can adequately match the "true" regional hazard. Candidate events may include historical, maximum credible, or user-defined earthquakes; or area sources. Note that unlike a full PSHA in which it is critical to include all possible sources, in the HCPS approach, if a possible source is omitted, it just means that it will be unavailable for selection in the final reduced set. Only a small number are selected for the reduced set anyway. If the errors obtained from the analysis are acceptably small, the user can conclude that the candidate set was adequate; if not, the candidate set could be expanded and the analysis redone.

An optimization model accomplishes the second and third steps together so as to make the regional hazard estimated by the earthquakes in the reduced set match the "true" regional hazard as well as possible (Figure 1-1). Regional hazard is represented by the hazard curves (annual probability of exceedence vs. ground shaking) for all control points in the study region, or equivalently, a set of *r*-year return period ground shaking maps. Ground shaking can be in terms of any scalar metric, such as peak ground acceleration (PGA) or spectral acceleration at period *T* ($S_{a(T)}$). In the case study, we use PGA in g. Control points may be census zone centroids, evenly-spaced grid points, locations of key facilities of interest, or any other user-specified locations in the study region. The "true" regional hazard is assumed to be that determined by a full probabilistic seismic hazard analysis or Monte Carlo simulation, as represented by a set of *r*-year return period maps. The hazard curve at each control point is approximated by the points associated with those *r*-year return periods (Figure 1-1). The set of control point-return period combinations are the matching points.

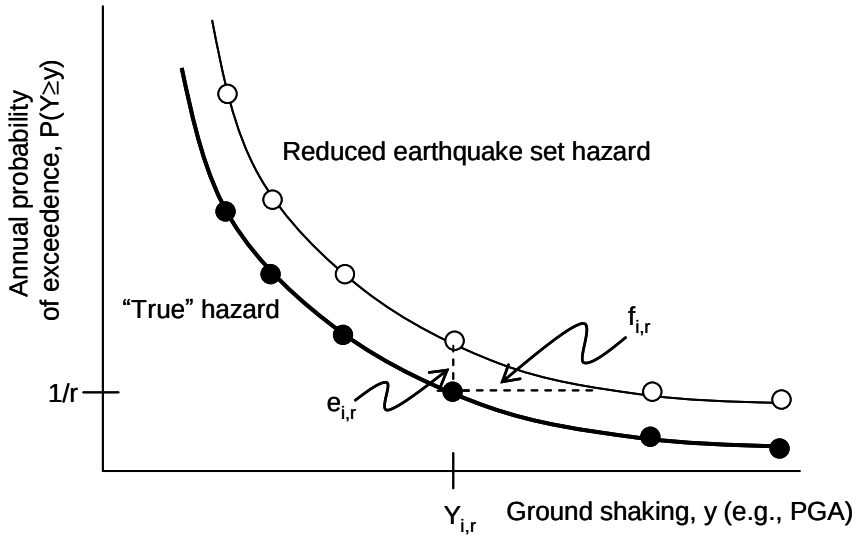

Figure 1-1 Schematic defining errors between "true" and reduced set hazard curves for control point *i*

1.3.2 Optimization Model Formulation

The objective of the optimization is to minimize the sum of the errors, over all control points and return periods, between points on the "true" hazard curves and the corresponding points on hazard curves developed with the reduced set of earthquakes and hazard-consistent annual occurrence probabilities (Figure 1-1):

$$Min \quad \sum_{i=1}^{M}\sum_{r=1}^{R}(e_{ir}^{+} + e_{ir}^{-}) \tag{1.1}$$

where e_{ir}^{+} and e_{ir}^{-} are the errors resulting from overestimating and underestimating, respectively, the "true" hazard curve for return period *r* at control point *i*. The error e_{ir}^{+} is positive if the "true" value is overestimated and zero otherwise; e_{ir}^{-} is positive if the "true" value is underestimated and zero otherwise.

Suppose P_j is the hazard-consistent annual occurrence probability for earthquake $j \in (1, N)$, N is the number of candidate earthquakes, $Y_{i,r}$ is the ground shaking from the "true" hazard curve for return period *r* at control point *i*, and $y_{i,j}$ is the ground shaking at control point *i* caused by earthquake *j*. The following constraint defines the error terms, for each control point-return period combination, as the difference

between the "true" annual exceedence probability, $1/r$, and the annual exceedence probability estimated using the reduced set of earthquakes:

$$\sum_{j=1}^{N}\{P_j * P(y_{i,j} \geq Y_{i,r})\} - e_{i,r}^{+} + e_{i,r}^{-} = \frac{1}{r} \quad \forall i, r \tag{1.2}$$

If c is the annual probability that no earthquake occurs and the probability of two or more earthquakes in a unit time is negligible compared to the probability of only one, we can assume the sum of no earthquake and all possible earthquakes equals one:

$$\sum_{j=1}^{N} P_j + c = 1 \tag{1.3}$$

Finally, the probability of earthquake j must be between 0 and P_{max}, where $0 \leq P_{max} \leq 1$, and the errors must be nonnegative.

$$0 \leq P_j \leq P_{\max} \quad \forall j \tag{1.4}$$

$$e_{ir}^{+}, e_{ir}^{-} \geq 0 \quad \forall i, r \tag{1.5}$$

One would typically assume $P_{max}=1$, but if desired, the user can specify a $P_{max}<1$. While the probabilities estimated by the model for each earthquake are really for all "earthquakes like that one" and not the probability of a single event, it may be awkward to explain a very large value of P_j. Hence, it may be desirable to include a limit significantly less than one. Including an arbitrary limit $P_{max}<1$ may result in a worse match between the reduced set and "true" hazard because it adds an additional constraint. It will also tend to increase the number of earthquakes identified by the model, which may be undesirable because the larger the set of earthquakes the more computation is required in subsequent analyses. The value of P_{max} is the user's decision and should depend on the particular analysis. In the case study, we conduct the analysis with P_{max} equal to 0.05 and 1 and compare the solutions.

The optimization model is a linear program in which the objective function is given in Expression (1.1) and the constraints are given in Expressions (1.2) to (1.5). The model determines the hazard-consistent annual occurrence probability P_j for every

earthquake *j* in the candidate set. If P_j=0, earthquake *j* is not included in the reduced set of earthquakes. It also provides the errors, $e^{+}_{i,r}$ and $e^{-}_{i,r}$, for each control point *i* and return period *r*, so the user can see how big the errors are and how they are distributed.

1.4 CASE STUDY

This section presents a case study application of the model for Tehran, the capital, and political and economic center of Iran. Tehran is located at the foot of the Alborz Mountains, which form part of the Alps-Himalayan Orogenic Zone. It is a highly seismic area surrounded by many active faults. Tehran's population has exploded in recent decades, growing from 1.0 to 7.0 million from 1950 to 2000 (UN 2002).

1.4.1 Input Data

The optimization model requires as input: (1) a candidate set of earthquakes, (2) the "true" ground shaking $Y_{i,r}$ associated with each control point *i* and return period *r*; (3) the probability that candidate earthquake *j* will cause ground shaking greater than or equal to $Y_{i,r}$ at control point *i*, $P(y_{i,j} \geq Y_{i,r})$, for every *i*-*j*-*r* combination; (4) the annual probability of no earthquake, *c*; and if desired, (5) the user-defined maximum allowable occurrence probability, P_{max}, of each earthquake *j*. For the case study, the candidate set of earthquakes was based on an earthquake catalogue developed as part of a microzoning study of the Greater Tehran Area conducted by the Japan Cooperation International Agency (JICA) for the government of Iran (JICA et al. 2000). The JICA database includes 6,114 historical events from 734 to 1999. For each, the database contains the latitude and longitude of the epicenter, date, and magnitude in M_w (which were converted to M_s, assuming M_s=M_w+0.1).

The $Y_{i,r}$, $P(y_{i,j} \geq Y_{i,r})$, and *c* values were based on a probabilistic seismic hazard analysis of Tehran by Amiri et al. (2003). In that study, the authors compiled a catalogue of historical and instrumental events in a 200 km radius of Tehran, from the 4th century BC to 1999. The logic tree method was used to integrate two methods of

estimating seismicity parameters, and three attenuation relationships. Kijko (2000) and Tavakoli (1996), considered appropriate for regions in which there is substantial uncertainty in the earthquake catalogue, were used to estimate seismicity parameters. Because of uncertainty in the catalogue, specific earthquakes could not be related to specific sources, so both studies determined a single set of seismicity parameters for the Tehran study region. The attenuation relationships were based on Iranian (Ramazi 1999), regional (Ambraseys and Bommer 1991), and global (Sarma and Srbulov 1996) earthquake catalogues. Seismic hazard assessment was conducted for 132 evenly spaced grid points in Tehran using SEISRISK III software (Bender and Perkins 1987).

In our case study, the control points were taken as the centroids of the 3,070 census zones in Tehran. We selected the 198 events from the JICA catalogue for which $4 \leq M_s < 6$ and $D \leq 200$ km, or $M_s \geq 6$ and $D \leq 500$ km, where D is the epicentral distance from the center of Tehran. Other earthquakes are not expected to cause significant ground shaking in Tehran, and thus were not considered. To ensure coverage of higher intensity ground shaking, we included an additional 8 earthquakes that Amiri et al. (2003) identified as the maximum earthquakes associated with the 8 main faults near Tehran. Figure 1-2 shows the locations of the 198 events from the JICA historical database and the 8 faults identified by Amiri et al. (2003). The 8 faults with their maximum magnitudes are (Amiri et al. 2003): Mosha 7.5, North Tehran 6.9, Niavaran 6.0, North Rey 6.1, South Rey 6.2, Kahrizak 6.6, Garmsar 6.9, and Pishva 6.5. Fault locations were obtained from the JICA et al. (2000) study. The ground shaking values $Y_{i,r}$ were obtained by digitizing 475-year and 950-year return period PGA maps from Amiri et al. (2003).

Since these were the only return period maps available, only r=475 and r=950 were considered. This means the hazard curves at each census zone is approximated

by two points. If we had access to the complete PSHA, more return periods could easily be considered, providing a better description of the hazard.

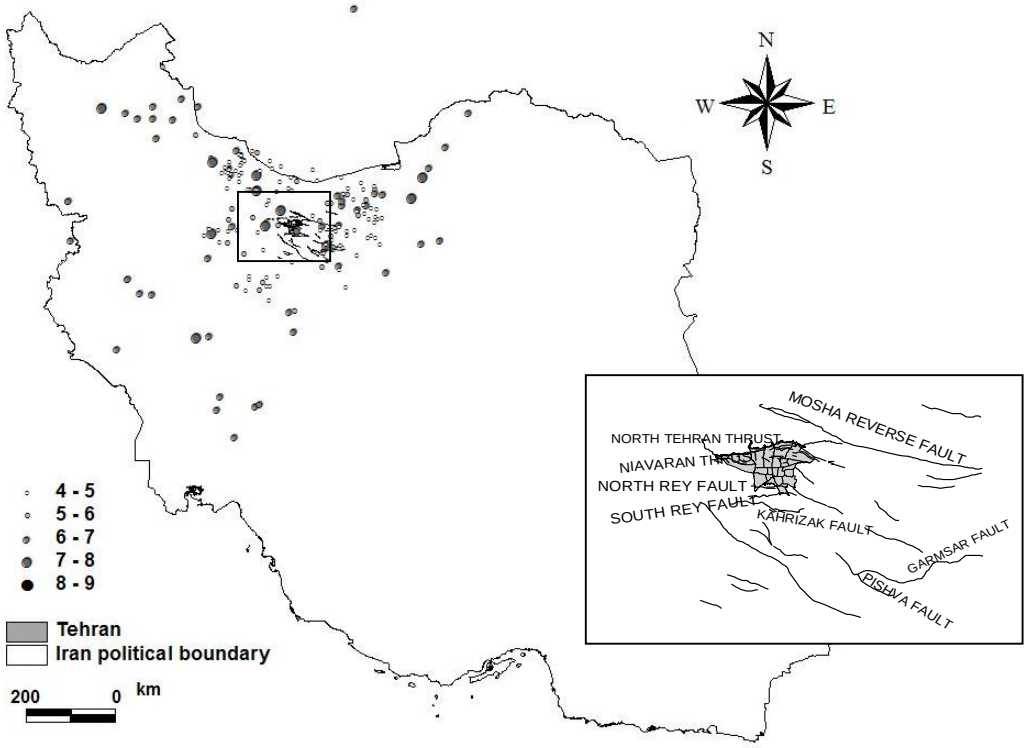

Figure 1-2 Earthquakes included in the candidate set of events, 198 epicenters and MCEs for 8 faults

Following Amiri et al. (2003), a logic tree approach was used to calculate the probability that each candidate earthquake *j* would cause ground shaking greater than or equal to $Y_{i,r}$ at census zone *i*, $P(y_{i,j} \geq Y_{i,r})$, for every *i-j-r* combination. The Ramazi (1999), Ambraseys and Bommer (1991), and Sarma and Srbulov (1996) attenuation relationships were each applied and a weighted average of the values was used, where the weights were, from Amiri et al. (2003), 0.4, 0.35, and 0.25, respectively. Specifically, we used the hard site equation in Ramazi (1999), Eq. 7 in Ambraseys and Bommer (1991), and Eq. 6 in Sarma and Srbulov (1996). In Ramazi (1999), since no distribution was specified, based on the form of the equation, we assumed that $\ln(a_h)$ is

normally distributed with a mean of ln(a_h) and standard deviation of 0.62 (estimated to be similar to the distribution in the other two relations).

The annual probability of no earthquake occurring that would affect the study region, *c*, was taken to be one minus the annual probability of an earthquake with $M_s \geq 4$ within 200 km of Tehran. From Amiri et al. (2003), c=0.505. We ran the analysis for two possible values of P_{max} (0.05 and 1) to see the effect of imposing that constraint.

1.4.2 Errors in terms of PGA

The errors in the model formulations are defined in terms of probabilities (vertical differences between the curves in Figure 1-1, $e_{i,r}^{+}$ and $e_{i,r}^{-}$, but it is easier to interpret errors defined in terms of the ground shaking parameter, PGA (horizontal differences in Figure 1-1, $f_{i,r}^{+}$ and $f_{i,r}^{-}$. To translate the probability error for census zone *i* and return period *r* into the associated PGA error, we first use the reduced set of earthquakes to develop a new hazard curve for each census zone (as in Figure 1-1). This is done by calculating the annual probability of exceeding each PGA value, *y*, in the range of interest as $\sum_{j \in \text{reduced set}} P_j * P(y_{i,j} \geq y)$, where P_j is the optimization-estimated annual occurrence probability for earthquake j and $P(y_{i,j} \geq y)$ are calculated using the logic tree approach described in the Input Data section. Interpolating on the hazard curve, we then find the reduced set estimated PGA associated with return period *r*, and compare it to the "true" PGA, $Y_{i,r}$, for census zone *i* and return period *r*. To facilitate interpretation, results are presented in terms of PGA errors.

1.4.3 Results

The linear optimization model was solved using AMPL software, with CPLEX by ILOG, for both P_{max}=1.0 ($\text{Model}_{1.0}$) and P_{max}=0.05 ($\text{Model}_{0.05}$). We first present results for $\text{Model}_{1.0}$, then compare them to $\text{Model}_{0.05}$ results. Figure 1-3 shows the historical

earthquakes selected in one or both models, and Table 1-1 lists the hazard-consistent annual occurrence probability P_j estimated for each. Eight of the 206 candidate earthquakes were selected in $\text{Model}_{1.0}$, with two having large hazard-consistent occurrence probabilities of 0.34 and 0.12. (Note that P_j does not represent the occurrence probability of a single real earthquake, but rather all earthquakes "like that one," so it should not necessarily be of the same magnitude as typically seen.)

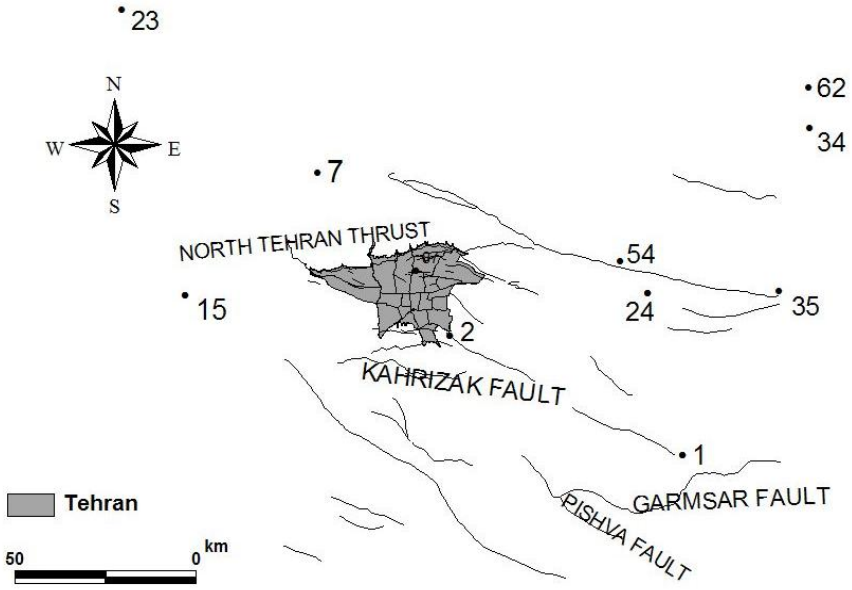

Figure 1-3 Earthquakes selected in $\text{Model}_{0.5}$ and/or $\text{Model}_{1.0}$ with earthquake number or fault name

Figure 1-4 and Figure 1-5 show the geographic distribution of 475-year and 950-year PGAs, respectively, estimated with the $\text{Model}_{1.0}$ reduced earthquake set. Figure 1-6 and Figure 1-7 show the $\text{Model}_{1.0}$ errors (reduced set PGA minus "true" PGA) for 475 and 950 years, respectively, which indicate no discernible geographic pattern. (Figures are in UTM-WGS84, Zone 39N.)

Table 1-1 Earthquakes selected in each model run with corresponding P_j values

EQ ID or fault name	Magnitude	P_j for $Model_{1.0}$	P_j for $Model_{0.05}$
1	7.1	0.1241	0.0500
2	7.0	0.0001	0.0003
7	7.7	0.0025	—
15	7.1	0.0112	0.0290
23	7.6	—	0.0500
24	6.4	0.3425	0.0500
34	6.6	—	0.0500
35	7.0	—	0.0500
54	5.4	—	0.0500
62	6.7	—	0.0484
87	4.1	0.0064	0.0083
Garmsar MCE	6.9	—	0.0500
Kahrizak MCE	6.6	0.0037	0.0037
North Tehran MCE	6.9	0.0044	0.0057
Pishva MCE	6.5	—	0.0500

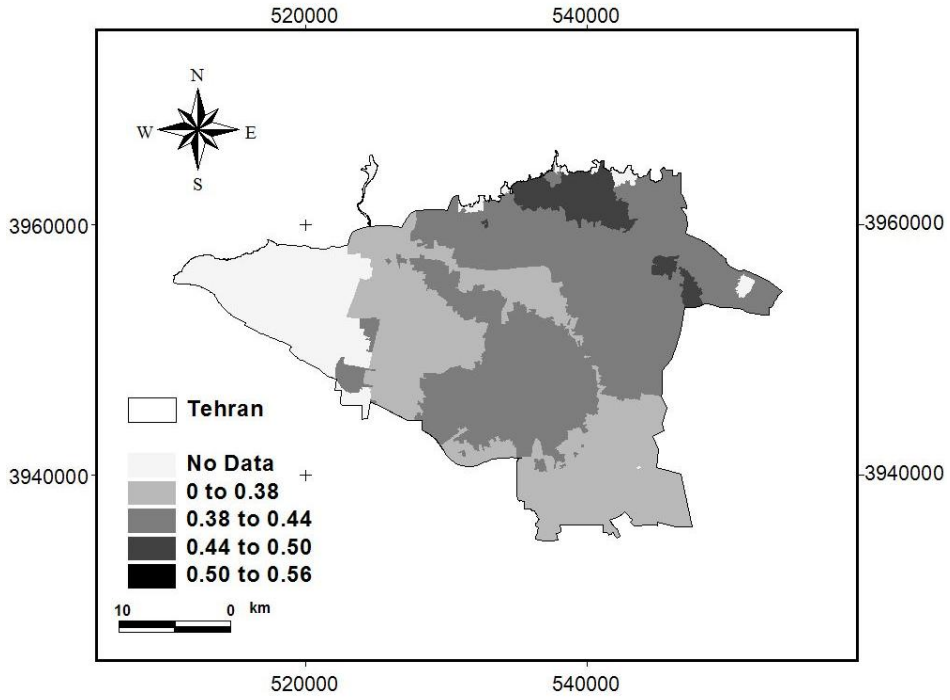

Figure 1-4 $Model_{1.0}$ reduced set PGA (g) for 475-year return period

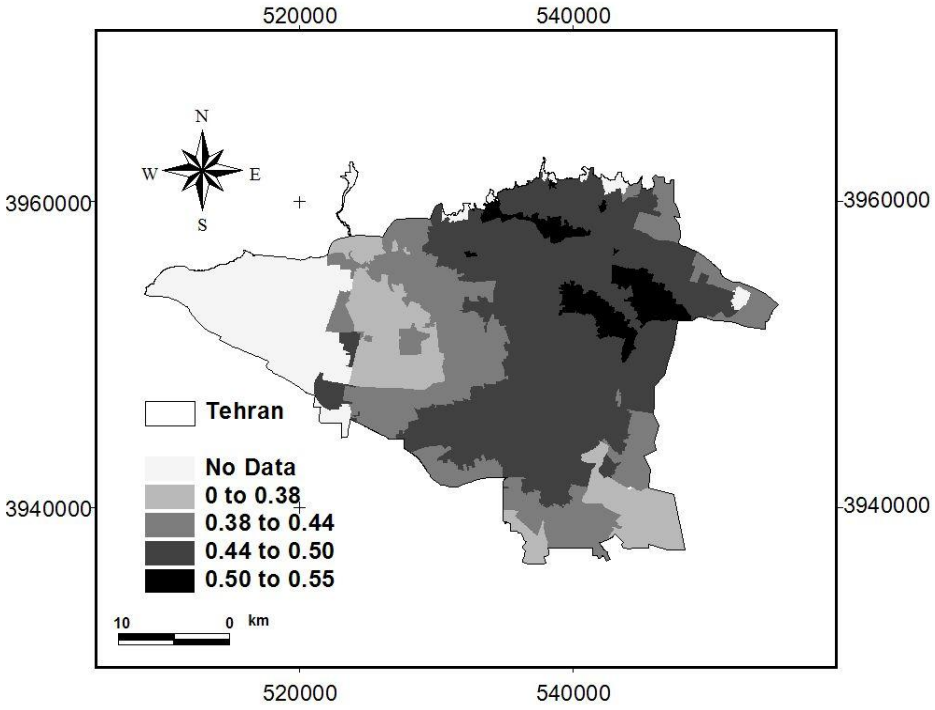

Figure 1-5 Model$_{1.0}$ reduced set PGA (g) for 950-year return period

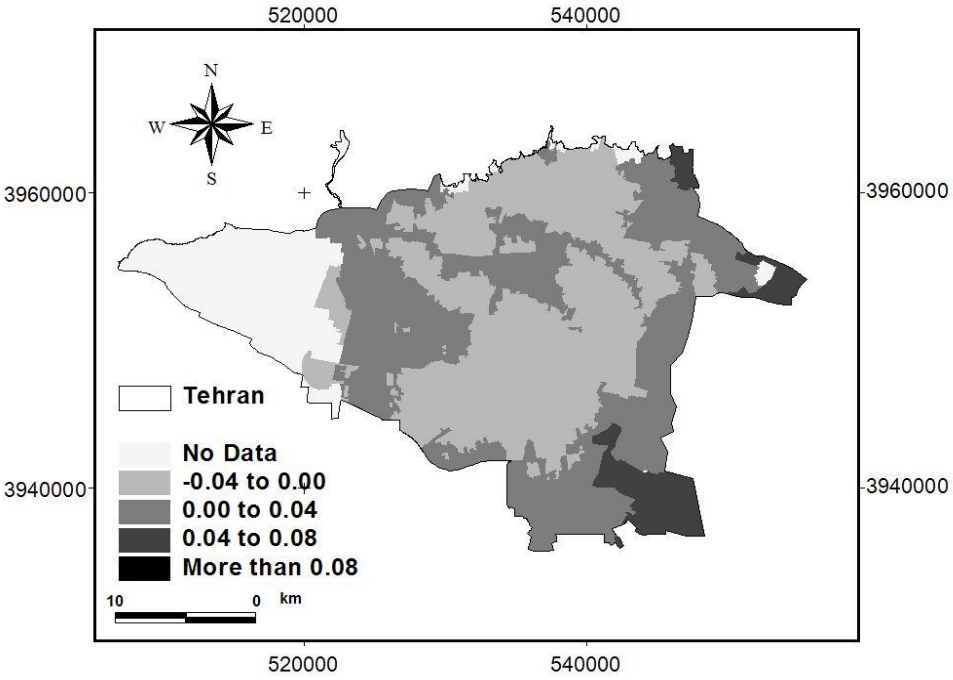

Figure 1-6 Model$_{1.0}$ error for 475-year return period

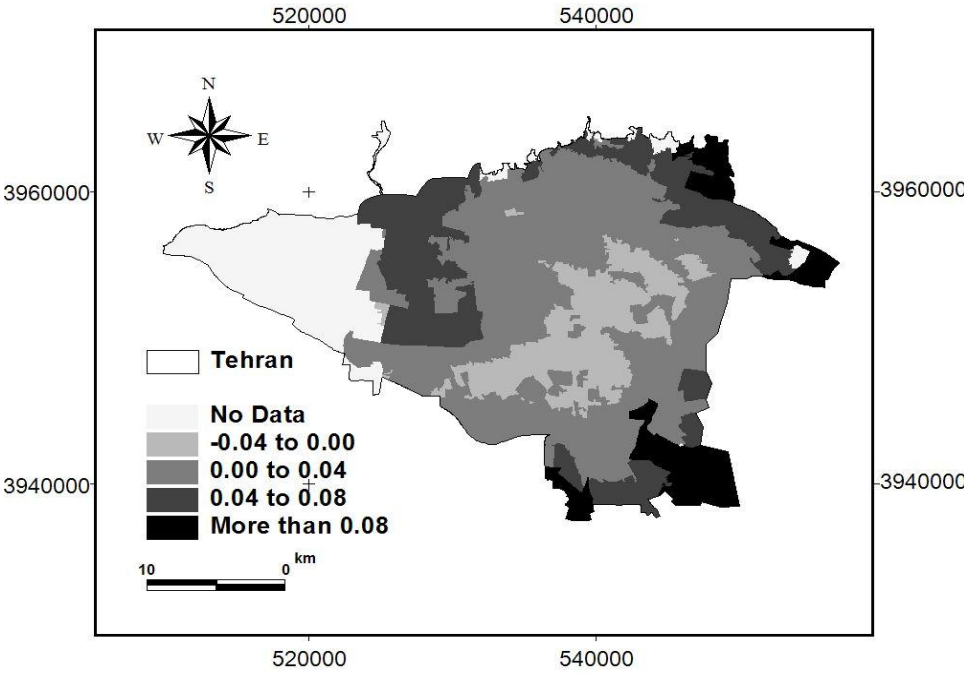

Figure 1-7 $Model_{1.0}$ error for 950-year return period

Figure 1-8 shows a histogram of the errors for $Model_{1.0}$, with one observation for each return period-census zone. Since PGA is typically modeled as having a lognormal probability distribution, Figure 1-8 is in terms of ln(reduced set PGA) – ln("true" PGA). With a mean of 0.006, median of -0.001, and positive skew of 1.1, Figure 1-8 shows an approximately normal distribution with little bias and small errors in general. There is no statistically significant difference in the errors by return period and no outliers of concern. In terms of PGA, both the expected value and median error are 0.003g (or 1%), 84% of errors are within ±0.02g, and 95% of errors are within ±0.04g. In practical terms, for this case study, the errors are not large enough to affect damage and loss estimations, and will be dominated by the uncertainty in other aspects of loss estimation.

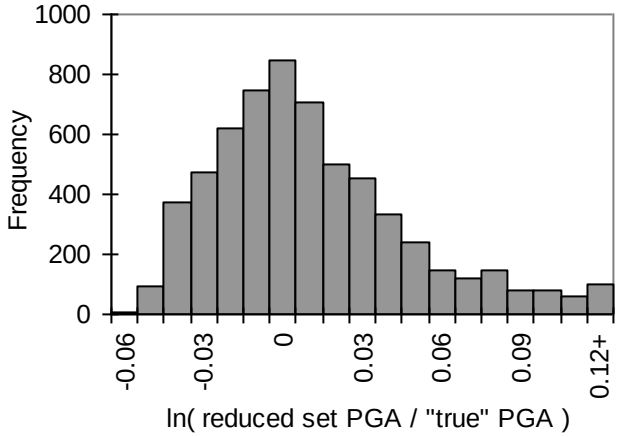

Figure 1-8 Histogram of errors (ln(reduced set PGA) minus ln("true" PGA)) for $\text{Model}_{1.0}$

To understand why the selected earthquakes were chosen and how each contributes to matching the "true" hazard, we define the contribution of earthquake *j* to matching the "true" hazard associated with census zone *i* and return period *r* as:

$$\frac{P_j P(y_{i,j} \geq Y_{i,r})}{\sum_{j \in J_r} P_j P(y_{i,j} \geq Y_{i,r})} \tag{1.6}$$

where J_r is the reduced set of earthquakes. The contributions vary greatly by census zone and return period, with a few earthquakes contributing much more than the others. If we average the contributions over all census zones and both return periods, the eight earthquakes contribute 44% (MCE on North Tehran fault), 19% (MCE on Kahrizak fault), 13% (earthquake 7), 12% (earthquake 24), 6% (earthquake 1), 3% (earthquake 15), 2% (earthquake 2) and 2% (earthquake 87), respectively. Figure 1-9shows the geographic distribution of contribution for the MCE on the North Tehran fault for the 475-year return period. Notice that this earthquake contributes significantly to the match in most of the region except the south.

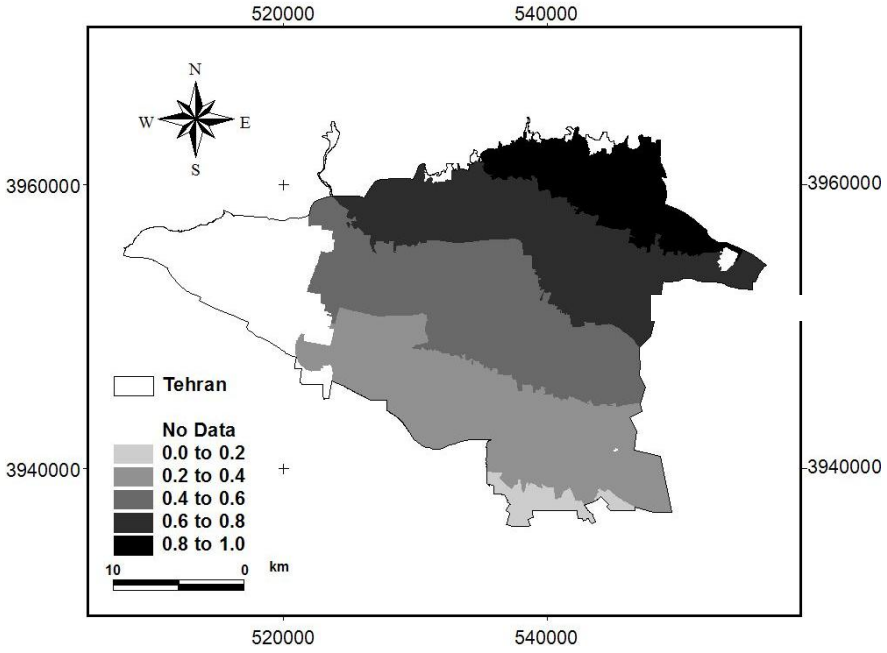

Figure 1-9 Map of Tehran showing the contribution (defined in Eq. 6) for the MCE earthquake on the North Tehran fault for $\text{Model}_{1.0}$ and the 475-year return period.

To see the effect of setting a maximum allowable annual occurrence probability for each earthquake, we compare the results from the two models. The objective function values are 0.820 and 0.927 for $\text{Model}_{1.0}$ and $\text{Model}_{0.05}$, respectively, indicating that imposing the additional constraint on P_{max} results in a worse match to the "true" hazard. However, the PGA errors for the two models are comparable in terms of distribution, magnitude, and practical significance. For $\text{Model}_{0.05}$, both the expected value and median error are 0.006g, 78% of errors are within ±0.02g, and 93% of errors are within ±0.04g (versus 0.003g, 84%, and 95% for $\text{Model}_{1.0}$). The two solutions are essentially equally good and the choice between them depends on the intended use. As expected, $\text{Model}_{0.05}$ resulted in more earthquakes in the reduced set, 14 instead of 8 (Figure 3). Eight of the 14 earthquakes in the $\text{Model}_{0.05}$ solution have $P_{\max} = 0.05$, indicating that the constraint restricting the maximum probability for an earthquake was binding.

The more matching points (i.e., return period-census zone combinations) there are, the more complete the representation of the "true" hazard. However, in general, one would expect more matching points and more constraints to make it more difficult to closely match the "true" hazard. More earthquakes in the reduced set will generally improve the match.

1.5 CONCLUSION

This paper presents a new formulation of the hazard-consistent probabilistic scenario approach to representing regional earthquake hazard for use in loss estimation. A set of candidate earthquakes is identified, and a linear program is used to select a reduced set of earthquakes and determine the hazard-consistent annual occurrence probability for each, such that together the earthquakes in the reduced set represent the "true" regional hazard. Losses can then be estimated for each earthquake in the reduced set to obtain loss exceedence curves. The reduced set represents the contributions of all possible earthquakes, but requires far less computation than simulation with tens of thousands of synthetic earthquakes.

The optimization formulation and solution method are novel in a few main ways. For the first time, they ensure that the error between the "true" hazard and the reduced set hazard is minimized. They allow the model to select the earthquakes included in the reduced set, rather than requiring the user to do that *a priori* without understanding the implications of the choice for the final error. Finally, they clarify the magnitude and distribution of errors so that the user can make informed decisions about the tradeoff between computational savings and introduction of errors. The simple linear program formulation is easily solved for any size region. The method results in a single set of earthquake scenarios (unlike PSHA or Campbell and Seligson 2003), is reproducible, and can be adapted to other hazards.

Opportunities exist to extend this new formulation and overcome some limitations it shares with other HCPS methods. Currently the "true" hazard is measured only by PGA. It would be possible, however, to add terms to the objective function that represent errors in other ground motion parameters or collateral hazards. One could also force errors to be smaller for certain census zones or return periods that are of particular interest by adding weights to penalize the corresponding error terms in the objective function. Although it would be less straightforward to do, future efforts might also try to minimize errors in spatial correlation. In any case, the method is only as good as the representation of "true" hazard on which it is based.

APPENDIX

This appendix contains the following information in support of the paper titled "Identification of hazard-consistent probabilistic earthquake scenarios for regional loss estimation":

1. Maps illustrating the digitized 475-year and 950-year return period PGA(g) maps from Amiri et *al.*(2003)
2. Maps of errors ("reduced set" minus "true" hazard) for $\text{Model}_{0.05}$ for (a) 475-year and (b) 950-year return periods in terms of PGA(g)
3. The contributions of each earthquake in the reduced set for $\text{Model}_{1.0}$ and $\text{Model}_{0.05}$ by census zone and return period
4. Discussion and illustration of how to compute $P(y_{i,j} \geq Y_{i,r})$

All figures are in UTM-WGS84, Zone 39N.

1. Digitized maps from Amiri et al.(2003)

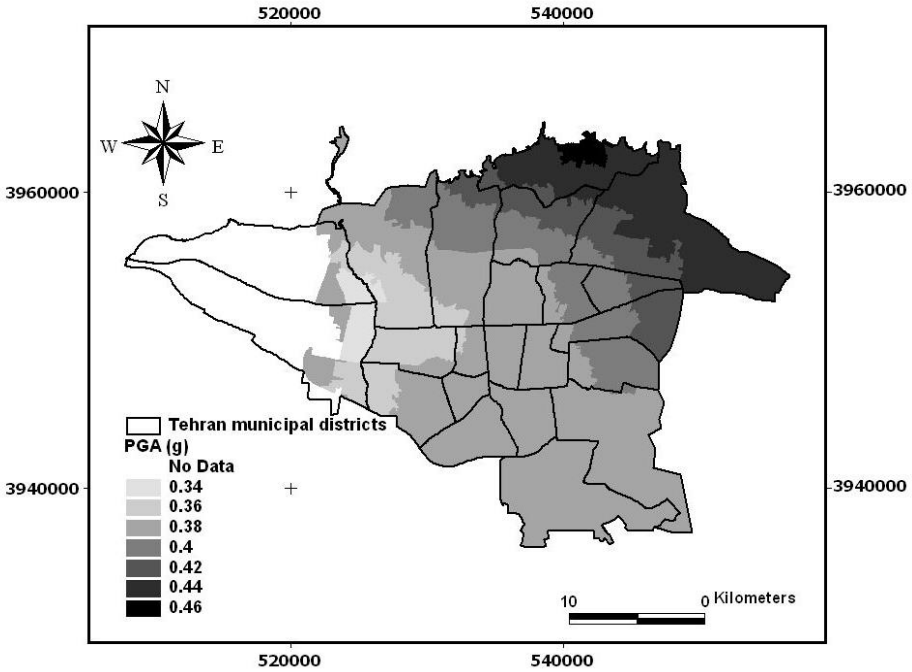

Figure 1-10 Map of 475-year return period bedrock PGA (g) in Tehran based on Amiri et al. (2003)

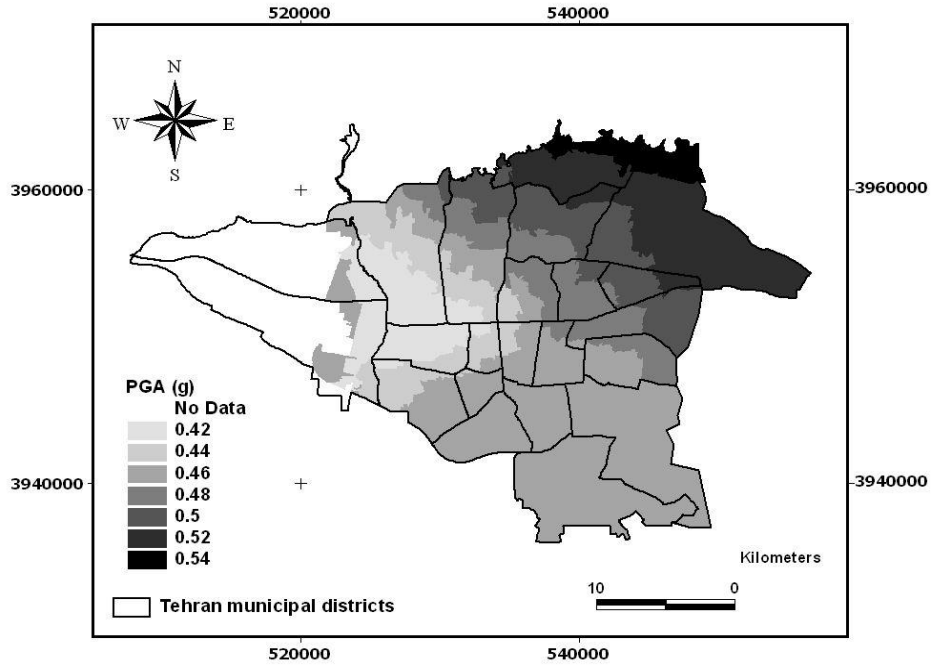

Figure 1-11 Map of 950-year return period bedrock PGA (g) in Tehran based on Amiri et al. (2003)

2. Maps of errors ("reduced set" minus "true" hazard) for Model0.05

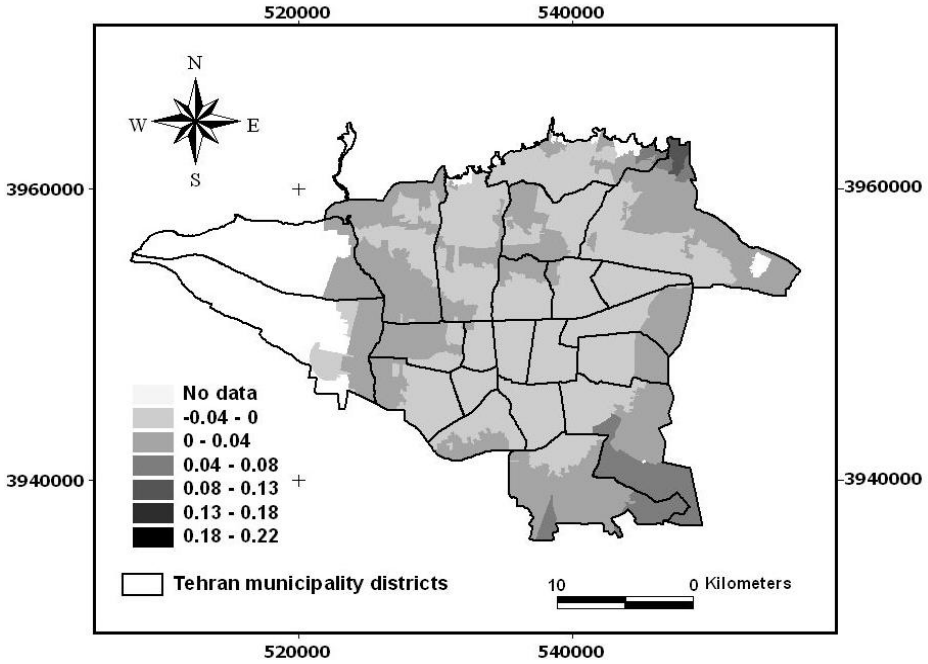

Figure 1-12 Model$_{0.05}$ error for 475-year return period

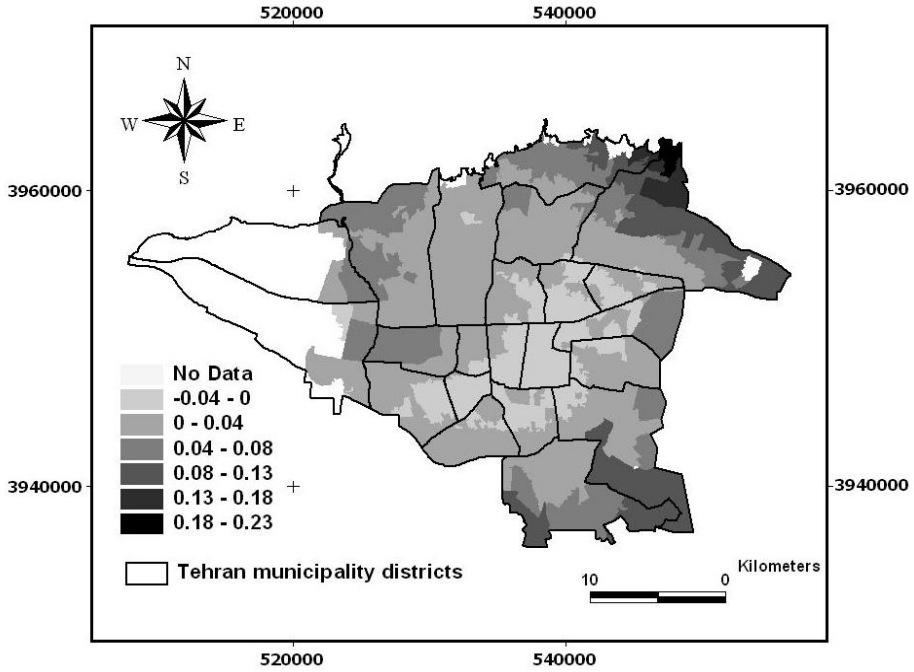

Figure 1-13 $Model_{0.05}$ error for 950-year return period

3. Maps of Contributions of Earthquakes

All figures are in UTM-WGS84, Zone 39N and are based on Equation(1.7)

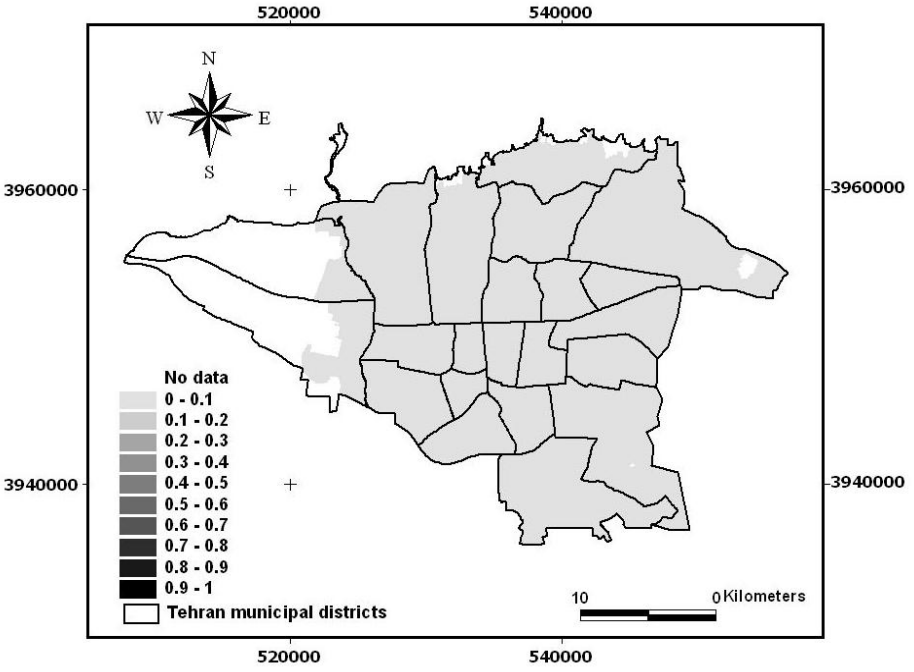

Figure 1-14 Map of Tehran showing the contribution for the earthquake ID 2 for $Model_{0.05}$ and the 475-year return period

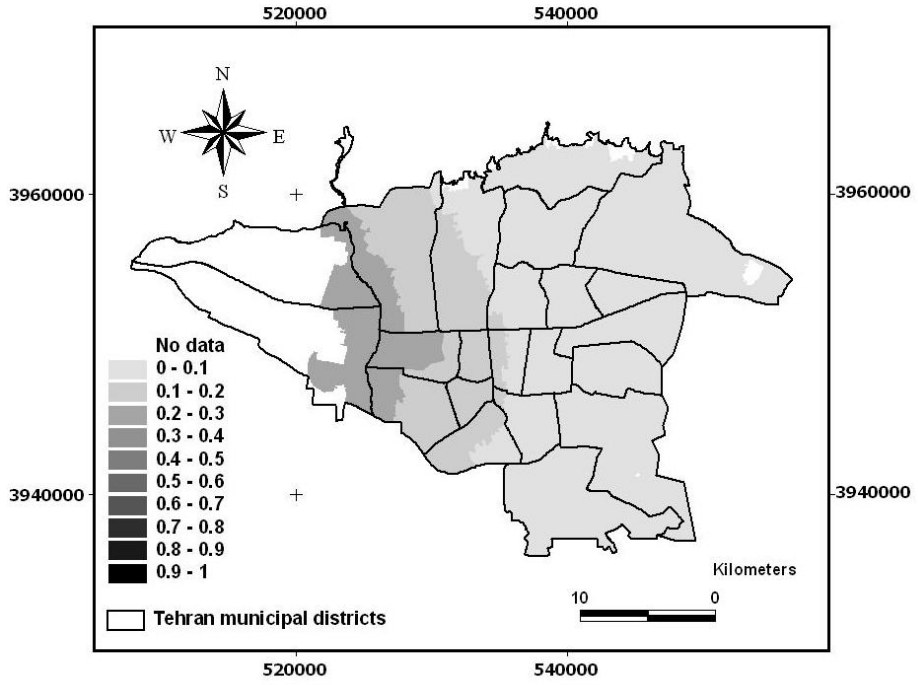

Figure 1-15 Map of Tehran showing the contribution for the earthquake ID 15 for $Model_{0.05}$ and the 475-year return period

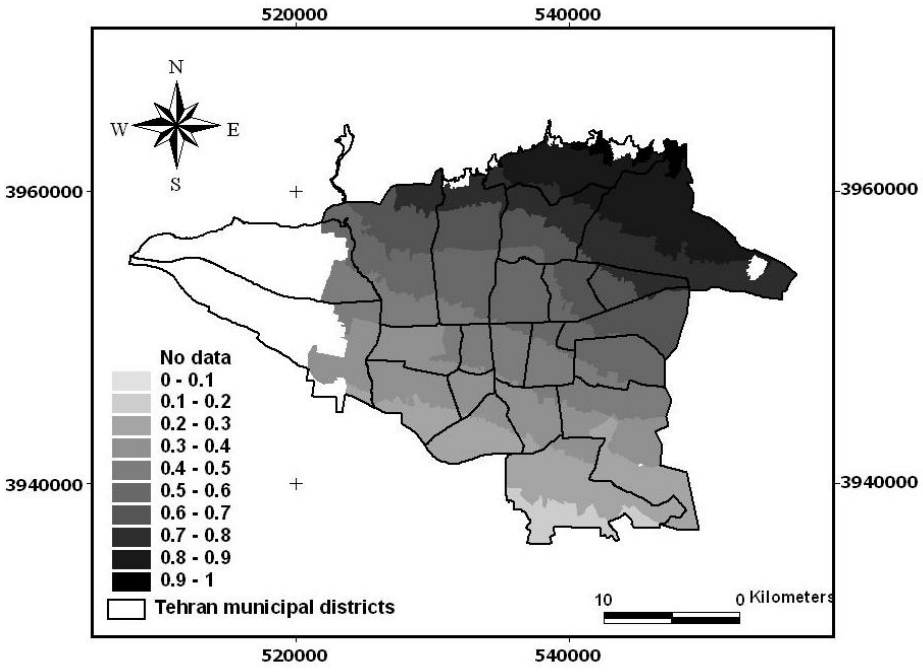

Figure 1-16 Map of Tehran showing the contribution for the earthquake ID 199 for $Model_{0.05}$ and the 475-year return period

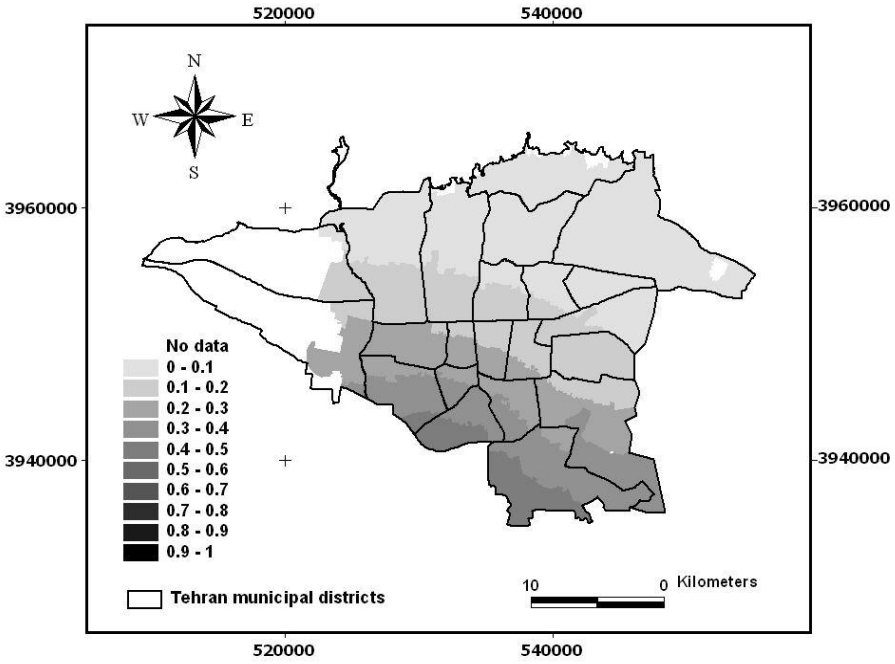

Figure 1-17 Map of Tehran showing the contribution for the earthquake ID 204 for $Model_{0.05}$ and the 475-year return period

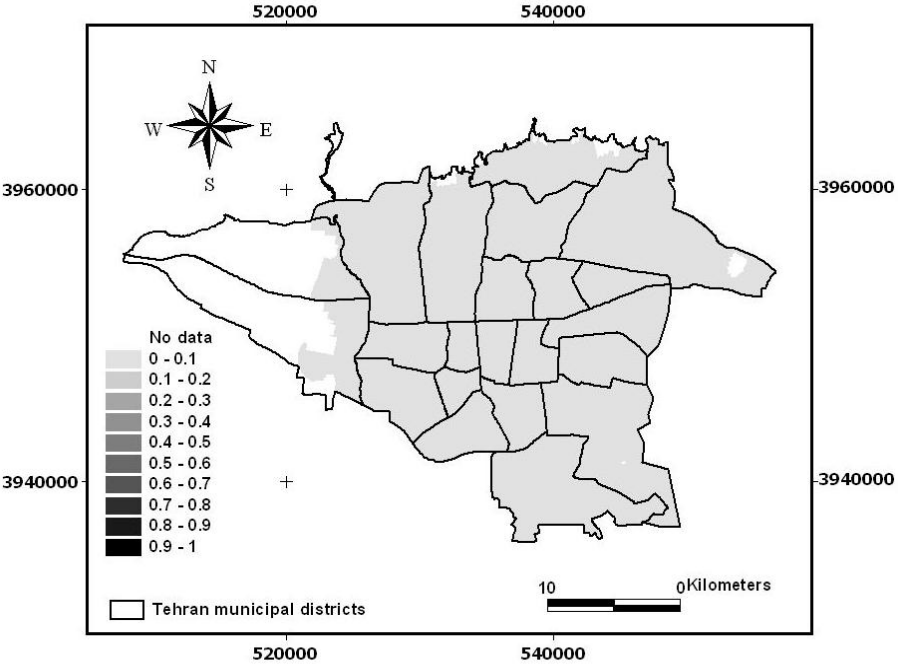

Figure 1-18 Map of Tehran showing the contribution for the earthquake ID 205 for $Model_{0.05}$ and the 475-year return period

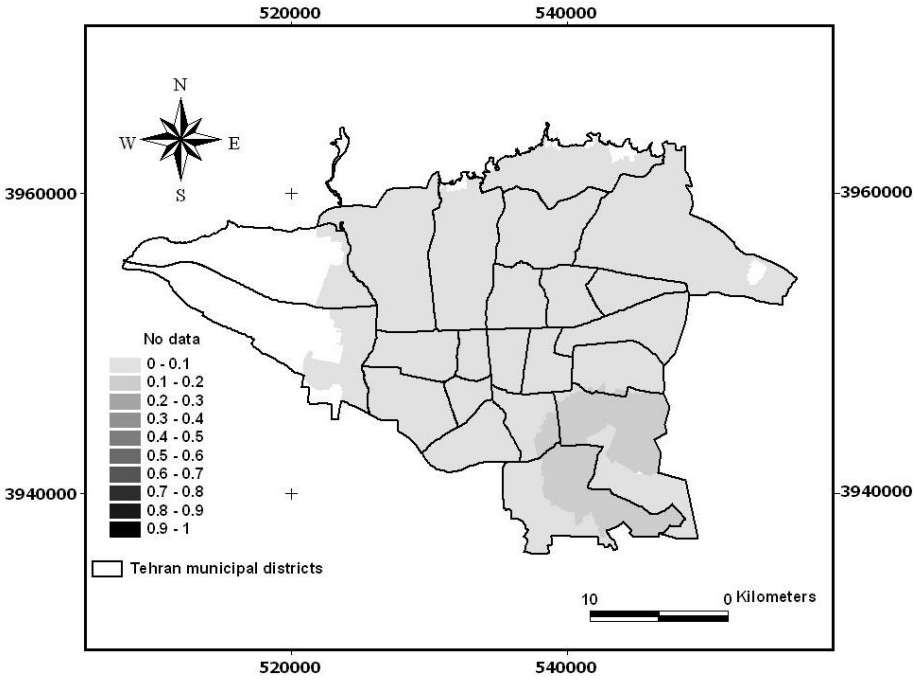

Figure 1-19 Map of Tehran showing the contribution for the earthquake ID 2 for $Model_{0.05}$ and the 950-year return period

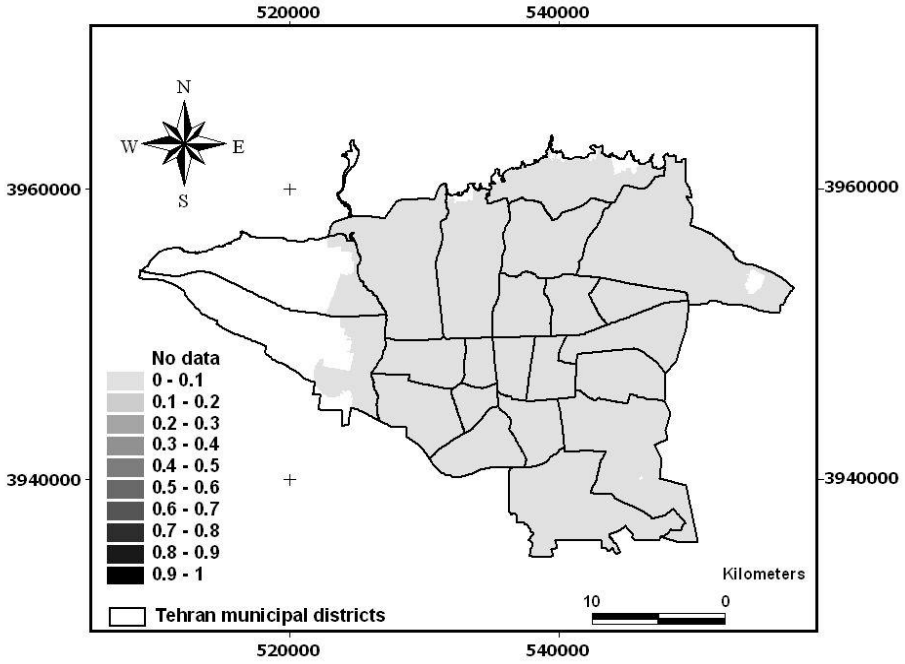

Figure 1-20 Map of Tehran showing the contribution for the earthquake ID 15 for $Model_{0.05}$ and the 950-year return period

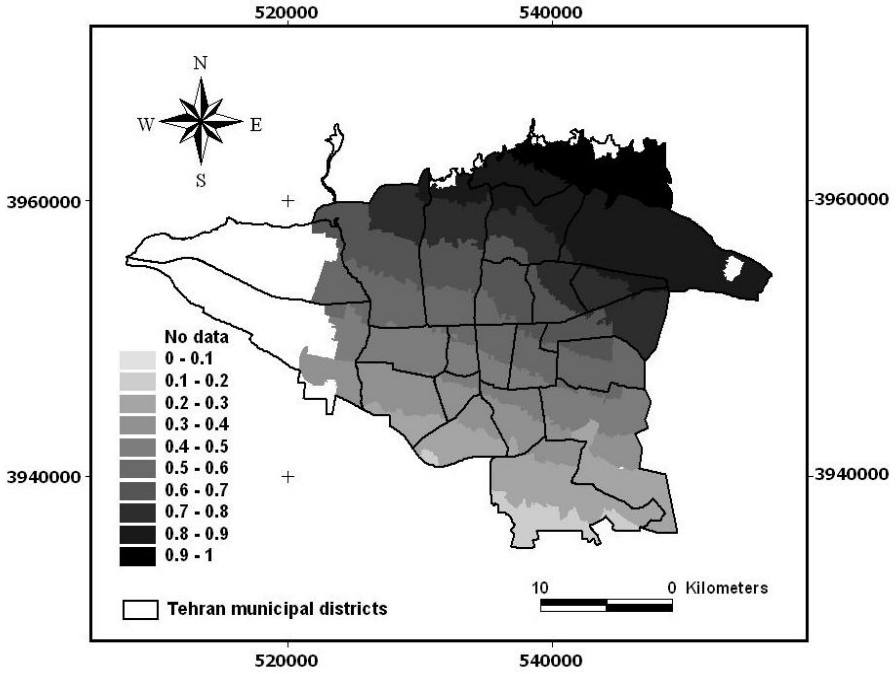

Figure 1-21 Map of Tehran showing the contribution for the earthquake ID 199 for $Model_{0.05}$ and the 950-year return period

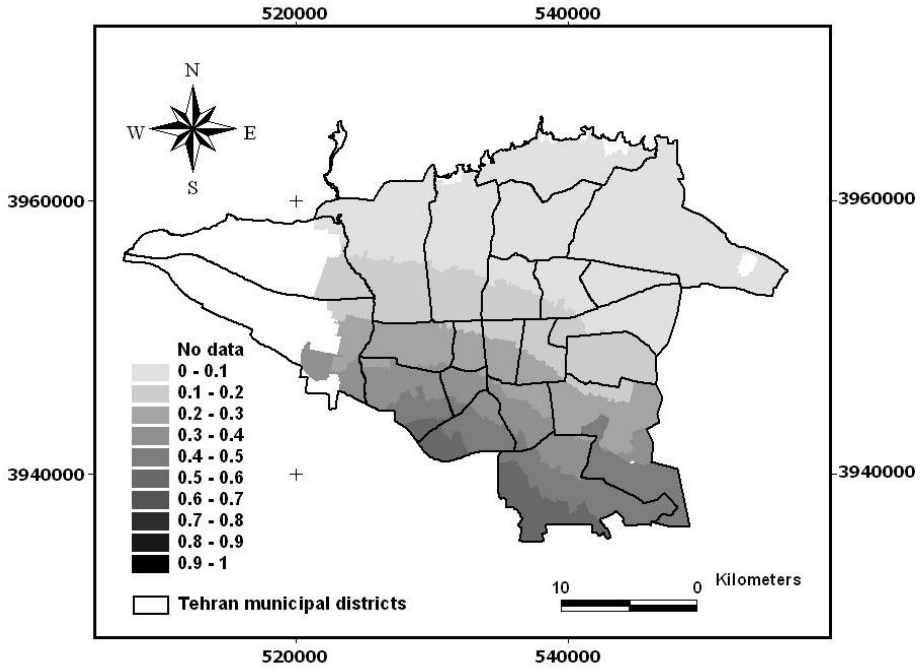

Figure 1-22 Map of Tehran showing the contribution for the earthquake ID 204 for $Model_{0.05}$ and the 950-year return period

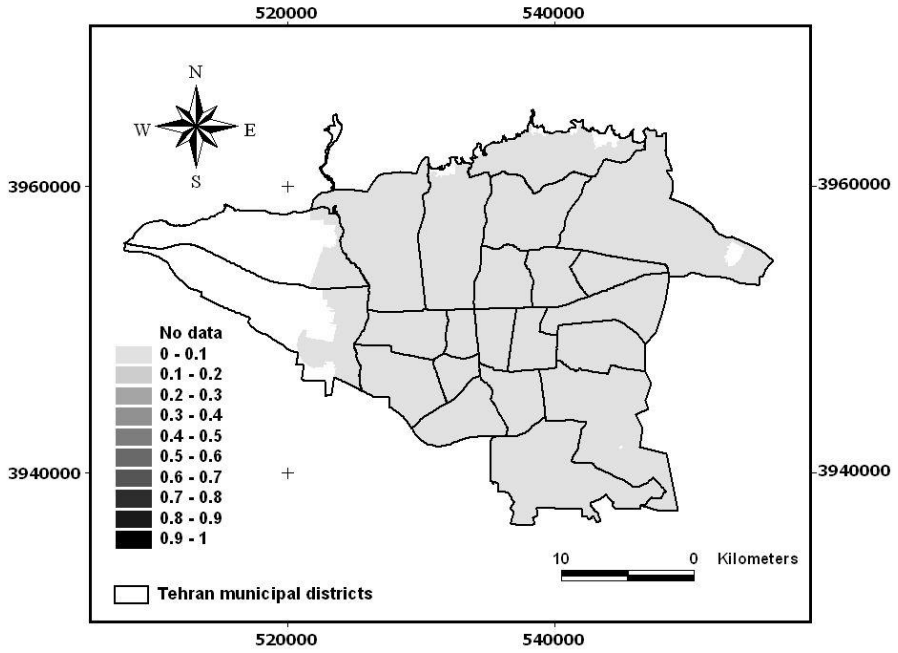

Figure 1-23 Map of Tehran showing the contribution for the earthquake ID 205 for $Model_{0.05}$ and the 950-year return period

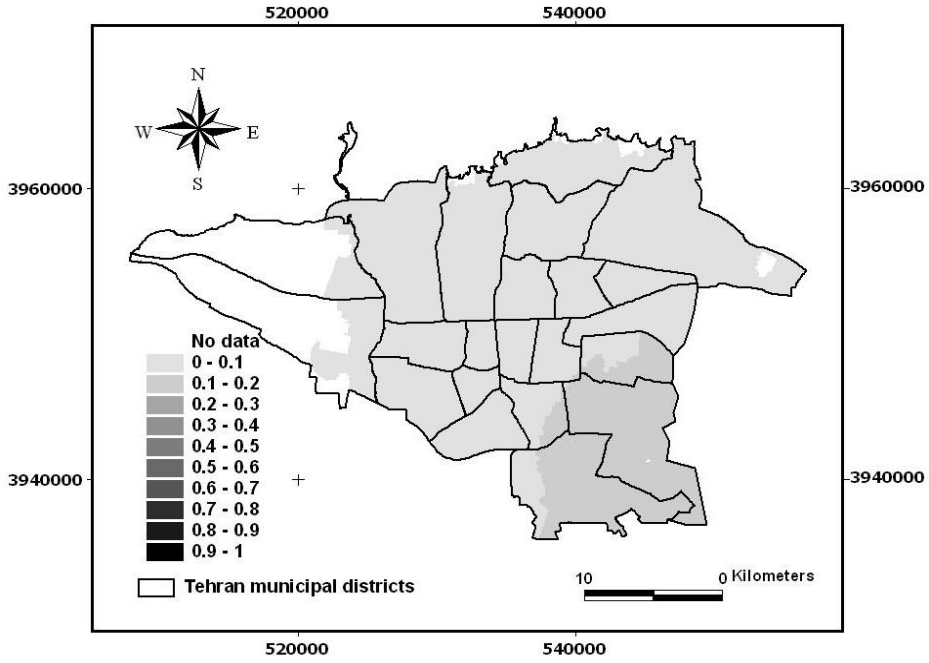

Figure 1-24 Map of Tehran showing the contribution for the earthquake ID 1 for $Model_{1.0}$ and the 475-year return period

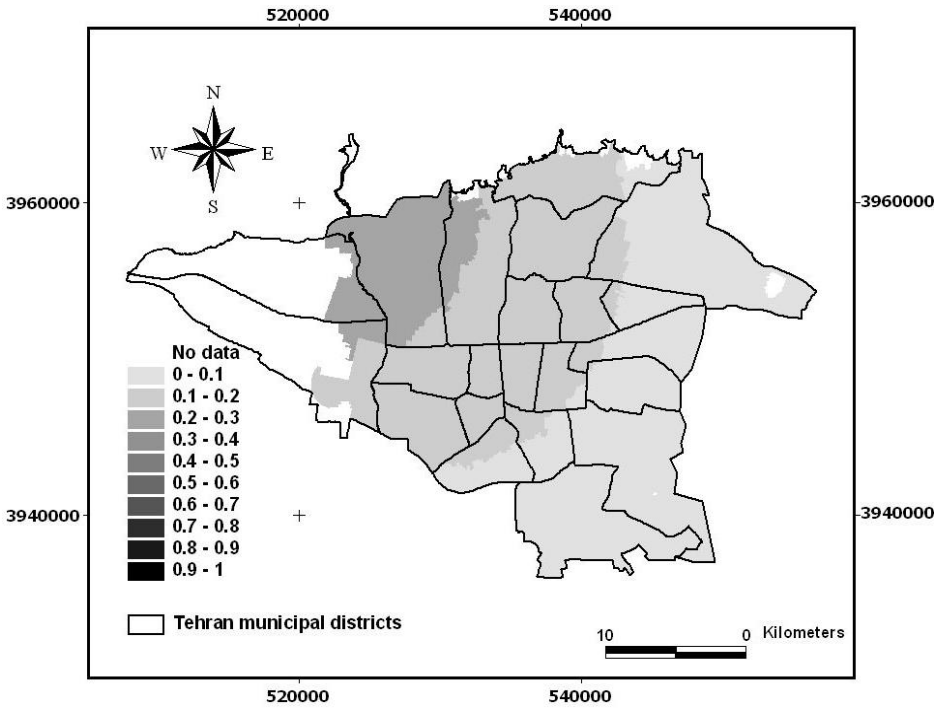

Figure 1-25 Map of Tehran showing the contribution for the earthquake ID 7 for $Model_{1.0}$ and the 475-year return period

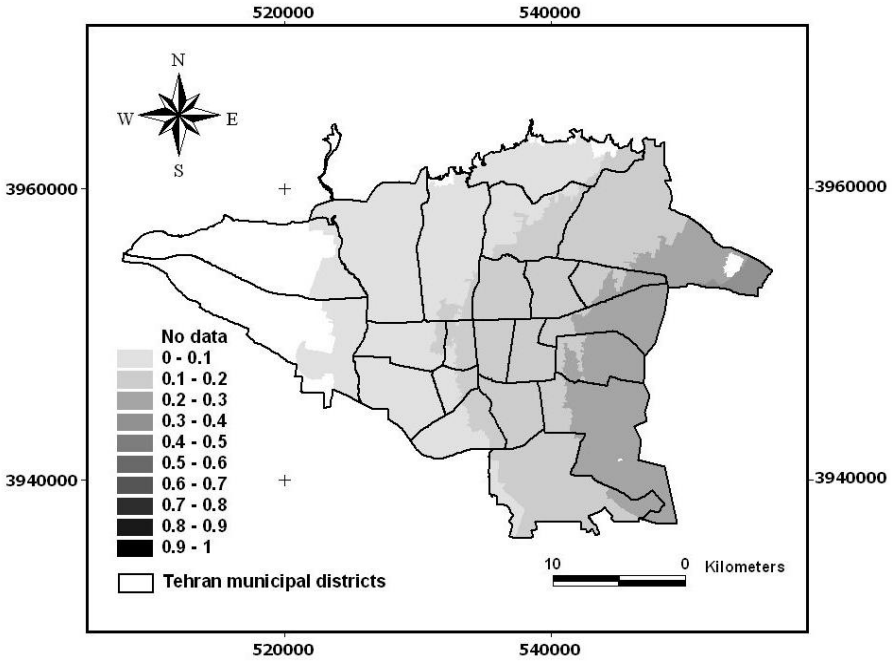

Figure 1-26 Map of Tehran showing the contribution for the earthquake ID 24 for $Model_{1.0}$ and the 475-year return period

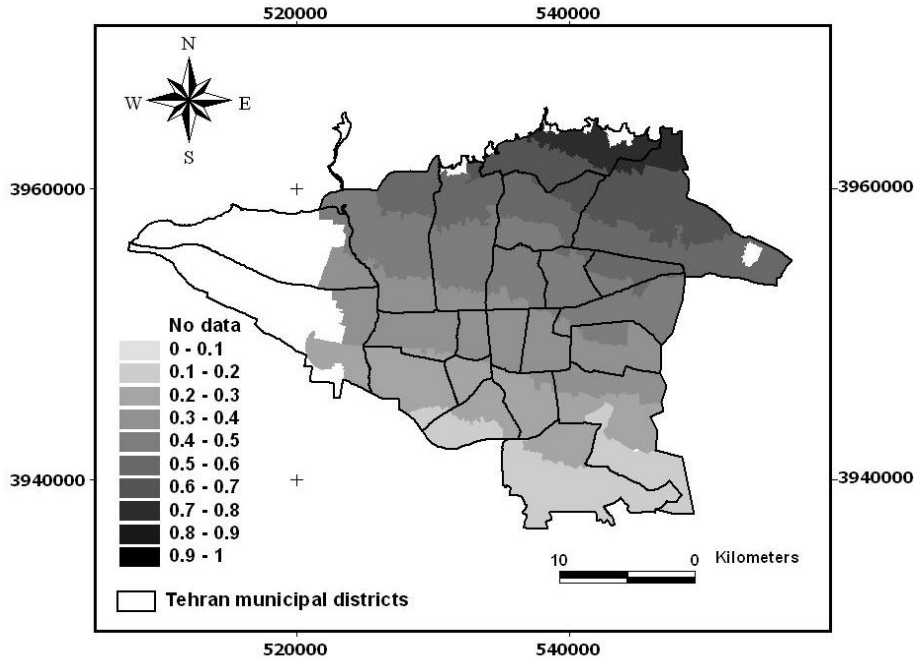

Figure 1-27 Map of Tehran showing the contribution for the earthquake ID 199 for $Model_{1.0}$ and the 475-year return period

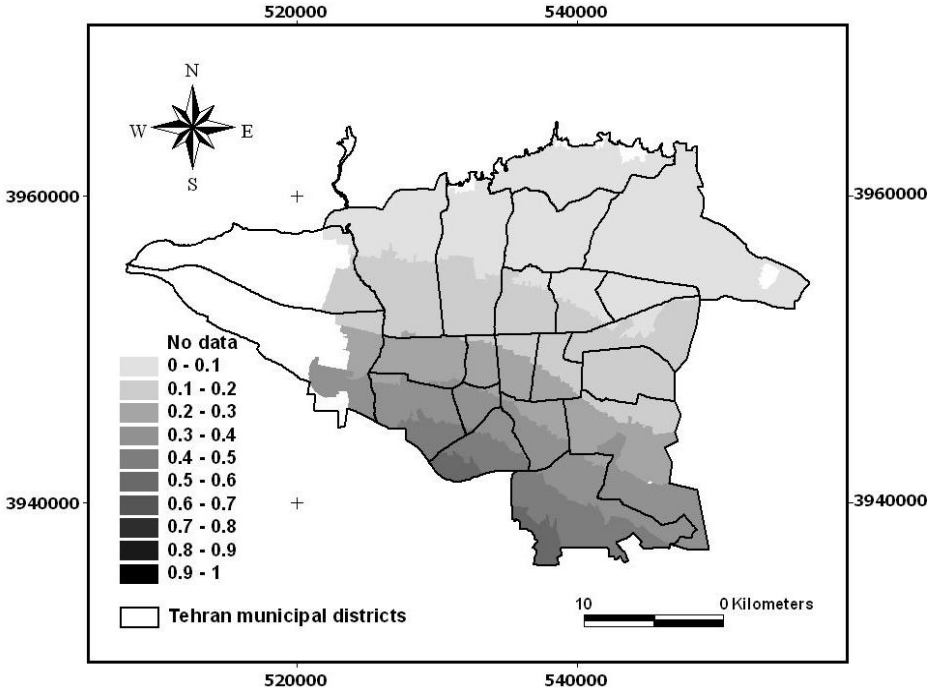

Figure 1-28 Map of Tehran showing the contribution for the earthquake ID 204 for $Model_{1.0}$ and the 475-year return period

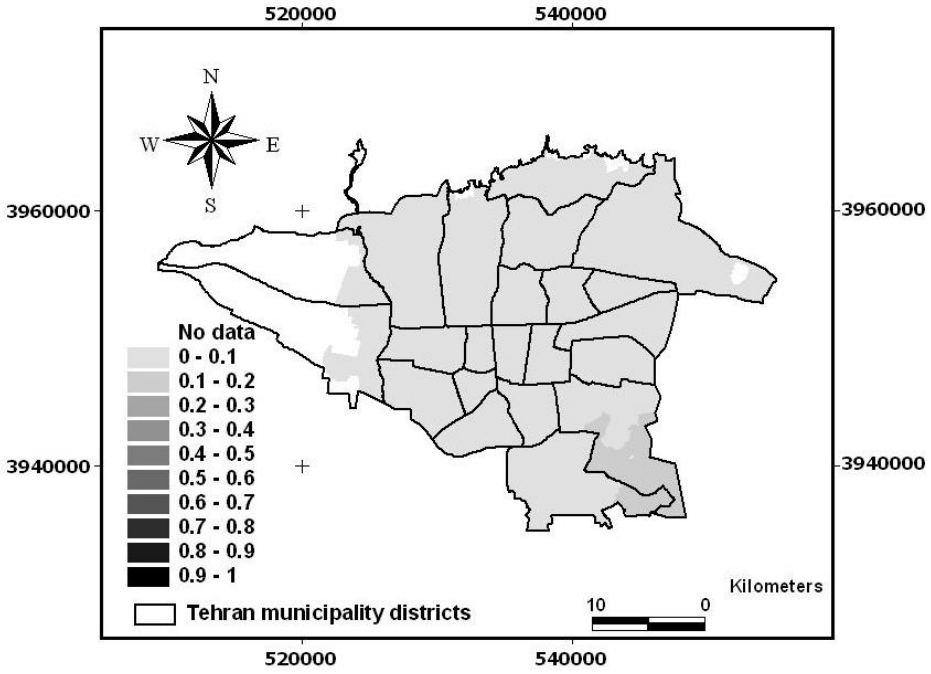

Figure 1-29 Map of Tehran showing the contribution for the earthquake ID 1 for $Model_{1.0}$ and the 950-year return period

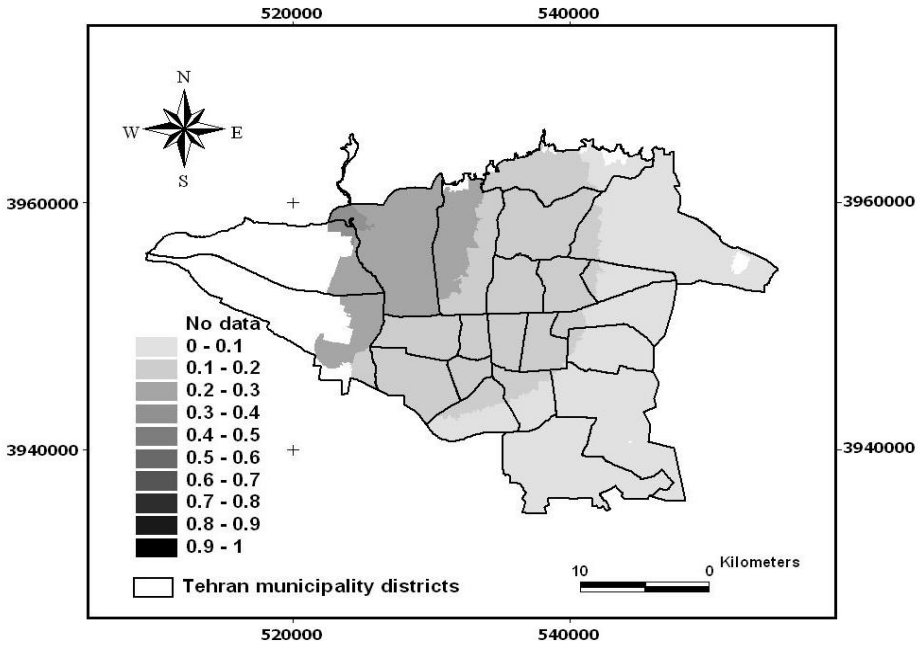

Figure 1-30 Map of Tehran showing the contribution for the earthquake ID 7 for $Model_{1.0}$ and the 950-year return period

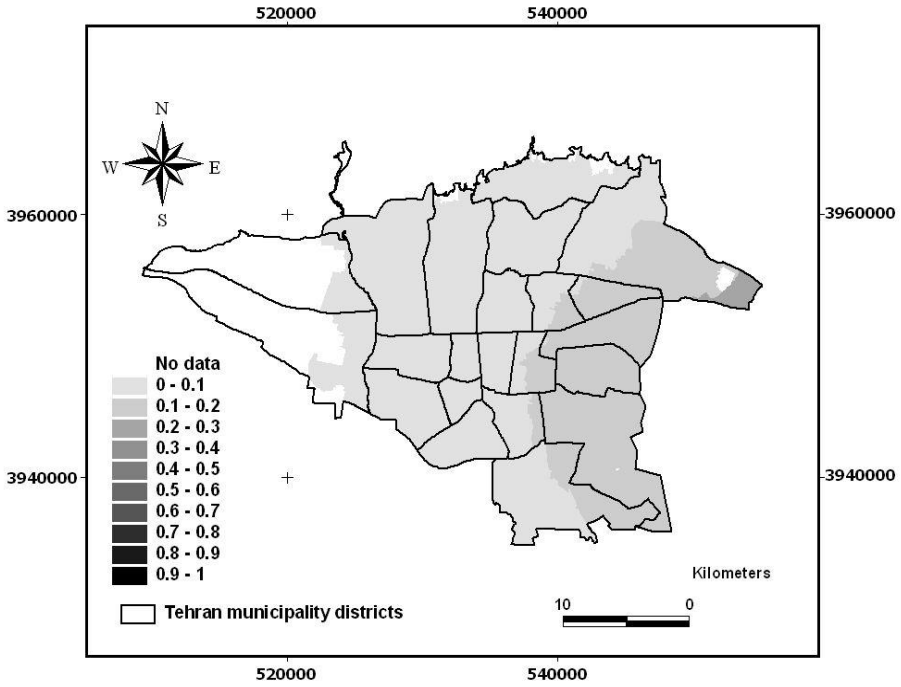

Figure 1-31 Map of Tehran showing the contribution for the earthquake ID 24 for $Model_{1.0}$ and the 950-year return period

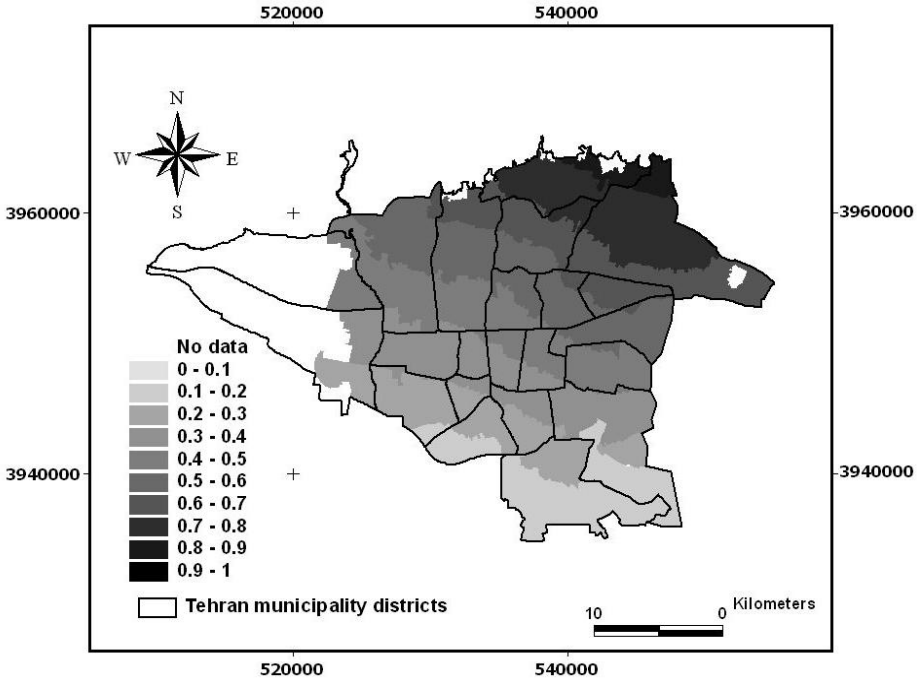

Figure 1-32 Map of Tehran showing the contribution for the earthquake ID 199 for $Model_{1.0}$ and the 950-year return period

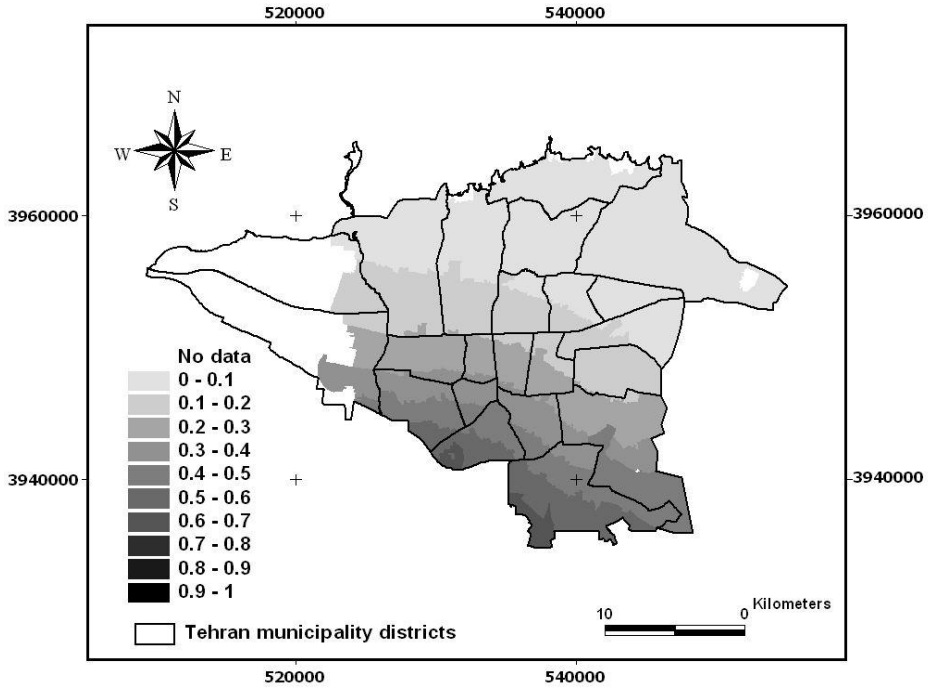

Figure 1-33 Map of Tehran showing the contribution for the earthquake ID 204 for $Model_{1.0}$ and the 950-year return period

4. Discussion and illustration of how to compute "exceedence probabilities"

This paper tries to match the estimated annual exceedence probabilities to the "true" exceedence probability of the map, *1/r* as shown in constraint (2) in the paper which is also shown in equation(1.8):

$$\sum_{j=1}^{N}\left\{P_j * P\left(y_{i,j} \geq Y_{i,r}\right)\right\} - e_{i,r}^{+} + e_{i,r}^{-} = \frac{1}{r} \quad \forall i, r \tag{1.8}$$

where P_j is the hazard-consistent annual occurrence probability for earthquake $j \in (1, N)$, N is the number of candidate earthquakes, $Y_{i,r}$ is the ground shaking from the "true" hazard curve for return period r at control point i, and $y_{i,j}$ is the ground shaking at control point i caused by earthquake j, e_{ir}^{+} and e_{ir}^{-} are the error terms for overestimations and underestimations, respectively, and $P(y_{i,j} \geq Y_{i,r})$ is called the "exceedence probability". This section describes the calculation of these exceedence probabilities $P(y_{i,j} \geq Y_{i,r})$, which are coefficients in the optimization. Note that for the analysis in this paper we focus on PGA as the measure of ground shaking.

An "exceedence probability" is the probability that when earthquake *j* occurs, the PGA at control point *i* will be greater than or equal to $Y_{i,r..}$ The calculation of this probability is done using attenuation relationships.

Attenuation relationships give the ground motion level (PGA in this paper) as a function of magnitude M_j, distance d_{ij}, and possibly other parameters to allow for different site types or fault styles (Field, 2007). All attenuation relationships are developed by fitting a curve to observations and these observations usually have significant scatter. This introduces uncertainty in the prediction of the fitted curve as illustrated in Figure 1-34.

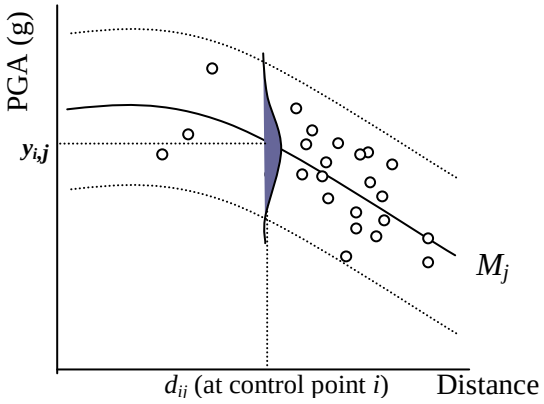

Figure 1-34 The scatter in the observations introduces uncertainty in the attenuation relationships. A lognormal distribution for PGA is often assumed with the mean value being the attenuation relationship (solid line)

To represent the uncertainty in the calculation of these ground shaking values it is typically assumed that they will have a lognormal distribution around the calculated average value at any given control point *i* (at distance d_{ij}) with a constant standard deviation which is estimated when the attenuation relationship is estimated (see Figure 1-34). Therefore, the probability that y_{ijr} exceeds $Y_{i,r}$ for the j^{th} earthquake at the i^{th} control point is given by equation (1.9) where F is the Normal cumulative distribution function with mean $\ln y_{ij}$ and standard deviation of σ .

$$P(y_{i,j} \geq Y_{i,r}) = 1 - F_Y(\ln Y_{i,r}) \quad (1.9)$$

(Note that some attenuation relations use $\log_{10} Y_{i,r}$ instead of $\ln Y_{i,r}$).

4.1. Calculations

Since the calculations in this paper are based on the method proposed by Amiri et al. (2003), the calculation of exceedence probabilities are done separately for each of the three attenuation relationships they have used (Ambraseys and Bommer, 1991; Sarma and Srbulov, 1996; Ramazi, 1999) and the weighted average of the three is used in Equation(1.2) of the paper. In other words, for every control point *i*, earthquake *j*, and return period *r*, the calculations consist of three main steps:

1. Calculation of the mean $y_{i,j}$ using each attenuation relationship given in Amiri et al. (2003).

2. Calculation of probability of exceeding $Y_{i,r}$ for each attenuation relationship

3. Calculation of weighted average using the weights in Amiri et al. (2003)

The details of the steps are as follows:

4.1.1.Calculate mean yi,j using each attenuation relation

(Ambraseys and Bommer, 1991)

Based on Ambraseys and Bommer (1991), the mean value at every control point *i*, for every earthquake *j* is calculated by equation (1.10)

$$\log_{10}(y_{ij}) = -1.09 + 0.238 M_s - \log_{10}(r) + 0.28P \quad (1.10)$$

$y_{i,j}$ PGA in g

Ms Surface wave magnitude

r $= (d_{ij}^2 + h_0^2)^{1/2}$

d_{ij} Shortest distance from the control point *i* to the surface projection of the fault rupture which is the source of the earthquake *j* in km

h_0 Constant with the value of 6

P 0 for 50-percentile and 1 for 84 percentile. We use P=0 to get the median.

It is assumed that $\log_{10}(y_{ij})$ is normally distributed with mean calculated using Equation (1.10) (with P=0) and standard deviation of 0.28.

(Sarma and Srbulov, 1996)

Similarly, based on Sarma and Srbulov (1996), the mean value at every control point *i*, for every earthquake *j* is calculated by equation (1.11):

$$\log_{10}(y_{ij}) = -1.507 + 0.240M_s - 0.5421\log_{10}(r) - 0.00397r + 0.26 \qquad (1.11)$$

Same definitions as in (1.10) except:

h_0 Constant with the value of 3

It is assumed that $\log_{10}(y_{ij})$ is normally distributed with mean calculated using Equation (1.11) (with P=0) and standard deviation of 0.26.

(Ramazi, 1999)

Similarly, based on Ramazi (1999), the mean value at every control point *i*, for every earthquake *j* is calculated by equation(1.13):

$$y_{ij} = \frac{4000}{9.81*100} * (20 + d_{ij} + H)^{-2.11} e^{0.79M}, \quad H = \left|16M - d_{ij}\right|^{0.63} \qquad (1.12)$$

or

$$\ln(y_{ij}) = \ln(\frac{4000}{9.81*100}) - 2.11*\ln(20 + d_{ij} + H) + 0.79M, \quad H = \left|16M - d_{ij}\right|^{0.63} \qquad (1.13)$$

Same definitions as in (1.10) except:

M Paper does not specify the magnitude scale, so to be consistent with previous two attenuation relationships, M_s is assumed.

We further assume that $\ln(y_{ij})$ is normally distributed with mean calculated using Equation (1.13) and standard deviation of 0.62. The value of 0.62, corresponds to 0.27 (like in the other attenuation relations) if $\log_{10}(y_{ij})$ is normally distributed, i.e.,

$10^{0.27}=e^{0.62}$. Since this paper does not present a standard deviation value, we assume a standard deviation that it is similar to the other attenuation relationships.

4.1.2. Calculate probability of exceeding Yi,r for each attenuation relation

For each attenuation relation, there is a normal distribution for either $\log(y_{ij})$ or $\ln(y_{ij})$. So, we use the equation describing a normal distribution to determine the probability of exceeding some specified probability $Y_{i,r}$ (e.g., 0.05g). This is done by using equation (1.9) for every attenuation relationship. For the 3 attenuations used in Amiri et al. (2003), the formulas in Microsoft Excel are:

$$P(y_{ij,\ \text{Ambraseys and Bommer}} \geq Y_{i,r}) = 1\text{-normcdf}(\log_{10}(Y_{i,r}), \text{mean from Equation (1.10)}, 0.28) \quad (1.14)$$

$$P(y_{ij,\ \text{Sarma and Srbulov}} \geq Y_{i,r}) = 1\text{-normcdf}(\log_{10}(Y_{i,r}), \text{mean from Equation (1.11)}, 0.26) \quad (1.15)$$

$$P(y_{ij,\ \text{Ramazi}} \geq Y_{i,r}) = 1\text{-normcdf}(\ln(Y_{i,r}), \text{mean from Equation (1.13)}, 0.62) \quad (1.16)$$

4.1.3.Take the weighted average probability of exceeding Yi,r over all 3 attenuations

The weights for each of the three attenuation relation in Amiri et al. (2003) are 0.35, 0.25, and 0.4 respectively. Therefore, the weighted average of the exceedence probability for every earthquake *j*, at a certain control point *i*, for a specific return period *r* with a corresponding "true" ground shaking $Y_{i,r}$ calculated by equation (1.17). This value is used in Equation(1.2) of the paper as $P(y_{i,j} \geq Y_{i,r})$.

$$P(y_{ij} > Y_{i,r}) = 0.35*P(y_{ij,\ \text{Ambraseys and Bomme}}r > Y_{i,r}) + 0.25*P(y_{ij,\ \text{Sarma and Srbulov}} > Y_{i,r}) + 0.4*P(y_{ij,\text{Ramazi}} > Y_{i,r}) \quad (1.17)$$

4.2.Example

Consider census zones 1963 and 214 and earthquake 198 corresponding to the Maximum Credible Earthquake (MCE) for the fault Mosha (Figure 1-35) with surface magnitude (M_s) of 7.5. Assume we are calculating the exceedence probabilities for the 475-year return period map (r=475). Based on Amiri et al. (2003) the PGA for the zones 1963 and 214 in this map is 0.36g and 0.44g respectively ($Y_{1963,475}$ and $Y_{214,475}$). To do the calculations for these two zones, the shortest distance from the center of the zone to the fault is measured and the rest of the calculation is given equations (1.10) to (1.17) above.

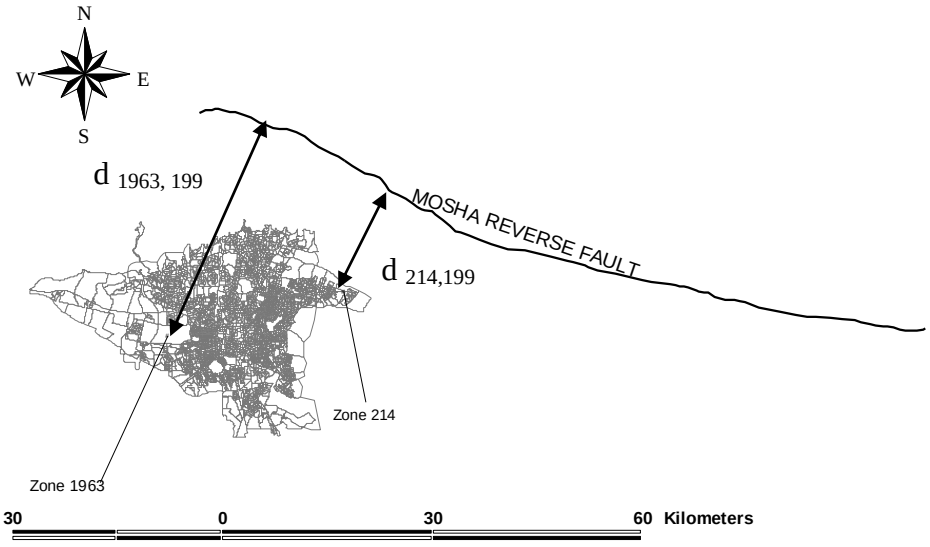

Figure 1-35 Census zones 214 and 1963 and their distances to Mosha fault

Distances $d_{1963,\,199}$ and $d_{214,\,199}$ are 30.09 and 15.62 kilometers respectively.

Step 1: The calculations for the mean values for the tree attenuation relationships are as follows:

(Ambraseys and Bommer, 1991):

Zone 1963: $\log_{10}(y_{1963,199}) = -1.09 + 0.238(7.5) - \log_{10}(30.6902) + 0 = -0.8073$

Zone 214: $\log_{10}(y_{214,199}) = -1.09 + 0.238(7.5) - \log_{10}(16.7327) + 0 = -0.5369$

(Sarma and Srbulov, 1996):

Zone 1963: $\log_{10}(y_{1963,199})$

$= -1.507 + 0.240(7.5) - 0.542\log_{10}(30.2471) - 0.00397*(30.2471) + 0 = -0.6275$

Zone 214: $\log_{10}(y_{214,199})$

$= -1.507 + 0.240(7.5) - 0.542\log_{10}(15.9055) - 0.00397*(15.9055) + 0 = -0.4203$

(Ramazi, 1999):

$Zone \quad 1963 : \ln(y_{1963,199})$

$= \ln(\frac{4000}{9.81*100}) - 2.11*\ln(20 + 30.098 + 17.0167) + 0.79(7.5) = -1.545$

$Zone \quad 214 : \ln(y_{1963,199})$

$= \ln(\frac{4000}{9.81*100}) - 2.11*\ln(20 + 15.62 + 18.6951) + 0.79(7.5) = -1.0986$

Step 2: The calculation of exceedance probabilities Based on equation (1.16) is as follows:

$P(y_{i,199,\text{ Ambraseys and Bommer}} \geq Y_{i,475})$

$= \begin{cases} \text{for zone 1963: 1-normcdf}(\log_{10}(0.36), -0.8073, 0.28) = 0.097 \\ \text{for zone 214: 1-normcdf}(\log_{10}(0.44), -0.5369, 0.28) = 0.2597 \end{cases}$

$P(y_{i,199,\text{ Sarma and Srbulov}} \geq Y_{i,475})$

$= \begin{cases} \text{for zone 1963: 1-normcdf}(\log_{10}(0.36), -0.6275, 0.26) = 0.2398 \\ \text{for zone 214: 1-normcdf}(\log_{10}(0.44), -0.4203, 0.26) = 0.4032 \end{cases}$

$P(y_{i,199,\text{ Ramazi}} \geq Y_{i,475})$

$= \begin{cases} \text{for zone 1963: 1-normcdf}(\ln(0.36), -1.545, 0.62) = 0.1993 \\ \text{for zone 214: 1-normcdf}(\ln(0.44), -1.0986, 0.62) = 0.3272 \end{cases}$

Step 3: The calculation of weighted average of exceedance probabilities is as follows:

$P(y_{i,199} \geq Y_{i,475})$

$= \begin{cases} \text{for zone 1963: } 0.35*0.097 + 0.25*0.2398 + 0.4*0.1993 = 0.1736 \\ \text{for zone 214: } 0.35*0.4032 + 0.25*0.3272 + 0.4*0.3272 = 0.3226 \end{cases}$

Notice that the exceedence probabilities are much higher for the zone closer to the source of the ground motion.

REFERENCES

Ambraseys, N., and Bommer, J., 1991. The attenuation of ground acceleration in Europe, *Earthquake Engineering and Structural Dynamics* 20(12), 1179-1202.

Amiri, G., Motamedi, R., and Rabet Es-Haghi, H., 2003. Seismic hazard assessment of metropolitan Tehran, Iran, *Journal of Earthquake Engineering*, 7(3), 347-372.

Anderson, J. G., 1997. Benefits of scenario ground motion maps, *Engineering Geology* 48, 43-57.

Bazzurro, P., and Cornell, C., 1999. Disaggregation of seismic hazard, *Bulletin of the Seismological Society of America* 89(2), 501-520.

Bazzurro, P., and Luco, N., 2005. Accounting for uncertainty and correlation in earthquake loss estimation, in *Proceedings, 9th International Conference on Structural Safety and Reliability (ICOSSAR'05)*, G. Augusti, G. Schuëller, M. Ciampoli (eds.), Rome, Italy, pp. 2687-2694.

Bender, B., and Perkins, D., 1987. *SEISRISK III, A Computer Program for Seismic Hazard Estimation*, U.S. Geological Survey, Bulletin 1772.

Çağnan, Z., Davidson, R., and Guikema, S., 2006. Post-earthquake restoration planning for Los Angeles electric power, *Earthquake Spectra* 22(3), 1-20.

Campbell, K., and Seligson, H., 2003. Quantitative method for developing hazard-consistent earthquake scenarios, in *Proceedings, Technical Council of Lifeline Earthquake Engineering, ASCE*, J. Beavers, (editor), Long Beach, Calif., pp. 829-838.

Chang, S., Shinozuka, M., and Moore, J., 2000. Probabilistic earthquake scenarios: Extending risk analysis methodologies to spatially distributed systems, *Earthquake Spectra* 16(3), 557-572.

Crowley, H., and Bommer, J., 2006. Modelling seismic hazard in earthquake loss models with spatially distributed exposure, *Bulletin of Earthquake Engineering* 4, 249-273.

Dodo, A., Xu, N., Davidson, R., and Nozick, L., 2005. Optimizing regional earthquake mitigation investment strategies, *Earthquake Spectra* 21(2), 305-327.

Ebel, J., and Kafka, A., 1999. A Monte Carlo approach to seismic hazard analysis, *Bulletin of the Seismological Society of America* 89(4), 854-866.

Federal Emergency Management Agency (FEMA), 2001. *FEMA 366: HAZUS Estimated Earthquake Losses for the United States*, Washington, D.C.

He, Y. 2006. *Earthquake Loss and Risk Estimation of Buildings by Monte Carlo Simulation*, Ph.D. dissertation, Department of Civil Engineering and Engineering Mechanics, Columbia University.

Ishikawa, Y., and Kameda, H., 1988. Hazard-consistent magnitude and distance for extended seismic risk analysis, in *Proceedings, 9th World Conference on Earthquake Engineering*, vol. 2, Tokyo.

Jain, V., and Davidson, R., 2007. Application of a regional hurricane wind risk forecasting model for wood-frame houses, *Risk Analysis* 27(1), 45-58.

Japan International Cooperation Agency (JICA), 2000. *The Study on Seismic Microzoning of the Greater Tehran Area in the Islamic Republic of Iran*, Final report to the Government of the Islamic Republic of Iran, Tokyo, Japan.

Kijko, A., 2000. Statistical estimation of maximum regional earthquake magnitude m_{max}, in *Workshop of Seismicity Modeling in Seismic Hazard Mapping*, Poljce, Slovenia, May 22-24.

Lee, J., Graf, W., Somerville, P., O'Rourke, T., and Shinozuka, M., 2005. *Developing a Hazard-Consistent Table of Earthquake Scenarios for Risk Analysis of the LADWP Water Systems*, Final Report to the Los Angeles Department of Water and Power.

McGuire, R., 1995. Probabilistic seismic hazard analysis and design earthquakes: Closing the loop, *Bulletin of the Seismological Society of America* 85(5), 1275-1284.

Ramazi, H., 1999. Attenuation laws of Iranian earthquakes, in *Proceedings of the 3rd International Conference on Seismology and Earthquake Engineering*, Tehran, Iran, pp. 337-344

Reiter, L., 1990. *Earthquake Hazard Analysis*. Columbia University Press, New York, 254 pp.

Rhoades, D., and McVerry, G., 2001. Joint hazard of earthquake shaking at two or more locations, *Earthquake Spectra* 17(4), 697–710.

Sarma, S. K., and Srbulov, M., 1996. A simplified method for prediction of kinematic soil-function interaction effects on peak horizontal acceleration of a rigid foundation, *Earthquake Engineering and Structural Dynamics*, 25(8), 815-836.

Tavakoli, B., 1996. *Major Seismotectonic Provinces of Iran*, International Institute of Earthquake Engineering and Seismology, Internal Document (in Persian).

Taylor, C., Werner, S., and Jakubowski, S., 2001. The walkthrough method for catastrophe decision making, *Natural Hazards Review* 2(4), 193-202.

United Nations (UN). 2002. *World Urbanization Prospects: The 2001 Revision*, New York.

Werner, S., Taylor, C., Cho, S., Lavoie, J-P., Huyck, C., Eitzel, C., Chung, H., and Eguchi, R., 2006. *REDARS2 Methodology and Software for Seismic Risk Analysis of Highway Systems*, Technical Manual. Prepared for the Multidisciplinary Center for Earthquake Engineering Research.

Wesson, R., and Perkins, D., 2001. Spatial correlation of probabilistic earthquake ground motion and loss, *Bulletin of the Seismological Society of America* 91(6), 1498–1515.

CHAPTER2 RESOURCE ALLOCATION FOR EARTHQUAKE RISK MITIGATION: CASE STUDY ON TEHRAN, IRAN

2.1 INTRODUCTION

There are many barriers to the adoption and implementation of regional earthquake risk mitigation plans, including for example, difficulty getting the issue on the political agenda, difficulty coordinating among multiple layers of government (local, state, and federal), and an apparent disconnect between who pays the costs of mitigation and who receives its benefits (e.g., Prater and Lindell 2000). Even if one had the will and complete authority to implement a comprehensive regional earthquake mitigation plan, however, for many reasons, it is difficult to know what to do. A large and diverse group of stakeholders is involved, each with different, sometimes competing objectives, constraints, and available strategies. Even a single stakeholder may have multiple competing objectives, including, for example, minimizing total costs, minimizing the chance of an extremely large loss, or ensuring that benefits that arise from mitigation investments are equitably distributed. There are an overwhelming number of possible mitigation alternatives, each with a different cost and effect on the risk. For example, FEMA (2003) groups mitigation alternatives into 6 categories: prevention, property protection, public education and awareness, natural resource protection, emergency services, and structural projects. Within each of those categories, in a given context, there are numerous combinations of alternatives. Focusing on structural upgrades, for example, one would still have to decide which of thousands of structures to upgrade, how, and when. The problem dimensions expand further because of the many types of impact an earthquake can have, including for example, deaths, injuries, structural damage, business interruption, environmental damage, and induced damage. Moreover, impacts across a region are spatially correlated, which should be considered because it affects the variability of total regional losses. The regional earthquake risk mitigation decision problem is also

highly uncertain and dynamic. There is substantial variability in possible mitigation investment outcomes because of the large uncertainty in earthquake occurrence. Because the return periods of damaging earthquakes are generally tens to hundreds of years, a long time horizon is required for analysis. Finally, an appropriate mitigation plan depends on the character of risk in the specific region of interest—what is driving it (e.g., frequent earthquakes, vulnerable structures) and what is "controllable." Each mitigation strategy targets a different aspect(s) of risk, so the best combination of efforts will be tailored to the issues particular to the region.

This paper describes a linear program designed to provide insight into these interactions and complexities of the regional earthquake risk mitigation decision problem and applies it to Tehran, Iran. Focusing on structural mitigation, the model addresses three main questions: (1) How much should be spent on pre-earthquake mitigation that aims to reduce future losses versus waiting until after an event and paying for reconstruction or simply not rebuilding damaged buildings?; (2) Which buildings should be mitigated and how?; and (3) Which buildings should be reconstructed and how? It builds on previously developed optimization models for regional earthquake mitigation resource allocation decision support, but as detailed in section 2.2, it extends those models to consider some particular issues that arise in seismically active developing countries like Iran. Section 2.2 summarizes the literature on modeling to support resource allocation for natural disaster risk management, and specifies how the model presented here extends that work. In section 2.3, the new optimization model formulation is presented, and the section 2.4 describes a case study application of the model for Tehran, Iran.

2.2 RESOURCE ALLOCATION FOR NATURAL DISASTER RISK MANAGEMENT

2.2.1 Previously developed models

Dodo et al. (2005) describes previous research related to resource allocation for natural disaster risk management by grouping it into four main approaches: Deterministic net present value (NPV) analysis, stochastic NPV analysis, multi-attribute utility models, and optimization models. Deterministic NPV (or benefit-cost), the simplest and most common method, involves simply (1) estimating the cost of implementing each mitigation alternative, (2) estimating the benefits of each mitigation alternative, where benefits are the losses avoided by implementing the alternative, and (3) comparing alternatives according to net present value or a similar criterion. Stochastic NPV is similar, except instead of a single point estimate, a probability density function of the benefits of each mitigation alternative is estimated, where the uncertainty is due to uncertainty in earthquake occurrence. A few studies have used multi-attribute utility theory or other decision criteria for analyses. Finally, while the first three previous approaches compare a small number of predefined mitigation alternatives, some studies have used optimization modeling, in which a set of mitigation alternatives is selected to maximize some stated objective(s) subject to constraints.

A few recent studies by two of the authors of this paper have used this optimization approach, which serves as the foundation for the new model described herein. Dodo et al. (2005) developed a linear program to support regional earthquake mitigation resource allocation and illustrated its use with a small case study area in Los Angeles County. The model determined which buildings—by structural type, occupancy type, and census tract location—should be upgraded so as to minimize total mitigation and expected post-earthquake reconstruction expenditures. Dodo et al. (2007) presented two efficient solution algorithms to solve the model for a realistic

application area. Davidson et al. (2005) extended this model to include the objective of ensuring equity among various groups of people in earthquake risk management. Xu et al. (2007) extended the original model into a stochastic optimization that explicitly models the *variability* in annual earthquake loss (and therefore net benefit of mitigation investments), allowing examination of the risk-return tradeoff between the original objective of minimizing the sum of mitigation and expected reconstruction expenditures, and a second objective to minimize the chance of an unacceptably large loss in any one earthquake. All of these models, and the one presented in this paper, focus on earthquakes and a regional (metropolitan area) public sector perspective, and share similar definitions of mitigation alternatives. They share key strengths of considering all possible earthquakes while capturing spatial correlation by using individual earthquake scenarios (as opposed to annual expected ground shaking); considering a very large set of mitigation alternatives; and allowing mitigation investments to occur over time as they do in real life (Dodo et al. 2005).

2.2.2 Comparison with the new model

This paper builds on the Dodo et al. (2005) optimization modeling approach, but modifies it in a few key ways with an eye towards applying the model in a highly seismically active developing country like Iran, in which economic resources may be more constrained, damage more widespread, and death tolls much higher than in the U.S. For example the five countries with greatest number of people killed by earthquakes between 1980 and 2000 are all from developing countries (Table 2-1). In comparison, countries in the developed world with comparable seismic activity have much lower fatalities. Japan with 23 events during this period had 5,626 casualties and United States with 10 events had only 130 deaths.

Table 2-1 Countries with greatest fatalities for earthquake 1980-2000 (UNDP, 2004)

Country Name	Number of events greater than 5.5 in Richter scale	Total number of people killed
Iran (Islamic Republic)	29	45,016
Armenia	1	23,810
Turkey	15	18,997
India	13	11,530
Mexico	15	8,545

To capture these differences, first, the model recognizes the likely possibility that limited economic resources will be available for post-earthquake reconstruction by incorporating budget limits, and although it is treated as a less desirable alternative, if economically necessary, allowing the possibility that some damaged buildings will not be reconstructed immediately. The model keeps track of any lost building inventory and allows it to be rebuilt at a later time when more funds are available. Second, the new model expands the set of possible mitigation alternatives to allow not just upgrading of a particular structural type, but a change in structural type as well. This is essential in the case of developing countries where many fatalities are due to non-engineered structures, such as adobe buildings, that can not be cost-effectively mitigated to a life safety performance level, and instead are best simply replaced by different structural types. Third, since a sound development plan will ideally use post-disaster reconstruction as an opportunity to introduce safer conditions, the model relaxes the assumption that all buildings should be reconstructed to their pre-earthquake condition, instead considering the possibility of reconstructing damaged buildings to any specified seismic design level and structural type. It also allows the decision maker to impose restrictions on mitigation and reconstruction decisions in case, for example, a certain design level or structural type is no longer allowed by the current building code. Finally, because death tolls may potentially be very high in a country like Iran, the model includes as one objective minimizing the chance of an extremely high death toll in any one earthquake (as well as minimizing the average

annual death toll across earthquakes). This involves inclusion of a risk-return tradeoff similar to that in Xu et al. (2007), but focusing on the risk of large life loss as opposed to large economic loss.

2.3 OPTIMIZATION MODEL

2.3.1 Scope

The mitigation alternatives considered in the new linear program are structural upgrading policies for groups of buildings. Buildings are grouped into categories based on their census zone locations, structural types (e.g., wood, steel), occupancy types (e.g., residential, hospital), and seismic design levels. One mitigation alternative is defined as upgrading some amount of building floor area (m^2) of a particular structural and occupancy type in a specified area unit (e.g., census zone) either from one seismic design level to another, or from one structural type to a more seismically resistant type (e.g., improving the design level of a steel structure or demolishing adobe structures and reconstructing them as reinforced concrete). Any area unit of analysis can be used without modifying the model formulation. The choice depends on data availability, computational demands, and a desire to choose a unit small enough that the hazard is relatively homogenous within it. From a computational perspective, modeling the decision variables as continuous variables (m^2 of floor area) instead of integers (number of buildings) produces a much simpler optimization and more appropriate one given the level of data available for regional planning. For clarity of discussion, the model is described in section 2.3.3 in terms of census zones, but in the case study, the area unit used is actually a cluster of census zones (Section 2.4.2).

The model assumes a finite set of earthquake scenarios with "hazard-consistent" annual occurrence probabilities can be identified to represent the region's seismicity as chapter one of this dissertation. This involves selecting a relatively small subset of all possible earthquakes and adjusting their annual occurrence probabilities so that each

of the subset of events represents all events "like that one" in terms of the frequency and distribution of ground motion it causes, and together the reduced set of events approximate the total regional seismic hazard, as described by *r*-year return period maps based on all possible events (first chapter of this dissertation). This model only deals with direct loss related to structural damage and deaths, not for example, indirect business loss. It also focuses only on structural upgrading and replacement as mitigation alternatives, not land use planning, insurance, or other types of alternatives. Population growth over time is not considered, and it is assumed that buildings' occupancy types do not change over time. Benefits and costs unrelated to earthquake risk are not considered. The migration of population is not considered in the model. The model does not allow the total floor area of each census zone exceed the initial value in the building inventory.

2.3.2 Modeling approach

Conceptually, the linear program is formulated to represent the evolving condition of the study area's building inventory, described in terms of the amount of floor area of each structural and occupancy type in each area unit (Figure 2-1).

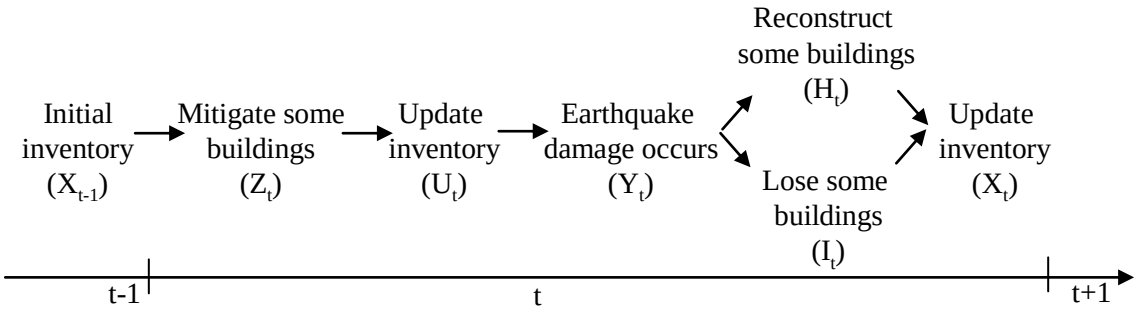

Figure 2-1 Evolution of building inventory in time period t, with variables used in model

In each time period, decisions are first made about which buildings to mitigate and how. Those decisions are implemented, and then the expected annual damage occurs,

calculated as the product of the expected damage given an earthquake and its hazard-consistent occurrence probability, summed over all possible earthquakes. The probability that a building of a given type enters a damage state after an earthquake is a function of the ground shaking at the site and the vulnerability of that structural type. While multiple damage states are possible in reality, given the precision of available data, it is assumed that only two damage states are possible: no damage and heavily damaged or collapsed. If desired, multiple damage states could be incorporated into the model as in Dodo et al. (2005). The model acknowledges that there may be insufficient resources to repair all the damage right away, and therefore the next decision is which buildings should be reconstructed and how (i.e., to which structural types and design levels). In other words, possible options after a building enters a damage state are to repair it to a specified structural type and design level or to not repair it at all, thus losing the floor area from the building inventory. The model keeps track of the cumulative floor area that is not reconstructed. This record of cumulative lost building inventory is updated after all reconstruction decisions are made. Finally, the state of the building inventory is updated for use in the beginning of the next time period.

2.3.3 Model formulation

Mitigation. Let $X^{c}_{ijk,t-1}$ be the floor area (m^2) of buildings at the end of time period *t-1* that are of structural type *i* and occupancy type *j*, are in census zone *k*, and are designed to seismic design level *c*. To simplify the notation, we defined *m* as a class of buildings in census zone *k* that are of occupancy type *j*. Without loss of generality, $X^{c}_{ijk,t-1}$ then becomes $X^{c}_{im,t-1}$. The first key decision to be made in the model is which buildings to mitigate and how. Let $Z^{i'c'}_{imct}$ be the floor area of buildings (m^2) of structural type *i*, in class *m*, designed to seismic design level *c* that are mitigated to

structural type *i'* and seismic design level *c'* during time period *t*. Then the mitigation decisions are represented by:

$$U_{imt}^{c} = X_{im,t-1}^{c} + \sum_{i'}\sum_{c'} Z_{i'mc't}^{ic} - \sum_{i}\sum_{c} Z_{imct}^{i'c'} \quad \forall i,m,t,c \tag{2.1}$$

where U_{imt}^{c} is the floor area (m^2) of buildings during time period *t* that are of structural type *i*, in class *m*, and designed to seismic design level *c*. Thus $X_{im,t-1}^{c}$ and U_{imt}^{c} describe the inventory at the beginning of the time step and after mitigation decisions have been implemented, respectively (Figure 2-1). Additional constraints are considered in the mitigation decisions. First, a building cannot be mitigated to a lower seismic design level. Second, buildings may not be mitigated to any structural type in a set Δ_Z of extremely seismically undesirable structural types (e.g., adobe), or in a set D_Z of undesirable design levels. Third, if the building inventory is partitioned into *N* mutually exclusive building type subsets (S_n, where $n \in (1,...,N)$), then change in structural type as a mitigation choice can be implemented between buildings within set S_n only. For example, if the subsets are low-rise and high-rise buildings as in the case study, then one could mitigate a low-rise building by replacing it with another low-rise structural type, but not a high-rise one. These constraints are represented by Equations (2.2) to(2.5):

$$Z_{imct}^{i'c'} = 0 \quad \forall m,t,i,i',c > c' \tag{2.2}$$

$$Z_{imct}^{i'c'} = 0 \quad \forall m,t,i,c,c',i' \in \Delta_Z \tag{2.3}$$

$$Z_{imct}^{i'c'} = 0 \quad \forall m,t,i,c,i',c' \in D_Z \tag{2.4}$$

$$Z_{imct}^{i'c'} = 0 \quad \forall m,t,c,c',i \in S_n, i' \notin S_n \tag{2.5}$$

Earthquake damage. If a_{im}^{cl} is the proportion of buildings of structural type *i*, class *m*, and seismic design level *c* that will be damaged if earthquake *l* happens, then

Y_{imt}^{cl}, the floor area (m^2) of buildings of structural type *i*, class *m*, and seismic design level *c* that are expected to be damaged in earthquake *l* in time *t* is:

$$Y_{imt}^{cl} = a_{im}^{cl} U_{imt}^{c} \quad \forall i,m,c,t,l \tag{2.6}$$

Reconstruction. As mentioned, one key component of the model that makes it more suitable for weaker economies or earthquakes causing more widespread damage is that it does not require the entire damaged inventory at every time period *t* to be reconstructed in the same time period. Let $H_{imct}^{i'c'}$ be the floor area (m^2) of buildings that were of structure type *i*, class *m*, and seismic design level *c* before they were damaged and are reconstructed as structural type *i'*, class *m*, and seismic design level *c'* in time period *t*. Let I_{imt}^{c} be the floor area (m^2) that are of structural type *i*, class *m*, and seismic design level *c* and are not reconstructed to any structure type by the end of time period *t*:

$$I_{imt}^{c} = I_{im,t-1}^{c} + \sum_{l} P^{l} Y_{imt}^{cl} - \sum_{i'} \sum_{c'} H_{imct}^{i'c'} \quad \forall i,m,t,c \tag{2.7}$$

As with mitigation decisions, some set of structural types (Δ_H) or seismic design levels (D_H) may be considered unacceptable options for reconstruction, perhaps because new seismic codes prohibit them. Thus,

$$H_{imct}^{i'c'} = 0 \quad \forall m,t,i,c,c',i' \in \Delta_H \tag{2.8}$$

$$H_{imct}^{i'c'} = 0 \quad \forall m,t,i,c,i',c' \in D_H \tag{2.9}$$

Moreover, similar to mitigation choices, if a unit area of a collapsed building is from a subset S_n, it should be rebuilt to a structural type from the same subset:

$$H_{imct}^{i'c'} = 0 \quad \forall m,t,c,c',i \in S_n, i' \notin S_n \tag{2.10}$$

After the effects of mitigation, earthquake damage, and reconstruction are determined, therefore, the total floor area (m^2) of buildings of structural type *i*, class *m*, and seismic design level *c* at the end of the time period *t* is given by:

$$X_{imt}^{c} = U_{imt}^{c} - \sum_{l} P^{l} Y_{imt}^{cl} + \sum_{i'} \sum_{c'} H_{i'mc't}^{ic} \quad \forall i,c,m,t \tag{2.11}$$

Budget. Recognizing financial realities, it is assumed that there is a maximum budget B_t to be spent in each period *t*. Let $F_{imc}^{i'c'}$ be the unit cost of mitigating a building of structural type *i*, class *m*, and seismic design level *c* to structural type *i'* and seismic design level *c'*. Let R_{im}^{c} be the unit construction cost of structural type *i*, class *m*, and seismic design level *c*. The decision of how to allocate the available budget between mitigation and reconstruction at every time period *t* is represented by:

$$\sum_{i} \sum_{m} \sum_{c} \sum_{i'} \sum_{c'} R_{im}^{c} H_{imct}^{i'c'} + \sum_{i} \sum_{c} \sum_{m} \sum_{i'} \sum_{c'} F_{imc}^{i'c'} Z_{imct}^{i'c'} \le B_t \quad \forall t \tag{2.12}$$

In practice, it may or may not be the case that mitigation and reconstruction expenditures are drawn from the same budget. Conceptually, however, there is a tradeoff between spending on pre-earthquake mitigation to reduce losses and post-earthquake reconstruction to repair damage and this constraint allows the user to examine that tradeoff. If desired, one could modify the formulation by defining separate mitigation and reconstruction budgets.

Risk of large death toll. A final constraint is included to represent the desire to guard against scenarios that would produce an unacceptably large number of casualties:

$$\sum_{i} \sum_{m} \sum_{c} \sum_{t} Y_{imt}^{cl} L_{im}^{c} - \gamma_{t}^{l} \le \kappa P \quad \forall t,l \tag{2.13}$$

where L_{im}^{c} is the expected number of people killed if a unit area (m^2) of building of structural type *i*, class *m*, and seismic design level *c* collapses; *P* is the study region's initial population; the user-defined parameter $\kappa \in [0,1]$ defines "large" death toll as a

percentage of the population; and γ_t^l is the number of deaths in earthquake *l* and period *t* beyond the threshold defining an unacceptably large death toll (κP). The following non-negativity requirements must also hold for the decision variables:

$$U_{imt}^c, X_{imt}^c, I_{imt}^c \geq 0 \quad \forall i,m,t,c \tag{2.14}$$

$$Z_{imct}^{i'c'}, H_{imct}^{i'c'}, \geq 0 \quad \forall i,c,m,t,i',c' \tag{2.15}$$

$$\gamma_t^l \geq 0 \quad \forall l,t \tag{2.16}$$

$$Y_{imt}^{cl} \geq 0 \quad \forall i,m,t,c,l \tag{2.17}$$

Objective. The objective of the model is to minimize the total mitigation cost, expected post-earthquake reconstruction cost, monetary value of the total expected loss of life, monetary value of total building inventory lost due to limited reconstruction resources, and risk of a large death toll, the terms in Expression (2.18), respectively.

$$Min \quad \sum_t \left(\begin{array}{l} \sum_i \sum_c \sum_m \sum_{i'} \sum_{c'} F_{imc}^{i'c'} Z_{imct}^{i'c'} + \sum_i \sum_m \sum_c \sum_{i'} \sum_{c'} R_{im}^c H_{imct}^{i'c'} \\ +\alpha \sum_i \sum_m \sum_c \sum_l P^l L^c{}_{im} Y_{imt}^{cl} + \sum_i \sum_c \sum_m V_{mict} I_{mict} + \mu \sum_l P^l \gamma_t^l \end{array} \right) \tag{2.18}$$

In this equation, α is the monetary value of a lost life; V_{imct} is the per-period, per unit floor area cost of not reconstructing buildings of structural type *i*, class *m*, and seismic design level *c*; and $\mu \geq 0$ represents a weight to characterize the relative importance of the objective of minimizing the chance of an extremely large death toll. A higher value of μ represents more risk aversion.

The final optimization model is a linear program in which the objective is given in Expression (2.18) and the constraints are given in Expressions (2.1) to(2.17). The model results indicate how to allocate the budget among mitigation ($Z_{imct}^{i'c'}$) and post-

earthquake reconstruction decisions ($H_{imct}^{i'c'}$); and how much lost building inventory (I_{imt}^{c}), how many deaths ($Y_{imt}^{cl}L_{im}^{c}$), and how many deaths over the "large death toll" threshold ($P^{l}\gamma_{t}^{l}$) are expected to result.

Input for the model can come from the region's census, engineering hazard and vulnerability studies, and user-defined parameters that represent the decision-maker's values. Table 2-2 summarizes the required input and where it came from for the case study analysis. It may be difficult to define "correct" values for the user-defined parameters and sensitivity analyses over a range of values will likely provide more insight.

Table 2-2 Summary of required input data and source of data for case study analysis

Variable	Description	Source
x_{im0}^{c}	Inventory of buildings of structural type *i*, class *m*, and seismic design level *c* at time 0	JICA (2000)
P	Initial population	JICA (2000)
R_{im}^{c}	Construction cost per unit area of structural type *i*, class *m*, and seismic design level *c*	Estimated by authors
$F_{imc}^{i'c'}$	Unit cost of mitigating a building of structural type *i*, class *m*, and seismic design level *c* to structural type *i'* and seismic design level *c'*	Estimated by authors
a_{im}^{cl}	Proportion of buildings of structural type *i*, class *m*, and seismic design level *c* that is expected to collapse or be heavily damaged in earthquake *l*	First chapter method
P^{l}	Per-period "hazard-consistent" occurrence probability of earthquake scenario *l*	First chapter method
V_{imct}	Per unit floor area cost of not reconstructing buildings of structural type *i*, class *m*, and seismic design level *c* at the end of time period *t*	Estimated by authors
L_{im}^{c}	Expected number of deaths if a unit of floor area of building of structural type *i*, class *m*, and seismic design level *c* collapses	Applied JICA (2000) method
μ	Penalty term in the objective function for solutions with an extremely large death toll	User-defined
κ	Percentage of the population that defines an extremely large death toll	User-defined
α	Monetary value of a lost life	User-defined
B_t	Available budget in period *t*	User-defined
Δ_H, Δ_Z D_H, D_Z S_n	Sets of prohibited structural types and design levels, and building type subsets	User-defined

2.4 CASE STUDY

2.4.1 Scope

To demonstrate application of the model, a case study analysis was conducted for Tehran, the capital and political and economic center of Iran, one of the most earthquake prone countries in the world. Tehran is located at the foot of the Alborz Mountains, which form part of the Alps-Himalayan Orogenic Zone. It is a highly seismic area surrounded by many active faults. Tehran's population has exploded in recent decades, growing from 1 to 7 million from 1950 to 2000 (UN 2002). Figure 2-2 shows the location of Tehran and its surrounding faults.

The case study analysis focuses on the ground shaking hazard, but the analysis could be refined by including the effects of liquefaction, landslide, or other collateral hazards with no or only minor modifications to the model formulation. For consistency, all monetary values and results are presented in terms of US dollars, using the 2005/06 IMF exchange rate of 9,026 Rials per US dollar (IMF 2007).

2.4.2 Input data

In the case study analysis, it was assumed that the time step is one year and the time horizon is 30 years. Part of the expected benefit from available mitigation and reconstruction options at every year depends on the number of remaining years for the city to enjoy those benefits. Therefore, to sustain incentive for the model to continue reconstruction or mitigation until the last years model is run for 60 years and the results for the first 30 years are presented. The set of earthquake scenarios assumed to represent the regional seismicity were the 14 earthquakes identified in the first chapter of this dissertation, 4 maximum credible earthquakes on specified faults and 10 other historical earthquakes. They are presented with their hazard-consistent annual occurrence probabilities in Figure 2-3 and Table 2-3. The 15^{th} scenario is the no-earthquake scenario with annual probability of 0.50.

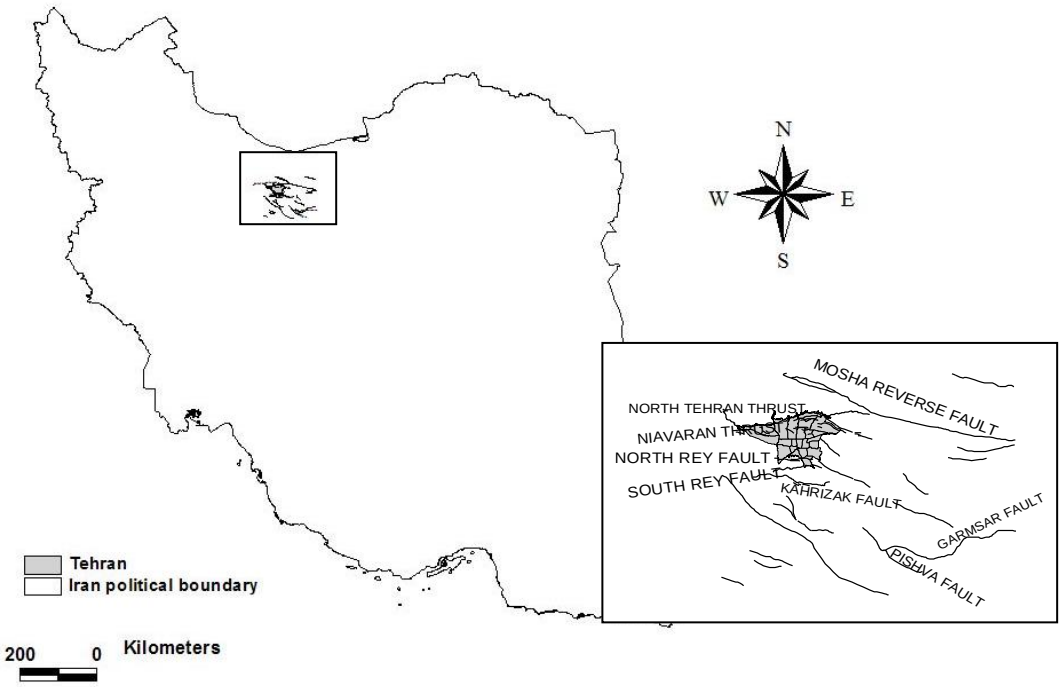

Figure 2-2 Tehran's location and its surrounding faults

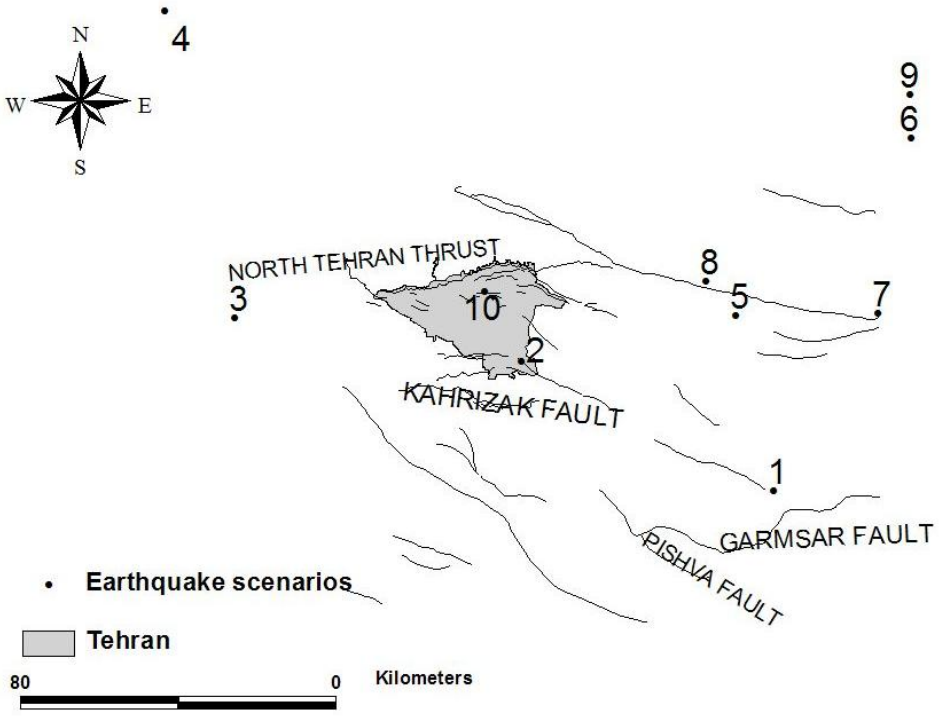

Figure 2-3 Geographic distribution of earthquake scenarios considered in case study

Table 2-3 Hazard-consistent annual occurrence probability and magnitude of the earthquake scenarios considered in the case study (Source: results from the first chapter)

EQ ID or fault name	Magnitude	Hazard-consistent probability
1	7.1	0.05
2	7.0	0.0003
3	7.1	0.029
4	7.6	0.05
5	6.4	0.05
6	6.6	0.05
7	7.0	0.05
8	5.4	0.05
9	6.7	0.0484
10	4.1	0.0083
11 Garmsar MCE[a]	6.9	0.05
12 Kahrizak MCE	6.6	0.0037
13 North Tehran MCE	6.9	0.0057
14 Pishva MCE	6.5	0.05

[a] MCE = Maximum credible earthquake

According to the 1996 census survey, Tehran is divided into 3,173 census zones (Figure 2-4). The case study covers only 3,070 census zones from the total due to limited ground motion data availability. To reduce the computational intensity of the example, the analysis unit of the model was taken to be clusters of contiguous census zones that experience similar ground motions. Clusters were formed such that for each earthquake *l*, the difference in ground motion between census zones within a cluster is no more than 0.03g, a difference that would have little effect on the estimated damage. The population and building statistics of the zones were summed to create the data for clusters. The ground motion of the clusters was assumed to be the weighted average of its component zones, where weights are the number of inhabitants of each zone. The 3,070 census zones were aggregated into 119 clusters, $k \in (1,...,119)$ (Figure 2-4).

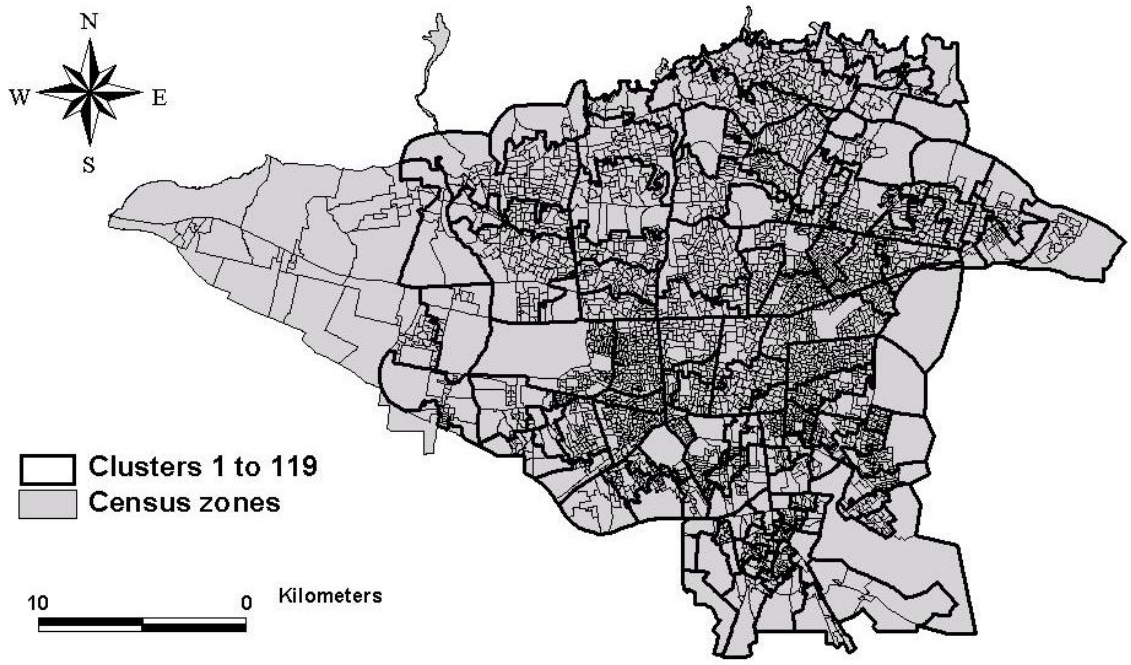

Figure 2-4 Census zones and census zone clusters used in case study

The statistical data on population and building inventory used in this case study were extracted from the data collected as part of a microzoning study of the Greater Tehran Area conducted by the Japan Cooperation International Agency (JICA) for the government of Iran (JICA 2000). Our study includes one occupancy type—residential (j=1), and 9 structural types, $i \in (1,...,9)$ (Table 2-4). Residential was the only occupancy type for which a complete set of data was available. Within the study area, there are 270 million m^2 of building floor area and P=6.3 million residents. JICA (2000) provided the population distribution among structural types and census zones, and it was assumed that the number of people per m^2 is constant across structural types and census zones so that the same distribution is true for floor area (Table 2-4). For each structural type, two seismic design levels were considered, $c \in (1,2)$, not mitigated and mitigated.

Table 2-4 Structural types in the case study with population distribution and unit mitigation and reconstruction costs in US dollars

Structural type i[a]	Description	High- or low-rise (S_n)[b]	Population (%)[c]	Unit mitigation cost ($F_{imc}^{i'c'}$)[d]	Unit reconst-ruction cost (R_{im}^{c})[d]
1. All wood (AW)	All wood	Low	0.1%	78	N/A[e]
2. Block and brick (BB)	Cement block (with any type of roof), brick and wood or stone and wood, all brick or stone and brick	Low	3.2%	100	166
3. Brick and steel (BS)	Brick and steel, or stone and steel	Low	46.2%	78	166
4. Reinforced concrete-0 (RC0)	Reinforced concrete, with more than 6 stories	High	1.9%	122	332
5. Reinforced concrete-1 (RC1)	Reinforced concrete, built after 1991 and with 1 or 2 stories	Low	0.8%	122	332
6. Reinforced concrete-2 (RC2)	Reinforced concrete, built before 1991 or with more than 3 stories	High	7.6%	122	332
7. Steel-1 (S1)	Steel, built after 1992, with 1 to 3 stories	Low	4.4%	133	332
8. Steel-2 (S2)	Steel, built before 1991 or with more than 4 stories	High	34.8%	122	332
9. Sun dried brick (SDB)	Sun-dried mud brick and wood, sun-dried mud brick and mud	Low	1.1%	N/A	N/A

[a] Structural type definitions and population distribution are from JICA (2000).
[b] Authors decided to consider each structural type to be high-rise or low-rise buildings.
[c] We assume the number of people per m^2 is constant, so the percentages in this column are the same for floor area.
[d] Unit mitigation and reconstruction costs were estimated by M. Hosseini.
[e] N/A means mitigation or reconstruction is not allowed for the associated structural type.

Figure 2-5shows the vulnerability curve for each structural type from JICA (2000). As in the JICA study, the ground shaking on the x-axis was converted from Modified Mercalli Intensity (MMI) to peak ground acceleration (PGA) using the formula in Trifunac and Brady (1975). To estimate the required input values a_{im}^{cl} (i.e., the proportion of buildings of structural type *i*, class *m*, and seismic design level *c* that will be damaged if earthquake *l* happens), three attenuation relationships were applied to

estimate the ground shaking at the centroid of each census zone *k* given earthquake *l*, and a weighted average of the resulting three PGA values was calculated (as in first chapter of this dissertation). The weighted average of PGA values for all census zones in a cluster was used to estimate the PGA for the cluster, and that value was then used with the vulnerability curves in Figure 2-5 to estimate the probability of damage in the cluster for each structural type *i*.

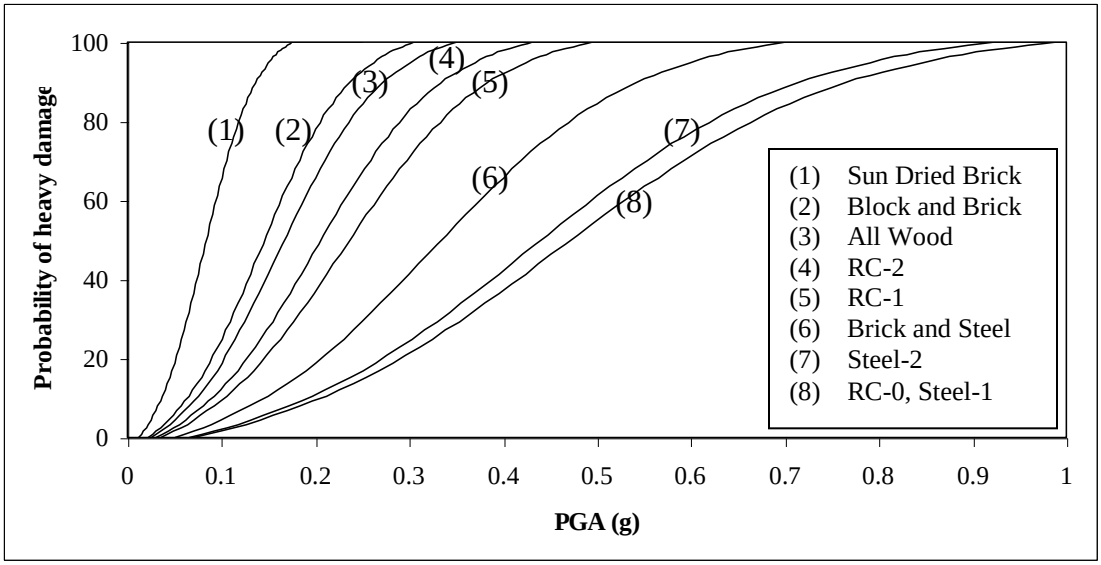

Figure 2-5 Vulnerability functions of residential structural types in the case study

Assuming mitigation and reconstruction costs vary by structural type but not census zone, and assuming that only one type of mitigation is possible, unit mitigation, $F_{imc}^{i'c'}$, and unit reconstruction costs, R_{im}^{c}, were estimated as in Table 2-4. The estimations are based on expert judgment from the International Institute of Earthquake Engineering and Seismology of Tehran, Iran. The effect of mitigation was defined as a rightward shift in the fragility curve of the specified structural type so as to double the PGA necessary to reach the same damage ratio.

Additional constraints were introduced to the model to make the set of mitigation and reconstruction alternatives more realistic. First, it was assumed that *Sun dried*

brick is an unacceptably weak structural type that is not an option for mitigation or reconstruction, and *All wood* is not acceptable for reconstruction because there is little wood available for construction in Tehran currently (i.e., $\Delta_Z = 1, \Delta_H = 2$). Second, structural types were divided into low-rise and high-rise (N=2), and it was assumed that demolishing a building from one category and reconstructing it to a structural type from the other category was not an option. High-rise includes structural types *Reinforced concrete-0*, *Reinforced concrete-2*, and *Steel-2*; low-rise includes the remaining structural types (Table 2-4).

Casualties were estimated as in JICA (2000) as a simple function of the number of collapsed buildings, number of people per building, occupancy at the time of the earthquake, percentage of occupants trapped by collapsed buildings, percentage of occupants killed immediately by building collapse, and percentage of injured that subsequently die before rescue. It was assumed that the earthquakes occur at night and no rescue is available. Other casualty scenarios could be incorporated with no modification in the model. The resulting values of L_{im}^{c} (expected number of people who will be killed if a unit area (m^2) of building of structural type i, class m, and seismic design level c collapses) are from 0 to 0.02. Note that because the model assumes that the number of people per m^2 remains constant, if the total building inventory decreases due to delayed reconstruction, it is implicitly assumed that the population declines as well, reducing future deaths as well (see Section 2.4.3.6). If desired, alternative assumptions could be made, such as assuming the city population remains constant and people will crowd into remaining buildings when some are not rebuilt, or adding a temporary structural type to house people displaced by earthquake damage.

The cost of lost building inventory was assumed to be three times the reconstruction cost of the same building type, assuming that it is less desirable to leave

inventory un-built than to reconstruct it right away. The lifetime of each building was assumed to be 30 years, so that a per-period value of $V_{imct} = 3R_{im}^{c} / 30$ could be estimated. Depending on data availability, other factors such as indirect economic losses, loss of income, relocation costs, and rental losses could be the basis for estimating this parameter. In the base case analysis, the user-defined parameters were assumed to be $\mu = 1$, $\kappa = 0.0001$, and $\alpha = US\$33,200$. Based on the 2005 Iran national report (Iran 2005b), Iran spends 2.5% of its annual budget on disaster reduction and mitigation efforts. Assuming half of this budget is allocated to earthquake risk reduction, since Tehran accounts for about 26% of Iran's GDP, and the total national 2005 budget was about 1600 trillion Rials (Iran 2005a), we estimate a base case annual budget of $B_t = US\$573$ million for all *t*.

2.4.3 Results

The linear optimization model was solved using AMPL software, with CPLEX by ILOG. The results from the model can be used to answer many questions, including: (1) How much should be spent on mitigation each year, and given those mitigation expenditures, as earthquakes occur, how much should be spent on reconstruction and how much building inventory should be allowed to not be rebuilt?; (2) Which buildings should be mitigated and how?; (3) Which buildings should be reconstructed and how, and which should not be rebuilt?; and (4) How do the time horizon, budget, and death risk aversion parameter (μ) affect the recommendations? Dissecting the results and investigating these and other questions can provide insight into the many tradeoffs in the regional earthquake risk mitigation problem. One can examine the tradeoffs between desires to minimize, for example, expenditures, the chance of a large death toll, and lost building inventory. One can also begin to understand the complicated, interacting influences of the different geographic patterns of ground shaking caused by the many possible earthquakes, distribution of the building

inventory across structural types, vulnerability of different structural types, budget constraints, and mitigation and reconstruction costs.

2.4.3.1 Recommended expenditures over time

Figure 2-6 shows the recommended expenditures by year for the base case analysis. It suggests that for the first six years, the total annual budget should be spent on mitigation. After year 6 the total annual budget should be spent on reconstruction. In the last seven years, the reconstruction expenditures drop by almost half because there is no remaining accumulated lost building inventory to reconstruct during those years. In those years, all the damage is reconstructed within the same year and almost half of the annual budget remains unspent.

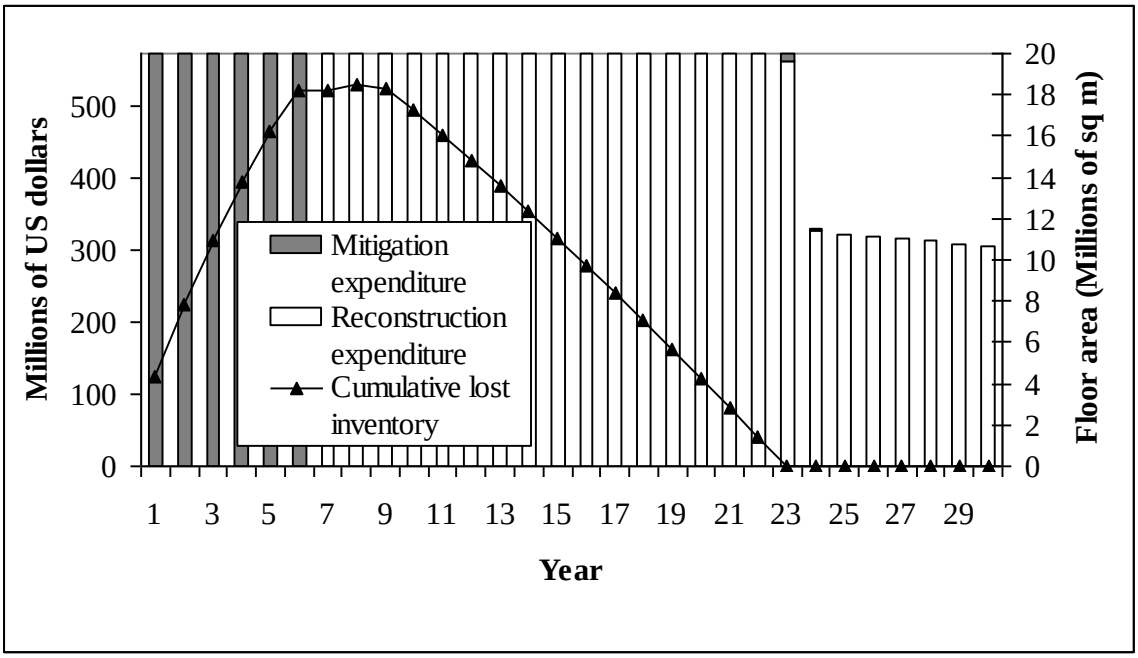

Figure 2-6. Recommended expenditures and total cumulative lost building inventory for base case

In the base case, the model recommends spending on mitigation only for the first 6 years for two reasons. First, as Figure 2-6 shows, while money is spent on mitigation and not reconstruction, the floor area of buildings that are not rebuilt accumulates.

After six years, the objective to minimize lost inventory becomes relatively more important, requiring that spending switch from mitigation to reconstruction. Second, after the cumulative lost inventory gets to zero (year 23) no mitigation is recommended because there is not enough time left in the time horizon to reap the benefits of mitigation. This is illustrated by Figure 2-7 which shows the recommended expenditures by year for the base case if the model is rerun with a 50-year time horizon instead. In this case, when the lost inventory goes to zero in year 23, the balance shifts back and it is then useful to spend on mitigation again for about 7 more years.

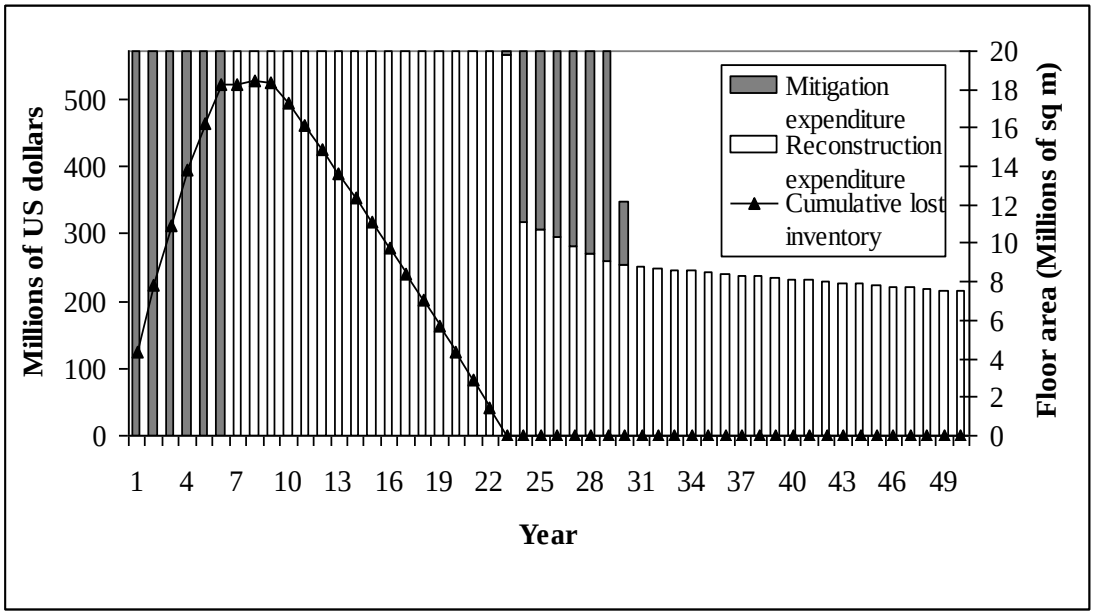

Figure 2-7 Recommended expenditures and total cumulative lost building inventory for base case for planning horizon of 50 years

There are also differences between the mitigation choices in the two runs with different time horizons. First, in the case of the 50-year time horizon, amount of mitigated *Reinforced concrete-1* increases by 2.4 times but *All wood* buildings are mitigated ten percent less in the initial periods because the longer planning horizon makes the more expensive investment more cost-effective. Second, in years 22 to 30,

the model switches back to mitigating stronger structural types that were not an appealing choice in the 30-year case in comparison with the benefits obtained from reconstructing the lost inventory. Figure 2-8 illustrates the total mitigated floor area in the two runs. In the 50-year time horizon, a significant amount of *Brick and Steel* and *Steel-2* are mitigated in the later years of planning horizon. As explained in Section 2.4.3.2, these structural types are among the least vulnerable types and therefore the expected reduction in damage is not as appealing in the beginning of the planning horizon in tradeoff with accumulation of lost inventory.

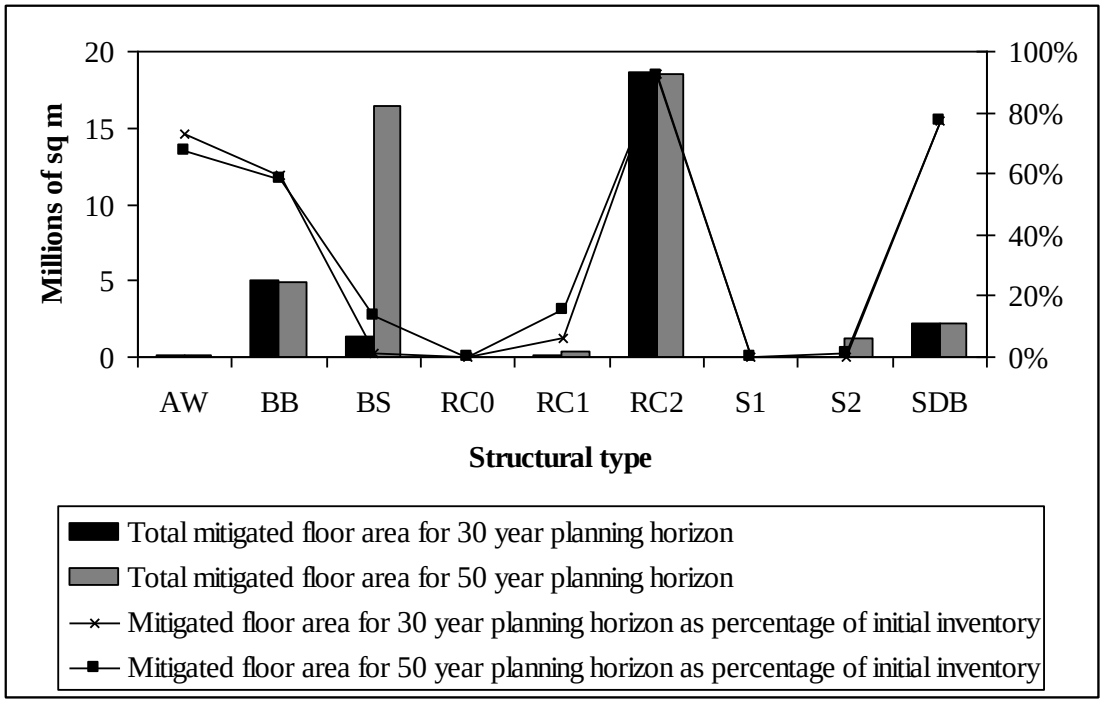

Figure 2-8 Recommended mitigation choices for base case for planning horizons of 30 and 50 years. Structural types are: *All wood* (AW), *Block and brick* (BB), *Brick and steel* (BS), *Reinforced concrete-0* (RC0), *Reinforced concrete-1* (RC1), *Reinforced concrete-2* (RC2), *Steel-1* (S1), *Steel-2* (S2), and *Sun dried brick* (SDB).

2.4.3.2 Mitigation choices

One would expect the choice of which structural types to mitigate would depend on a combination of factors including the relative prevalence of different types in the

initial inventory, the relative levels of ground shaking the different types experience (which depends on their locations relative to the possible earthquakes), the relative improvement in building performance achieved by mitigation, and their relative vulnerabilities and unit mitigation costs. Figure 2-9 shows the recommended total mitigation area by initial and final structural type.

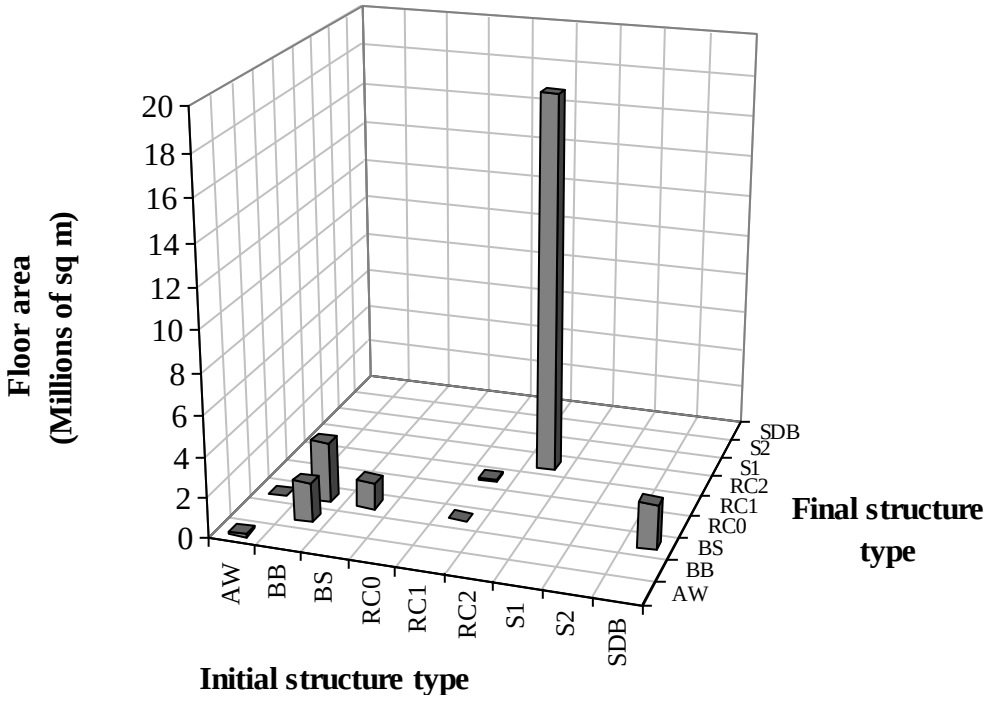

Figure 2-9 Recommended mitigation expenditures by initial and final structural type for base case. Structural types are: *All wood* (AW), *Block and brick* (BB), *Brick and steel* (BS), *Reinforced concrete-0* (RC0), *Reinforced concrete-1* (RC1), *Reinforced concrete-2* (RC2), *Steel-1* (S1), *Steel-2* (S2), and *Sun dried brick* (SDB).

It suggests that mostly *Reinforced concrete-2* should be mitigated. Most of the building inventory is *Brick and steel* (46%) and *Steel-2* (35%), but those are two of the least vulnerable structural types (within their respective subgroups of low-rise and high-rise). *Reinforced concrete-2* is the next most common structural type (8%) and is much more vulnerable (Figure 2-5), so it is an appealing target for mitigation. The choice of which structural types to mitigate seems to be driven largely by their relative

vulnerability. For each the four most vulnerable structural types (*Sun dried brick*, *Block and brick*, *All wood*, and *Reinforced concrete-2*), 59% to 92% of the initial inventory is mitigated; whereas for the five least vulnerable structural types, only 0% to 6% is.

The structural types selected for the buildings to be mitigated to are a function of the constraint that they must be the same height group (low or high rise) as the initial structural type, and a desire to choose a structural type with both low vulnerability (Figure 2-5) and low mitigation cost (Table 2-4). All *Reinforced concrete-2* is mitigated to *Reinforced concrete-2*. Although mitigating to *Reinforced concrete-0* or *Steel-2*, the other high-rise types, which are much less vulnerable, would also have been possible, they would have cost $\$332/m^2$ instead of $\$122/m^2$, and thus were not cost-effective. Similarly, *Brick and steel* could have been mitigated to *Steel-1*, which is also low-rise and less vulnerable, but it would have been more expensive ($\$332/m^2$ instead of $\$78/m^2$). *All wood*, *Block and brick*, and *Reinforced concrete-1* are all mitigated partly to their original structural type, and partly to *Brick and steel*, which is also low-rise and is less vulnerable though more expensive. With a larger available annual budget, however, *Brick and steel* would be chosen more often (Figure 2-12). Finally, the model does not allow *Sun dried brick* to be upgraded within the same structural type; so instead, it is mitigated by rebuilding it as *Brick and steel*, the most cost-effective, low-rise alternative.

Mapping the area mitigated per m^2 of initial inventory does not reveal any geographic pattern. The structural types (which determine vulnerability and unit mitigation cost) are distributed throughout the city, and the hazard does not exhibit strong enough geographic variability to dominate the pattern. Trying to understand the combination of mitigation strategies selected makes it clear that a number a factors interact in a complex way to determine the relative appeal of different available

mitigation alternatives. It would be impossible to anticipate what the recommended strategy should be ahead of time, without such a model.

2.4.3.3 Reconstruction choices

In this model, unlike Dodo et al. (2005), the decision maker is given the option of not rebuilding some collapsed inventory immediately if the budget is not available to do so effectively. Floor area in the initial inventory then can evolve in several different ways. It can remain unchanged, be mitigated to a higher seismic design level or a different structural type, collapse and be reconstructed in the same or another structural type, or collapse and not be reconstructed. Figure 2-10 summarizes the reconstruction choices recommended by the model for the base case analysis, by structural type reconstructed from and to.

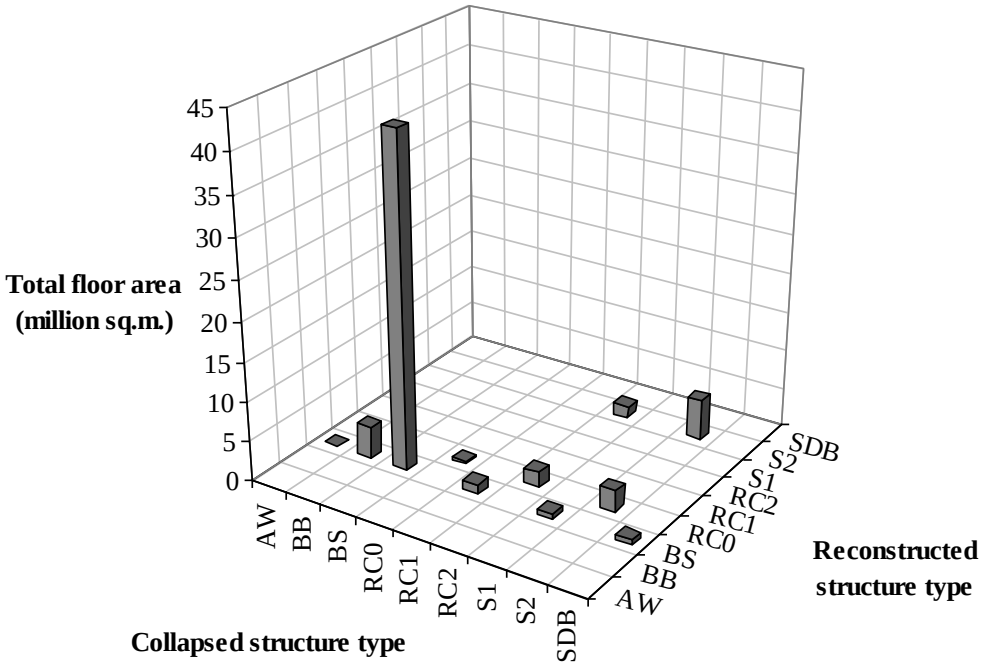

Figure 2-10 Recommended reconstruction expenditures by initial and final structural type for base case. Structural types are: *All wood* (AW), *Block and brick* (BB), *Brick and steel* (BS), *Reinforced concrete-0* (RC0), *Reinforced concrete-1* (RC1), *Reinforced concrete-2* (RC2), *Steel-1* (S1), *Steel-2* (S2), and *Sun dried brick* (SDB).

Since no cumulative lost inventory remains at the end of the base case analysis (Figure 2-6), all damaged buildings are eventually reconstructed. Most damaged

buildings are *Brick and steel* because they make up most of the building inventory (46%), and the other most common structural type, *Steel-2* (35%) is one of the least vulnerable. The decision of which structural types to reconstruct to is similar to the decision of which structural types to mitigate to, except that in mitigation, there is a bias towards retaining the same structural type, which tends to be less expensive than tearing a building down and reconstructing it as a different type (unit mitigation costs are $\$78/m^2$ to $\$133/m^2$; unit reconstruction costs are $\$166/m^2$ to $\$332/m^2$;Table 2-4). For the base case analysis, the model recommends that all low-rise structural types be reconstructed as *Brick and steel*, because it is the most cost-effective low-rise type (*Steel-1* is less vulnerable, but twice as expensive). The model recommends that all high-rise structural types be reconstructed as *Reinforced concrete-0* or *Steel-2*, which have almost identical vulnerabilities and reconstruction costs. *Reinforced concrete-2* is never chosen because it is more vulnerable and equally expensive.

2.4.3.4 Sensitivity to budget

Keeping all other parameters at their base case values, Figure 2-11 shows the recommended mitigation and reconstruction expenditures as a function of available annual budget. As the annual budget increases, a few things happen. First, mitigation expenditures increase suggesting that if more money is available, more should be spent on mitigation. Second, reconstruction expenditures increase as well, but then begin to decline above an annual budget of about $573 million as less accumulated lost inventory is available to be reconstructed. Similarly, the total expenditures increase, but then level off with reconstruction spending, leaving an increasing percentage of the annual budget unused. At the highest budget levels considered, it is not cost-effective to spend more on mitigation even if more funds are available.

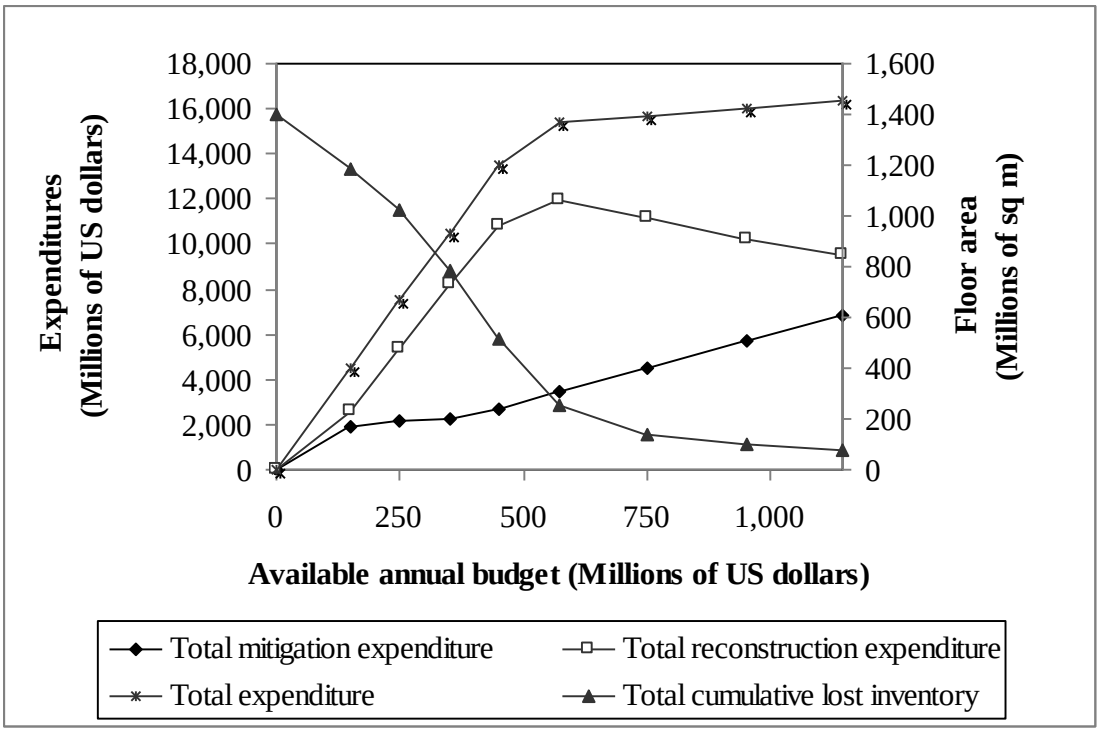

Figure 2-11 Sensitivity of recommended expenditures to available annual budget

The total cumulative lost building inventory decreases with annual budget because with more funds available, one can avoid postponing reconstruction, which is more expensive than reconstructing immediately after an earthquake due to the V_{imct} parameter (Figure 2-11). In addition, with more funds, reconstruction choices tend towards less vulnerable (but more expensive) structural types, which help reduce the cumulative lost inventory faster. Interestingly, the annual expected number of deaths declines as the budget increases. As the annual budget increases from \$150 million to \$1,145 million, the annual expected number of deaths declines from 1,655 to 1,502 (9%); whereas the cumulative lost inventory declines from 1,182 million m^2 to 79 million m^2 (93%). It is more difficult to eliminate all casualties than all lost inventory (especially when the death risk aversion parameter μ is small, as in the base case).

Figure 2-12 shows the sensitivity of mitigation choices to available annual budget. For the most part, as more funds are available, additional structural types are simply

added to the mitigation portfolio. In some cases, however, the strategy changes with the addition of more funds. For example, at an annual budget of $450 million, *Block and brick* buildings are mitigated to *Block and brick* (at a cost of $\$100/m^2$), but at an annual budget of $573 million, one can afford the $\$166/m^2$ required to mitigate *Block and brick* to *Brick and steel* instead, a less vulnerable structural type. When funds are limited, the priority is to mitigate *Reinforced concrete-2*. Although it is less vulnerable and more expensive to mitigate than *Block and brick*, for example, it is also much more expensive to reconstruct than *Block and brick* if it should collapse, and thus the benefit of the mitigation (avoided loss) is greater for *Reinforced concrete-2*.

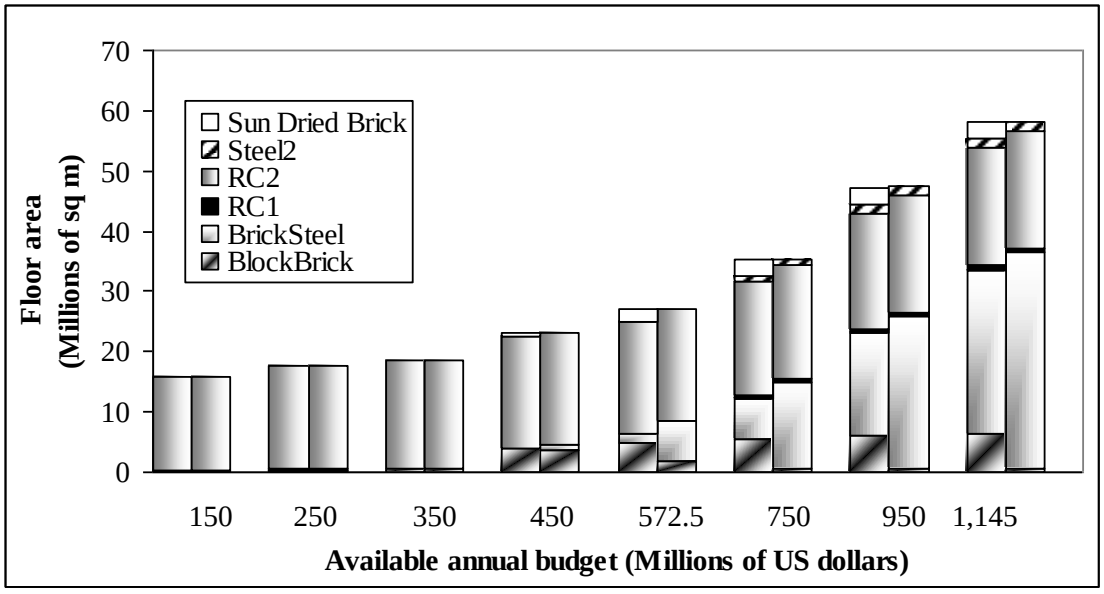

Figure 2-12 Sensitivity of mitigation recommendations to available annual budget, by initial structural type (left column) and final structural type (right column).

2.4.3.5 Sensitivity to death risk aversion parameter

As the death risk aversion parameter μ increases, indicating increased importance of the objective to minimize the chance of a large death toll, the model has two mechanisms to reduce the death toll. It can spend more money on mitigation (reconstruction does nothing to reduce life loss). Or it can increase the cumulative lost

inventory, which allows more money to be spent on mitigation and reduces the population exposed to earthquake damage since the model assumes that the population is proportional to the available building floor area (Section 2.4.2) (Figure 2-13).

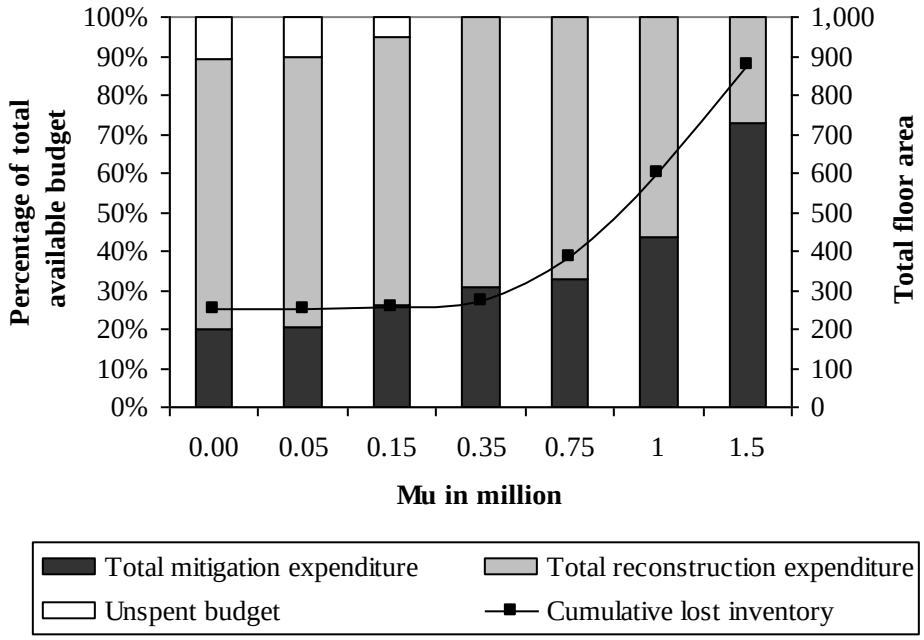

Figure 2-13 Sensitivity of recommended expenditures to risk parameter μ

Increasing the cumulative lost inventory comes at a cost (reflected in the V_{imct} parameter), since a city might not want to encourage emigration. Nevertheless, the model recommends both strategies, especially when the objective of reducing the chance of a large death toll becomes important, above about μ=0.35 million (Figure 2-13).

As discussed in Section 4.3.1, at μ=0 in the base case analysis, 10% of the total budget over the 30-year time horizon remains unspent because reconstruction in the last seven years declines when the cumulative lost inventory goes to zero. As μ increases, however, the unspent budget decreases to zero because it becomes increasingly important to reduce the possibility of large death toll through mitigation, even if that requires using mitigation alternatives that were considered less cost-effective at lower μ values (Figure 2-13).

As μ increases, the model recommends mitigating more, but mostly selects similar structural types. There are small changes, however. For example, when μ=0, a small amount of floor area is mitigated to *Block and brick*, but as μ increases above 0.35 million, it does not anymore because that structural type is too vulnerable and too likely to contribute to future deaths. Similarly, as μ increases and cumulative lost inventory is allowed to accumulate, less total area is reconstructed, but μ does not have a large effect on the structural types damaged buildings are reconstructed to.

Another interesting issue to explore is the effectiveness of different strategies in particular future earthquakes. That is, what should be expected in terms of number of deaths and damage, if one follows a recommended strategy for a specified μ, and then a particular earthquake occurs in Year 31? Figure 12 shows these results for the three most deadly earthquakes, which account for about 14%, 68%, and 16% of the annual expected number of deaths, respectively. For example, if one follows the strategy recommended when μ=0, all of the initial inventory would remain at the end of the time horizon in Year 30, but if Earthquake 2 occurred in Year 31, 702,000 deaths would result and 287 million m^2 of floor area would be damaged. On the other hand, if one follows the strategy recommended when μ=1.5 million, only 89% of initial inventory would remain in Year 30, but if Earthquake 2 occurred in Year 31, 59% as many deaths (415,565) would occur and 362 million m^2 of floor area would be damaged. Increasing μ from 0 to 1.5 million reduces the number of deaths by 41%, but does so not just by mitigating, but also by reducing the available inventory (and therefore the population). If instead, the North Tehran MCE or Kahrizak MCE occurred in Year 30, the death-lost inventory tradeoff would be less dramatic (Figure 2-14). This analysis demonstrates again that with a strong emphasis on minimizing deaths under fixed budget, the model suggests not rebuilding at all

because it cannot be done in a way that provides adequate life safety under a limited budget.

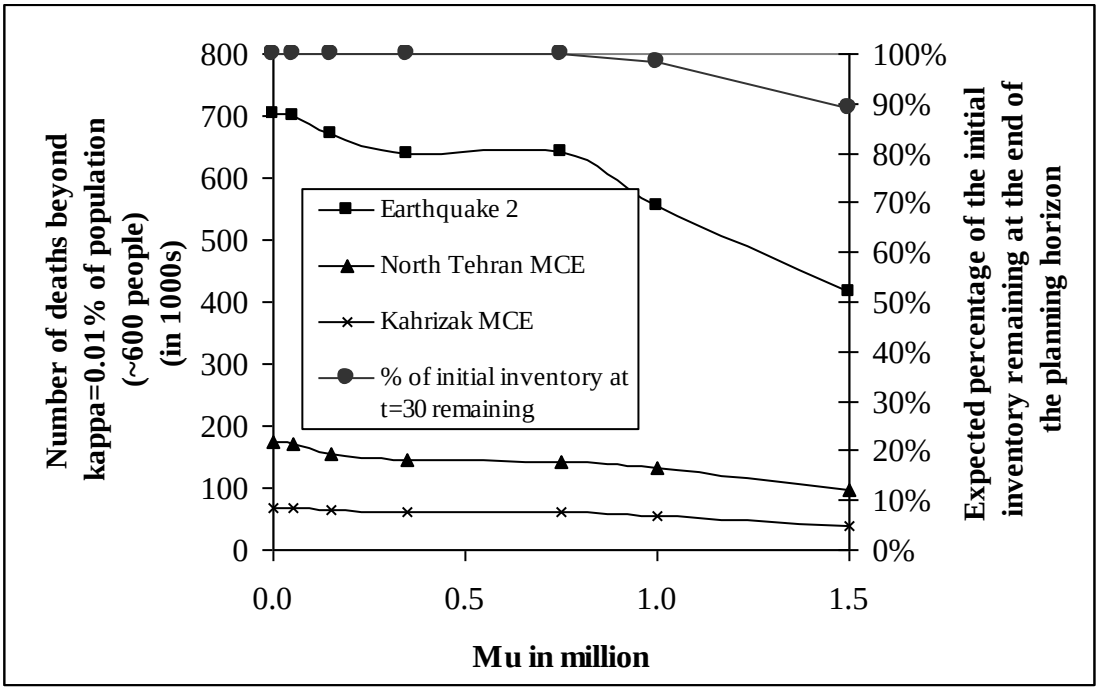

Figure 2-14 Sensitivity of death toll to risk parameter μ

2.5 CONCLUSIONS

Regional earthquake mitigation planning is difficult because the problem is characterized by multiple, competing objectives; numerous alternative courses of action; several different types of impact (e.g., deaths, economic loss); spatial correlation among the impacts; substantial uncertainty; dynamism; and dependence on the character of risk in the specific region of interest. In this paper, a linear program is developed to help explore these issues, and is applied to Tehran, Iran. The linear program builds on previously developed models (e.g., Dodo et al. 2005), but modifies them to account for features of particular importance in a seismically active developing country like Iran. Key modifications include: (1) allowing reconstruction to be delayed (at a penalty) if funds are not immediately available, (2) allowing changes in structural types either during mitigation or reconstruction, and (3)

including an objective to minimize the chance of an extremely large death toll. By running it with different values of key parameters and carefully disaggregating the results, this new model can help allow risk managers to explore the complex tradeoffs between the objectives to minimize mitigation expenditures, expected reconstruction expenditures, loss of building inventory (and associated loss of population), expected death toll, and chance of large death toll. It can also help the user understand the relative importance of the budget constraint, time horizon, and other key parameters.

Opportunities exist to continue to build on this effort, both in further modifying the model and in improving the input it requires. The model could be extended by including collateral hazards and indirect economic loss to give a more complete picture of the full impacts of an earthquake. If desired, one could implement an alternative assumption about what people do when buildings are not rebuilt immediately. Rather than assuming they leave the city until the inventory is rebuilt, for example, one could assume the population remains constant and increase the population density as building inventory is lost. In addition to modeling changes in the built environment resulting from mitigation activities, earthquake damage, and reconstruction efforts, the model could be modified to reflect the effects of normal population growth, infrastructure aging, and other non-earthquake-related changes. In developing countries in particular, economic instability can introduce sometime significant uncertainties in unit mitigation and reconstruction costs that might be considered in future versions. With more significant effort, the scope of the model might be expanded even further to include risk management alternatives other than structurally upgrading buildings (e.g., insurance). Finally, the results of the optimization model are only as good as the input data they rely on. This may be a particular challenge in developing countries where data are often less available or of lower quality. For the case study in this paper, some simplifying assumptions were

made in developing the input data (e.g., considering only two damage states and estimating the effect of mitigation as a simple shift in the fragility curves), but they are considered to be consistent with the state of seismic risk analysis in Tehran.

REFERENCES

Davidson, R., Nozick, L., Dodo, A., and Xu, N. 2005. Equity in regional earthquake mitigation investment. *Symposium on Risk Modeling and Loss Reduction Strategies for Natural and Technological Hazards,* Part of *Ninth International Conference on Structural Safety and Reliability – ICOSSAR'05, Rome, Italy, June 19-23, 2005*.

Dodo, A., Davidson, R., Xu, N., and Nozick, L. 2007. Application of regional earthquake mitigation optimization. *Computers and Operations Research* 34(8), 2478-2494.

Dodo, A., Xu, N. Davidson, R. and Nozick, L. 2005. Optimizing regional earthquake mitigation investment strategies. *Earthquake Spectra* 21(2), 305-327.

Federal Emergency Management Agency (FEMA). 2003. "State and local mitigation planning how to guide." *Rep. No. 386-3,* Washington, DC.

International Monetary Fund (IMF). 2007. IMF Executive Board Concludes 2006 Article IV Consultation with the Islamic Republic of Iran, Public Information Notice (PIN) No. 07/29, http://www.imf.org/external/np/sec/pn/2007/pn0729.htm. (Accessed June 17, 2008).

Iran, Islamic Republic. 2005a. National Budget Act of 1384, http://www.spac.ir/hoghoghi/ (Accessed May 15, 2008) (in Persian)

Iran, Islamic Republic. 2005b. National Report of Islamic Republic of Iran on Disaster Reduction, World Conference on Disaster Reduction, Kobe, Hyogo, Japan http://www.unisdr.org/eng/mdgs-drr/national-reports/Iran-report.pdf. (Accessed May 4, 2008).

Japan International Cooperation Agency (JICA). 2000. *The Study on Seismic Microzoning of the Greater Tehran Area in the Islamic Republic of Iran*, Final report to the Government of the Islamic Republic of Iran, Tokyo, Japan.

Prater, C., and Lindell, M. 2000. “Politics of hazard mitigation.” *Natural Hazards Review*, 1(2), 73-82.

Trifunac, M. D., and A. G. Brady 1975. On the correlation of seismic intensity scales with the peaks of recorded ground motion, 65, 139-162.

United Nations (UN). 2002. *World Urbanization Prospects: The 2001 Revision*, New York.

UNDP-BCPR, 2004, *Reducing Disaster Risk: A Challenge for Development*, New York, John S. Swift Co. (www.undp.org/bcpr/disred/rdr.htm, retrieved 02.23.2008).

Xu, N., Davidson, R., Nozick, L., and Dodo, A. 2007. The risk-return tradeoff in optimizing regional earthquake mitigation investment. *Structure and Infrastructure Engineering* 3(2), 133-146.

CHAPTER3 GEOGRAPHIC INEQUALITY IN REGIONAL EARTHQUAKE RISK MITIGATION PLANS

3.1 INTRODUCTION

Natural disasters do not affect people equally (Mileti 1999, Nuemayer and Plumper 2007). In fact, due to inequalities in exposure, and access to resources and opportunities, certain segments of the population are more likely to suffer from deaths, damages and economic losses than the others and some groups are less likely to be able to recover from loss when they experience it. There is a significant body of work investigating these differences in population segments using a number of characteristics, including gender (Nuemayer and Plumper 2007, Peacock et al. 1998), income (Philips 1993), age (Bolin and Stanford 1998), and ethnicity (Peacock et al. 1987).

In the context of providing public services and managing public sector resources, efficiency is not adequate. Savas (1978) introduces effectiveness and equity as measures that should be considered in providing public goods and services in addition to efficiency. Efficiency measures the cost to provide the service relative to the rate-of-return of providing it. Effectiveness is defined as the adequacy of services relative to the need and incorporates the notion of service quality. Equity refers to the fairness and impartiality of provided service. Athanassopoulos (1998) and Boiney (1995) develop models to incorporate these criteria in the decision making process for allocation of public goods.

Resource allocation for regional earthquake risk mitigation is an intervening act by a central decision maker (governmental body for instance) with consequences that may impact different groups of people in different ways. As Boiney (1995) argues, in such an act the decision maker's task is to assess the preferences and tradeoffs of those concerned and identify a defensible and implementable option. To be successful in

doing so requires attention to fairness. While Chapter 2 of this dissertation focuses on developing a framework to aid the selection of the most efficient option in the allocation of resources for earthquake risk management, this chapter begins to consider impacts on equity. This analysis aims to build awareness about identification of vulnerable groups and provide insight on the issue of fairness and how it is affected by different decision parameters. The equity in regional earthquake risk mitigation is discussed in the next section followed by a brief introduction to Lorenz curves and their application in inequity comparisons. An illustrative analysis of this application in Tehran, Iran is then described.

3.2 EQUITY IN REGIONAL EARTHQUAKE RISK MANAGEMENT

Davidson et al. (2005) provide an excellent discussion of key challenges that must be addressed in incorporating equity into regional earthquake risk mitigation. First, what groups of people or facilities should be examined with respect to equity? Second, what equity principle should be used, such as horizontal (similar people or facilities should be treated equally) or vertical equity (different people or facilities might need different treatments). Third, the equity principle could be applied to initial allocation (funds spent), final outcome (final risk or expected losses after risk reduction effort), or process by which risk reduction efforts are allocated. Fourth, one should define exactly what it is that should be distributed equitably among facilities or people. For example, the discussed outcome could be average per capita earthquake loss, percentage reduction in per person expected loss, or average earthquake loss for the whole group. Fifth, what metric should be used to best capture and address the specific characteristics and circumstances of the problem at hand?

Davidson et al.(2005) develop a linear optimization model based on Dodo et al.(2005) using the Gini coefficient. The optimization distributes resources for

earthquake mitigation so that the amount f "inequality" in per capita loss does not pass a threshold. The people group was based on income.

3.3 LORENZ CURVE AND EQUALITY COMPARISONS

The Lorenz curve is a graphical depiction of cumulative percentage of a certain characteristic, such as size or income, against cumulative percentage of (ordered) population, Figure 3-1(Lorenz 1905).

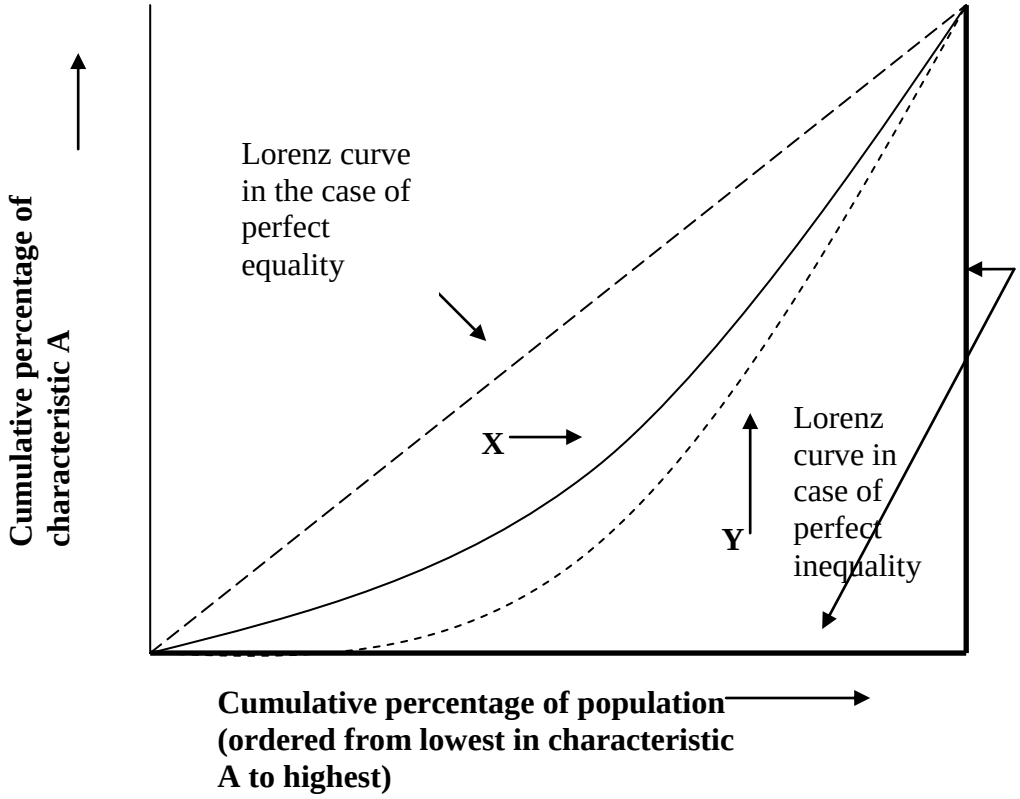

Figure 3-1 Lorenz curve when distribution X Lorenz dominates distribution Y (Fields 2001)

Since for a certain characteristic A, the population of recipients is ordered from lowest to highest, the change in the cumulative percentage of A is always larger for recipient *i* than it is for recipient *i-1*, and therefore the Lorenz curve always has a

convex shape (Figure 3-1). In the case of perfect equality in distribution, the curve is a 45° line, and for any distribution, the closer its Lorenz curve to this line, the more equal it is. In general, for two distributions X and Y, if the Lorenz curve for distribution X lies somewhere above and never below the Lorenz curve for distribution Y, then X is said to Lorenz-dominate Y, denoted $L_X > L_Y$ (Figure 3-1).

If the measure of equity is assumed to be the Lorenz curve of the distribution, then if one distribution Lorenz-curve dominates another, it is more equal than the dominated one. This conclusion however is not always consistent with what is derived based on the numerical inequality measures.

Numerical inequality measures are defined to be a function $I(.): R^n \to R$ determining how much inequality there is for a given vector of characteristic A. Some of the most common inequality measures in the literature are share of the richest *x* percent and poorest *y* percent, *R*%-*P*% ratio, Gini coefficient, Theil's measure, Atkinson's measure, variance, standard deviation, and log variance.

Gini coefficient is defined as the ratio of the areas in the Lorenz Curve (Figure 3-1). If the area between the perfect equality and Lorenz Curve is A and the area under the Lorenz Curve is B then the Gini coefficient is A/(A+B). The Gini coefficient of zero indicates perfect equality and a value of one indicates perfect inequality. Expression (3.1) shoes Theil's measure where x_i is the income (or any other characteristic) of recipient *i*, μ_x is the average income, and *n* is the total number of recipients.

$$T = \frac{1}{n}\sum_{i=1}^{n}\left(\frac{x_i}{\mu_x}.\ln\left(\frac{x_i}{\mu_x}\right)\right) \tag{3.1}$$

The first term inside the sum can be considered individual's share of aggregate income and the second term is that person's income relative to the mean. If everyone

has the same income (mean) then the index is zero and if one has all the income the index is equal to *n*. Expression(3.2) shows Atkinson's measure of inequality.

$$A_{\varepsilon} = \begin{cases} 1 - \left[\frac{1}{n} \sum_{i=1}^{n} \left(\frac{x_i}{\mu_x} \right)^{1-\varepsilon} \right]^{1/(1-\varepsilon)} & \varepsilon \in [0,1) \\ 1 - \prod_{i=1}^{n} \left(\frac{x_i}{\mu_x} \right)^{1/n} & \varepsilon = 1 \end{cases} \tag{3.2}$$

Atkinson's measure has the special feature that it is able to gauge the movement in different segments of the income with the weight ε. The measure becomes more sensitive to the changes at the lower end of the income as ε approaches one.

In ordering distributions based on their inequality, these numerical measures may or may not have the same outcome as the Lorenz-dominance. Fields (2001) divides inequality measures into three sets based on how they treat situations of Lorenz-dominance:

Inequality measure $I(.)$ is:

1. *Strongly Lorenz-consistent* if when $L_X > L_Y$ then $I(X) > I(Y)$ and when L_X coincides with L_Y then $I(X) = I(Y)$. Examples are the Gini coefficient, Theil's two measures, the Atkinson index, and the coefficient of variation.
2. *Weakly Lorenz-consistent* if when $L_X > L_Y$ then $I(X) \geq I(Y)$ when L_X coincides with L_Y then $I(X) = I(Y)$. Examples are share of the richest *x* percent and poorest *y* percent, *R*%-*P*% ratio, and the relative mean deviation.
3. *Lorenz-inconsistence* if ever, when $L_X > L_Y$ then $I(X) < I(Y)$. Examples are the variance, standard deviation, and the log variance.

As Davidson et al. (2005) points out, one of the challenges in equity analysis in regional earthquake risk mitigation is choosing the appropriate measure. However, if one distribution Lorenz-dominates another, then using the Lorenz Curve as the basis of comparison has the advantage that the conclusion can be extended to several strongly and weakly Lorenz-consistent measures that are widely used in the literature. Therefore, Lorenz curve comparisons can be a valid starting point. However, if the two curves cross, no dominance conclusion can be derived, and inequality of the distributions can not be compared using the Lorenz criterion alone. In such a case, the challenge of picking the appropriate measure entails close understanding of the decision maker's judgment and goals. Gini coefficient can also provide the same results because it is defined based on the Lorenz Curves.

3.4 ILLUSTRATIVE ANALYSIS

This section describes analysis of the results of the optimization model developed in the Chapter 2 from an equity perspective. The scope of the analysis is limited data is availability, but nevertheless is helpful in providing initial insights in to the interaction between efficiency and equity and its sensitivity to key parameters.

The analysis is based on comparison of differences in the distribution of damage (number of collapsed buildings per 1000 people) among different building clusters. Lorenz-curves of these distributions are drawn for the base case of Chapter 2 as well as variations in available annual budget and "death risk parameter".

3.4.1 Scope

The analysis is done for the 119 census zone clusters defined in Section 2.4 for Tehran, Iran. The study includes nine structural types (Table 2-4) and only residential occupancy. The total number of dwellings of each structure type *i* in each cluster *k* is given for the initial inventory of the buildings. Figure 3-8 to Figure 3-17 in the Appendix show the spatial distribution of the population and the different structural

types in the study area as a percentage of their total number. As explained in Section 2.4.2, the area of a typical building of structure type *i* in cluster *k* is used to convert the model damage results (Y variable) from total square meters lost to total number of buildings lost.

The analysis is based on the spatial distribution of damages. The buildings are grouped by their location. That is, all the buildings in each cluster belong to one group and it is assumed that all clusters should be treated equally (horizontal equity). This choice has been made because there is no data on income or other characteristics which might be more appropriate in identifying vulnerable groups. The analyses are outcome-based. The outcome is the total number of collapsed buildings per 1000 people. The equality comparisons are based on Lorenz curve analyses.

3.4.2 Results

3.4.2.1 Spatial distribution of loss

Figure 3-2 (figures are in UTM-WGS84, Zone 39N) shows the spatial distribution of damage in Tehran for the base case analysis (Section 2.4) as the total number of collapsed buildings over all 30 year planning horizon per thousand people. In general, overlaying such spatial distribution of damage on maps of different characteristics distribution in data, such as income distribution or similar indicators of vulnerable groups, will give the decision maker a clearer picture of the situation and will assist them in devising a more defensible policy.

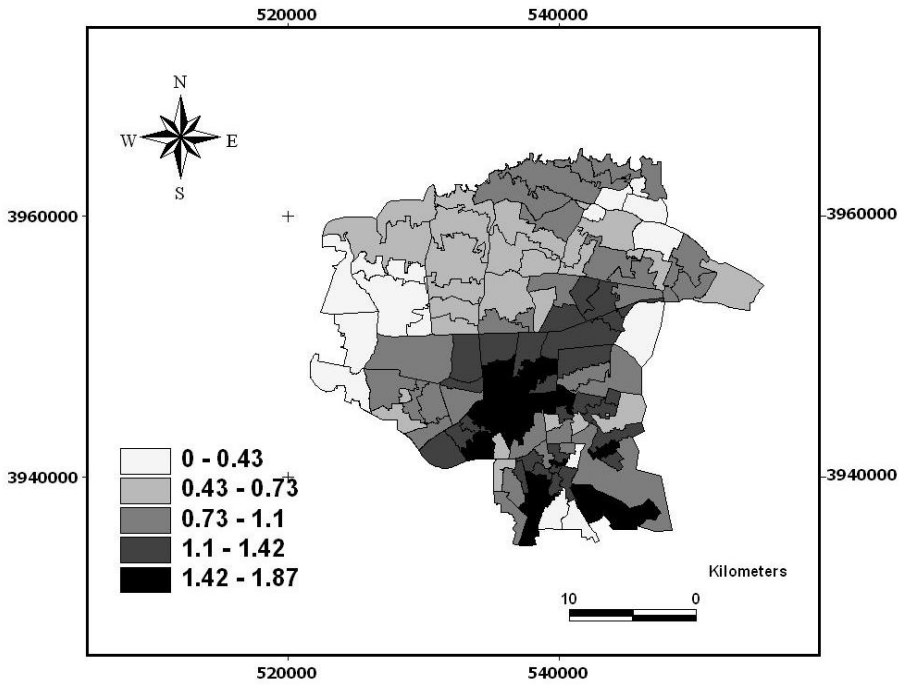

Figure 3-2 Number of collapsed buildings per 1000 people for the base case

Since the total damage in the planning horizon is a combination of many factors such as spatial distribution of different structure types, their vulnerability, the hazard they are exposed to and the decisions the model makes over the planning horizon for mitigation and reconstruction, it is hard to exactly explain specific factors behind this damage distribution. However, in terms of equality implications one notes that there is a significant concentration in the central and southern parts of the city, indicating unequal distribution of damage among residents in different areas. Considering the reconstruction cost and vulnerability of different structure types (Table 2-4, Figure 2-5) one can assume that structure types *All wood, Block and brick, Brick and steel,* and *Sun dried brick* are associated with lower income classes and Reinforced concrete and Steel structures are associated with higher incomes. Looking at the spatial distribution of the different structure types (Appendix) it is clear that the structure types associated with lower incomes are also mostly concentrated in central

and southern parts of the city. These two coinciding patterns suggest that the lower income class of residents may be shouldering the majority of damages in the city.

Presenting the same data from a different perspective, the Lorenz curve of damage distribution per thousand people is illustrated in Figure 3-3. This graph shows that 60% of the damage is concentrated in 40% of the population suggesting rather unequal distribution of damage among residents. Since the distribution of damage is a negative term it is desired to be distributed among the population as evenly as possible.

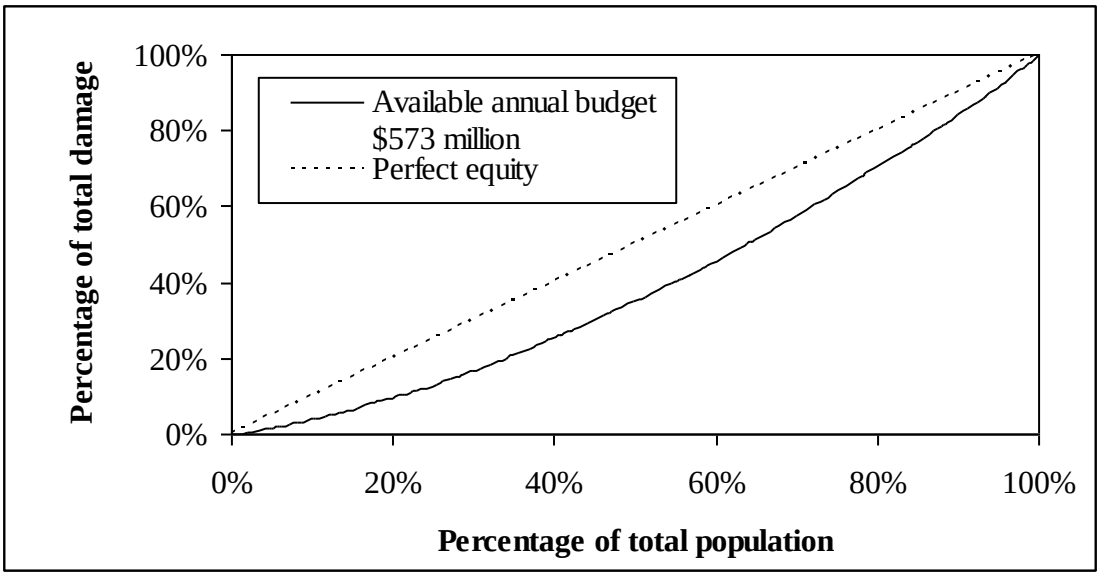

Figure 3-3 Lorenz curve for damage distribution among population for the base case

3.4.2.2 Sensitivity to annual available budget

Results are compared for the base case and highest available annual budgets used in Section 2.4.3—US$573 and US$1,145 million, respectively. Figure 3-4 shows the Lorenz-curve for the two budgets. As this figure illustrates, the two Lorenz curves cross. For the 20% of the population that receives only about 10% of the damage the Lorenz curve of $1,145 million dollars is actually above that of the base case. This might suggest that the higher income people may in fact be receiving greater proportion of benefits from an equity perspective. In general however, the cross of the two curves means that no dominance conclusions can be derived from the graph alone.

However, one could conclude that increasing the available annual budget does not necessarily decrease the inequality of damage distribution and the final conclusion will in fact be dependent on the inequality measure used.

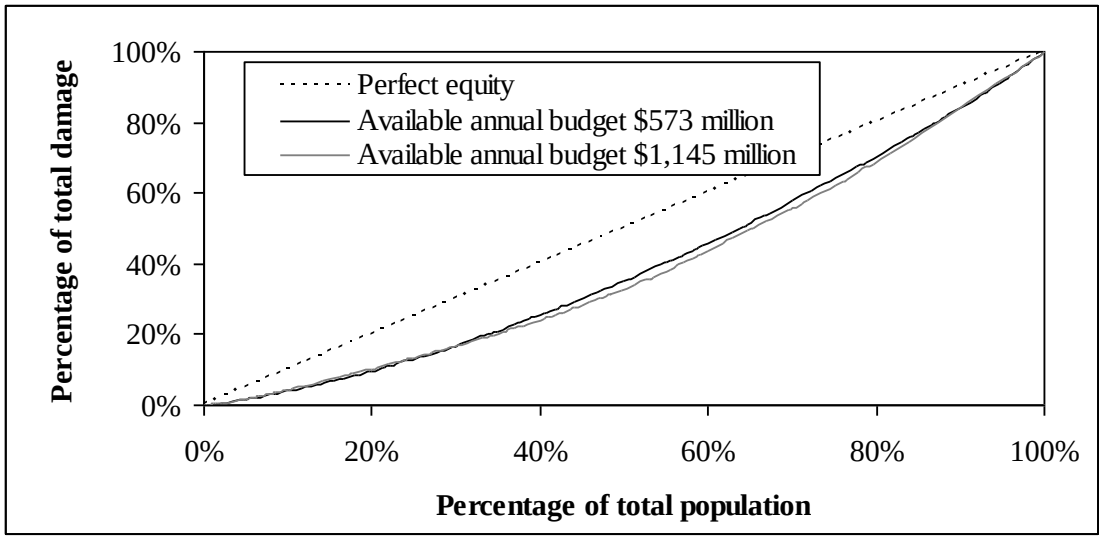

Figure 3-4 Lorenz curve comparison for base case and when budget is 1145 million US dollars

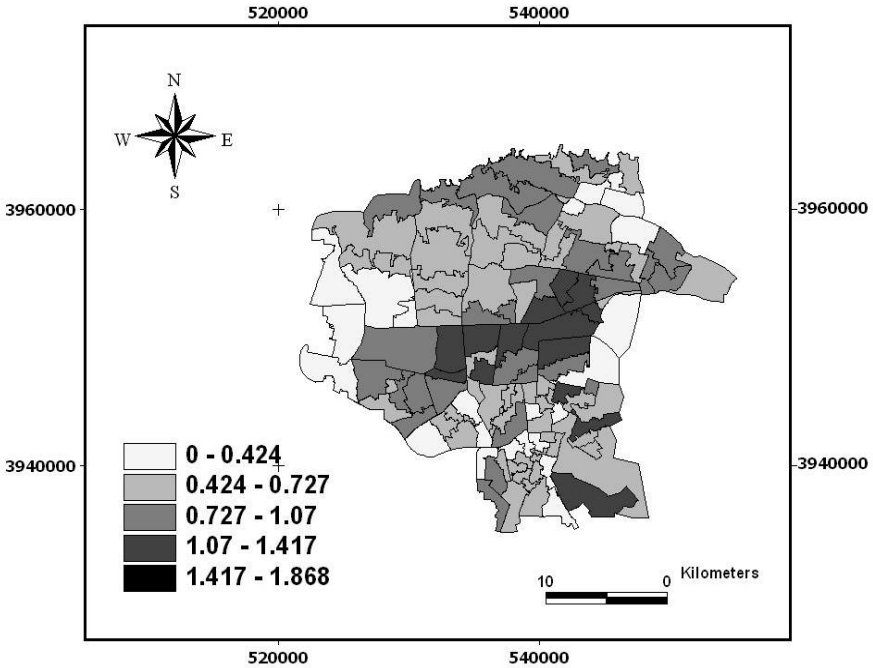

Figure 3-5 Number of collapsed buildings per 1000 people for the budget of 1,145 million US dollars

Figure 3-5shows the damage distribution for the budget of US$1,145 million as the total number of collapsed buildings per thousand people. Compared to Figure 3-2 it shows that over all number of collapsed buildings has decreased but the rate of this decrease is greater in central zones than the northern and eastern parts.

3.4.2.3 Sensitivity to death risk aversion parameter

Figure 3-6 shows the Lorenz curves for the base case (budget of $573 million and risk parameter μ=0) and the case in which μ=1 million. In this case, the damage distribution of the base case is Lorenz-dominant the damage distribution of μ=1 million. This means that putting more emphasize on guarding against casualties of rare but big earthquakes in fact increases the inequality in the damage distribution in the city in this analysis.

Looking at the spatial damage distribution in the city for μ=1million (Figure 3-7), it is obvious that the model has reduced the damage in southern clusters adjacent to earthquake 2 and 12 (Kahrizak Fault Maximum Credible Earthquake) as well as in northern clusters adjacent to earthquake 11 (Northern Tehran Fault Maximum Credible Earthquake) (Figure 2-3). The damage for the more central clusters on the other hand is increased because these central clusters are not adjacent to any major events, which means that as the model increasingly emphasizes guarding against large death risk, it drives resources away from clusters with less death risk. This creates the sort of spatial inequality that is illustrated in Figure 3-6and Figure 3-7

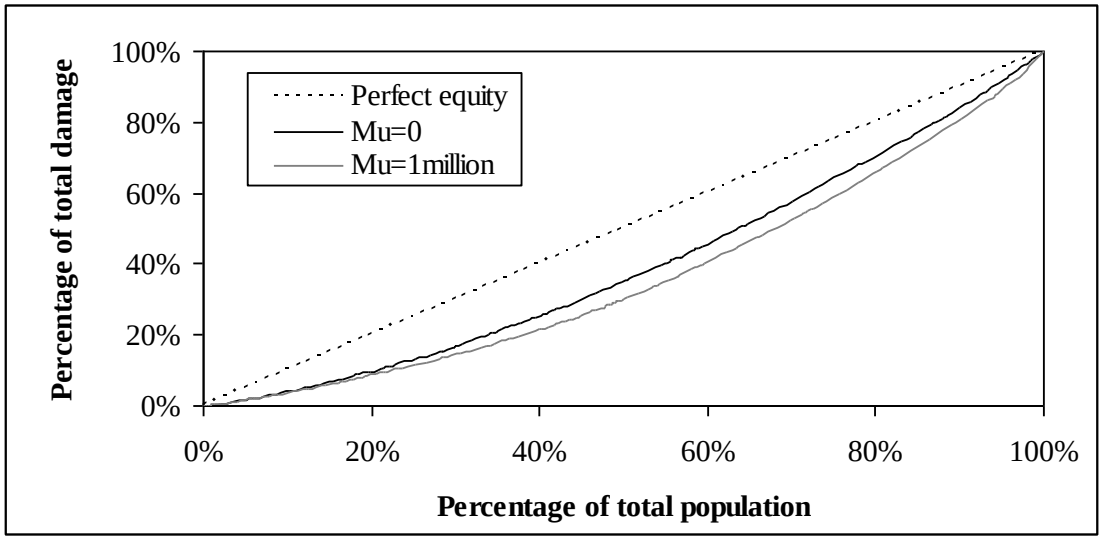

Figure 3-6 Lorenz curve comparison for base case and when μ is one million

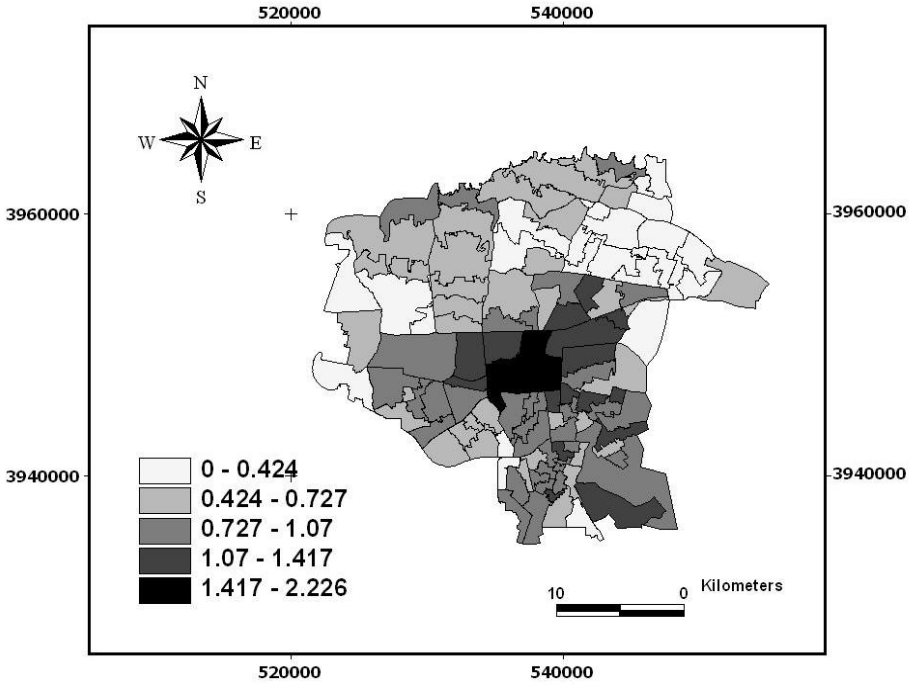

Figure 3-7 Number of collapsed buildings per 1000 people for the μ=1million

3.5 CONCLUSION

In this chapter the concept of equity in regional earthquake risk mitigation investment was explored. A brief review on the concept of Lorenz-curve dominance and its relationship to inequality comparisons was provided. An illustrative analysis on

the result of the mathematical model developed in Chapter 2 provides a simplified demonstration of how equity might be interpreted from these results.

Opportunities exist to continue to build on this effort. The model could be extended to allow relocation of current population in the city. Currently it is assumed that the total floor area of building inventory and population in each cluster can not exceed the initial value. This means that population from clusters with more hazard exposure can not relocate to places with lower hazard level. In reality, relocation might be a cost effective way to reduce the over all risk and improve the equity in distribution of damage. Although it might also increase the overall risk due to over population of some areas that are considered safe and creating secondary risks. When Lorenz curves cross different numerical measures can be calculated to explore the implications of different parameters for equity in damage distribution. The analysis can significantly improve in identifying and tracking the vulnerable groups with regard to equity if better data is available on population segmentation such as income or ethnicity. If the model improves to consider uncertainties in the costs then this might have different impacts on lower and higher income segments (lower income might have less tolerance for uncertainty) and might have specific implications on equity of damage distribution. Similar to Davidson *et al*.(2005) different numerical measures can be incorporated into the optimization as specific constraints.

.

APPENDIX

This appendix consists of maps of the distribution of initial population and initial building inventory for each structure type as a percentage of total of that type.

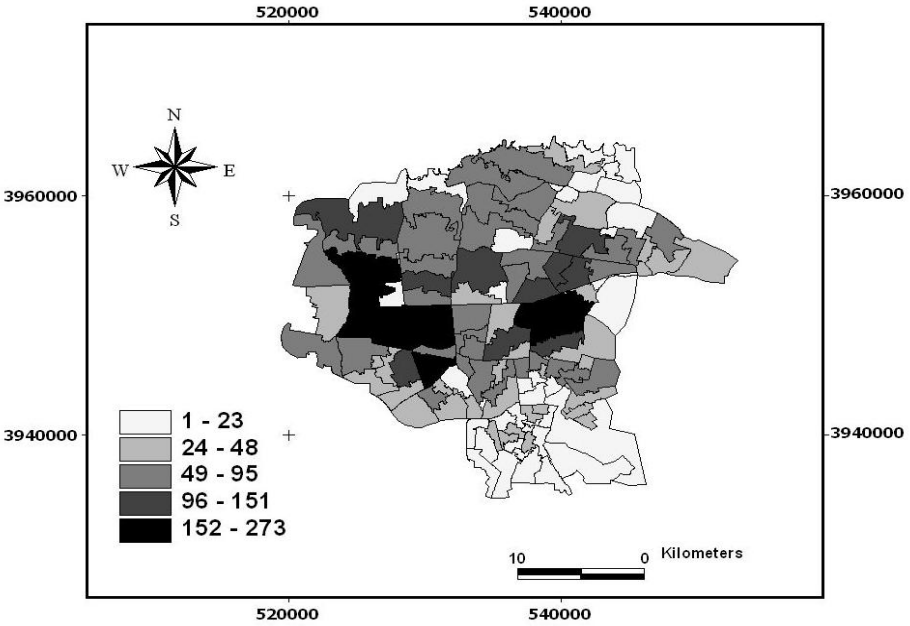

Figure 3-8 Initial population distribution in 1000 people

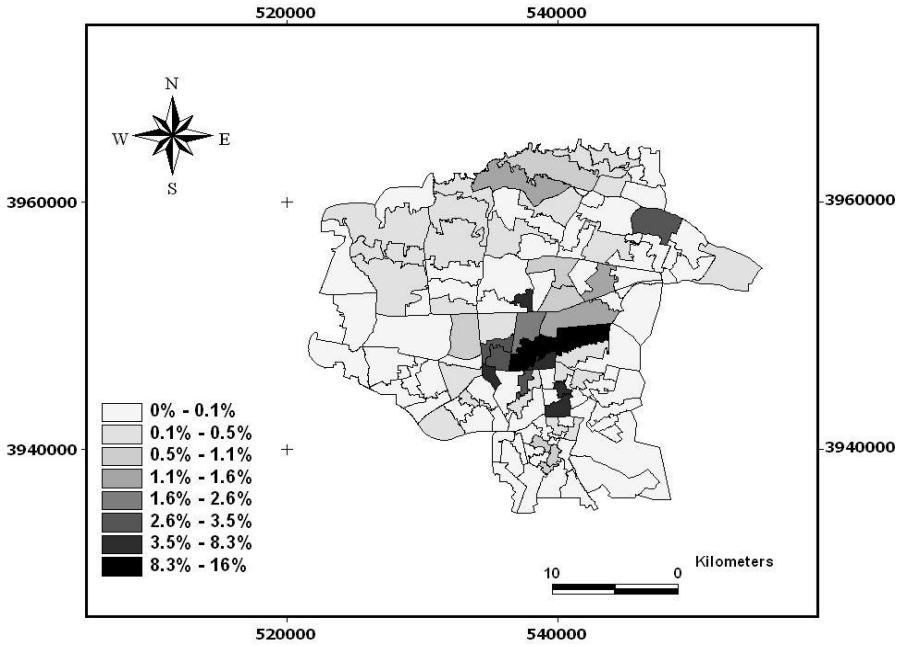

Figure 3-9 The distribution of *All Wood* structures in the initial inventory as a percentage of total number of buildings in that structural type

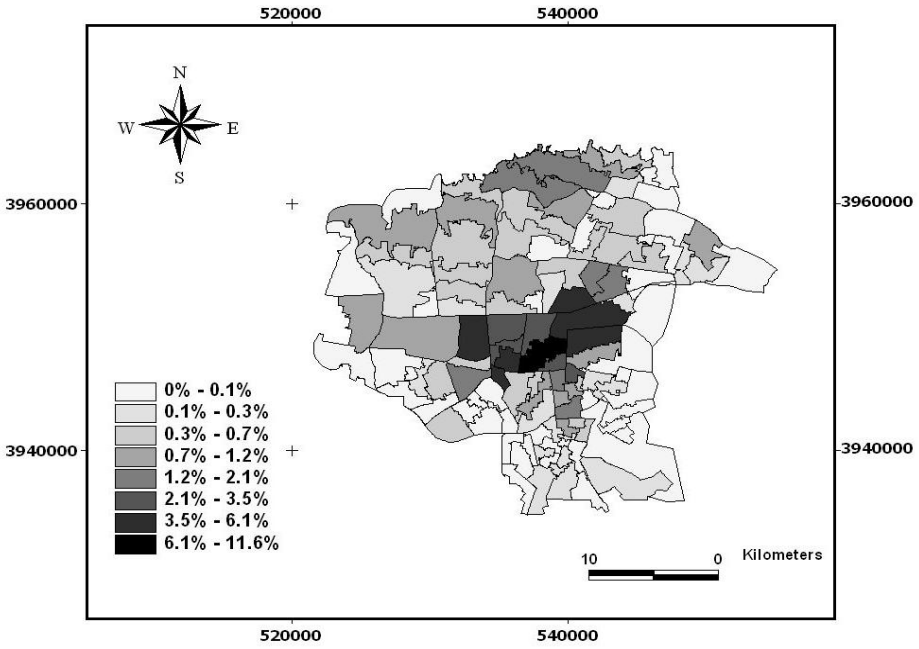

Figure 3-10 The distribution of *Block and Brick* structures in the initial inventory as a percentage of total number of buildings in that structural type

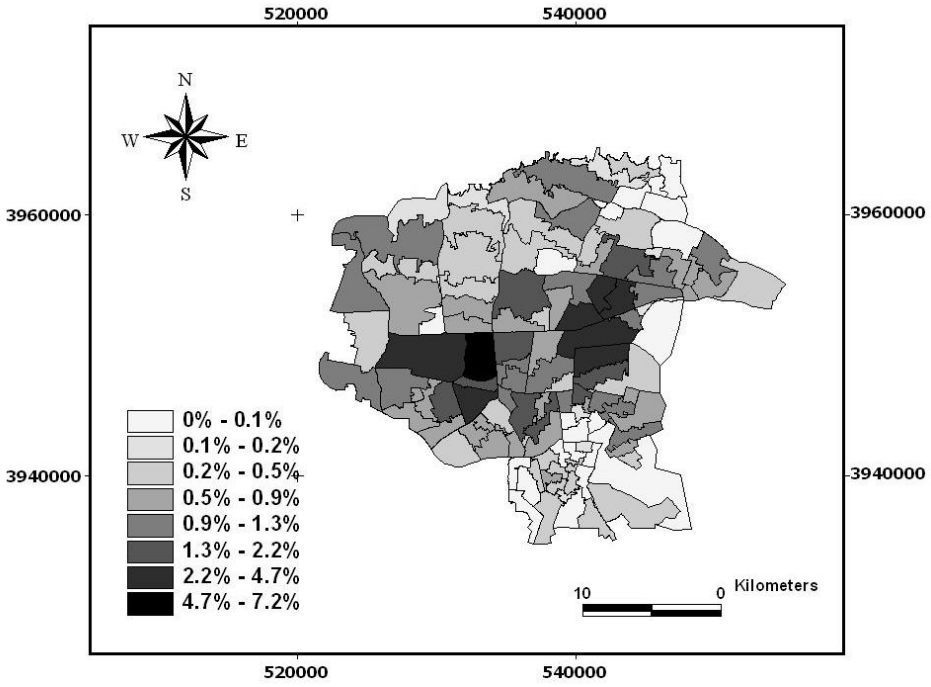

Figure 3-11 The distribution of *Brick and Steel* structures in the initial inventory as a percentage of total number of buildings in that structural type

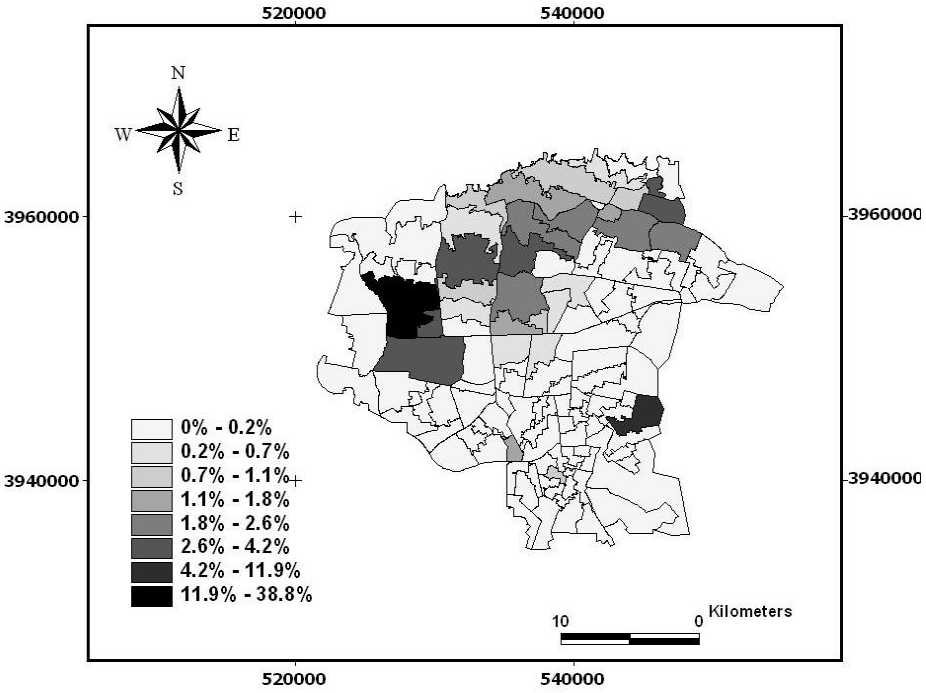

Figure 3-12 The distribution of *Reinforced Concrete-0* structures in the initial inventory as a percentage of total number of buildings in that structural type

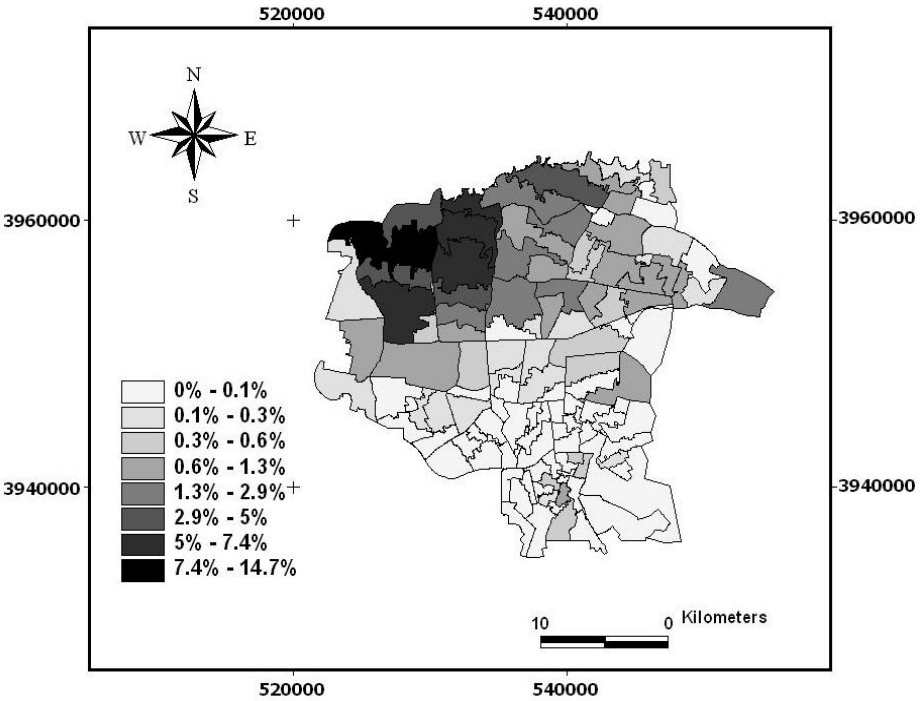

Figure 3-13 The distribution of *Reinforced Concrete-1* structures in the initial inventory as a percentage of total number of buildings in that structural type

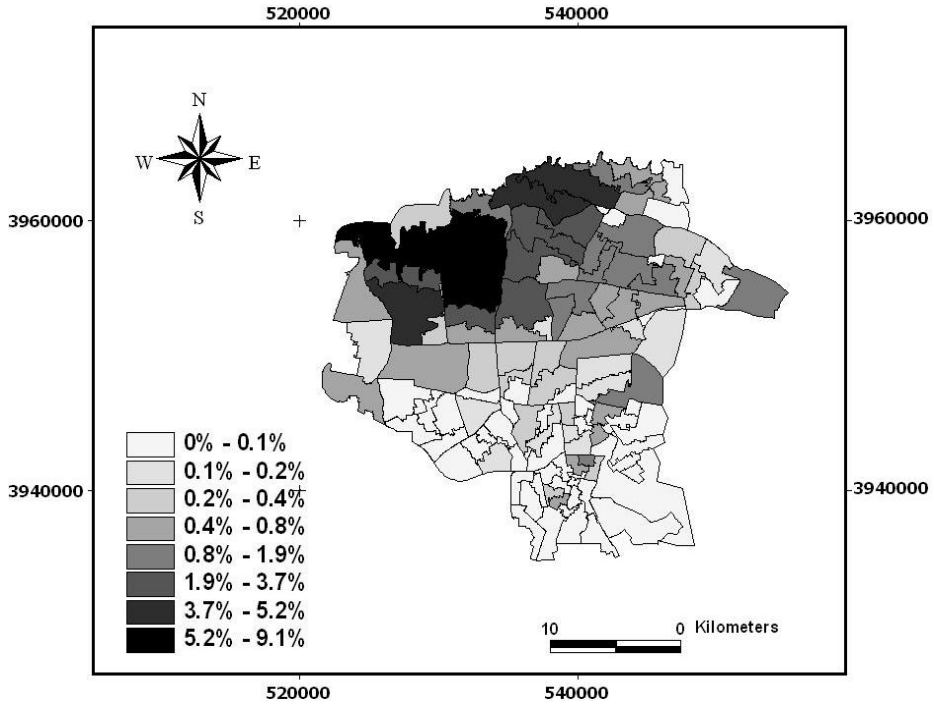

Figure 3-14 The distribution of *Reinforced Concrete-2* structures in the initial inventory as a percentage of total number of buildings in that structural type

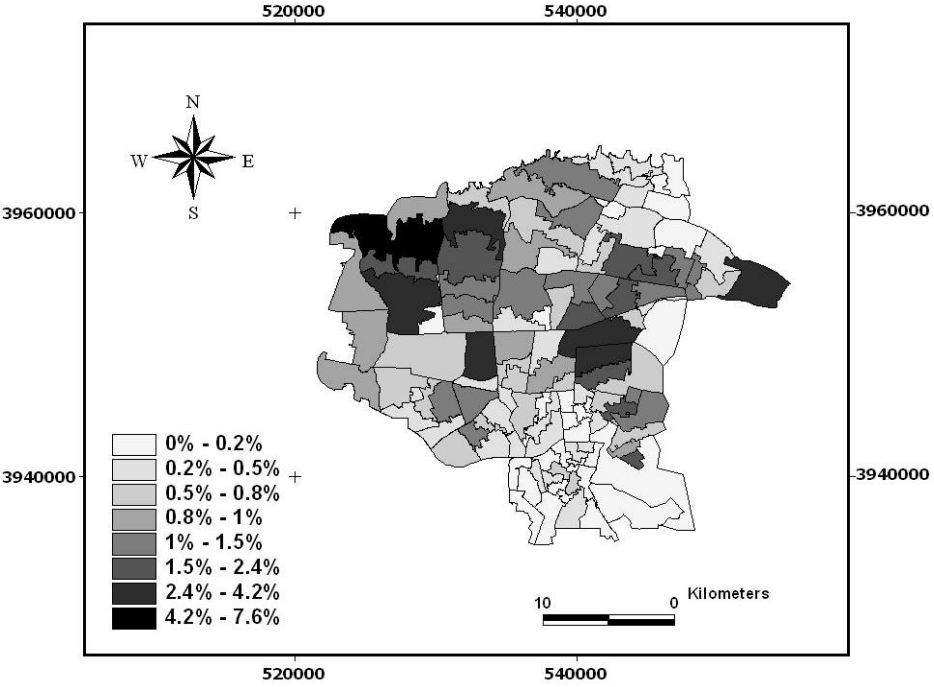

Figure 3-15 The distribution of *Steel-1* structures in the initial inventory as a percentage of total number of buildings in that structural type

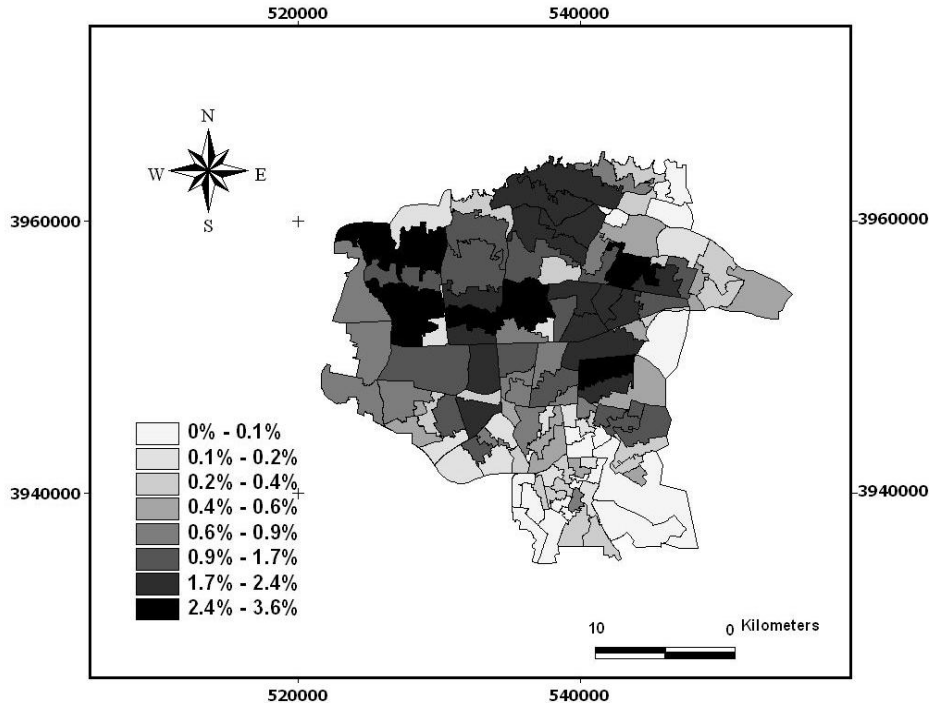

Figure 3-16 The distribution of *Steel-2* structures in the initial inventory as a percentage of total number of buildings in that structural type

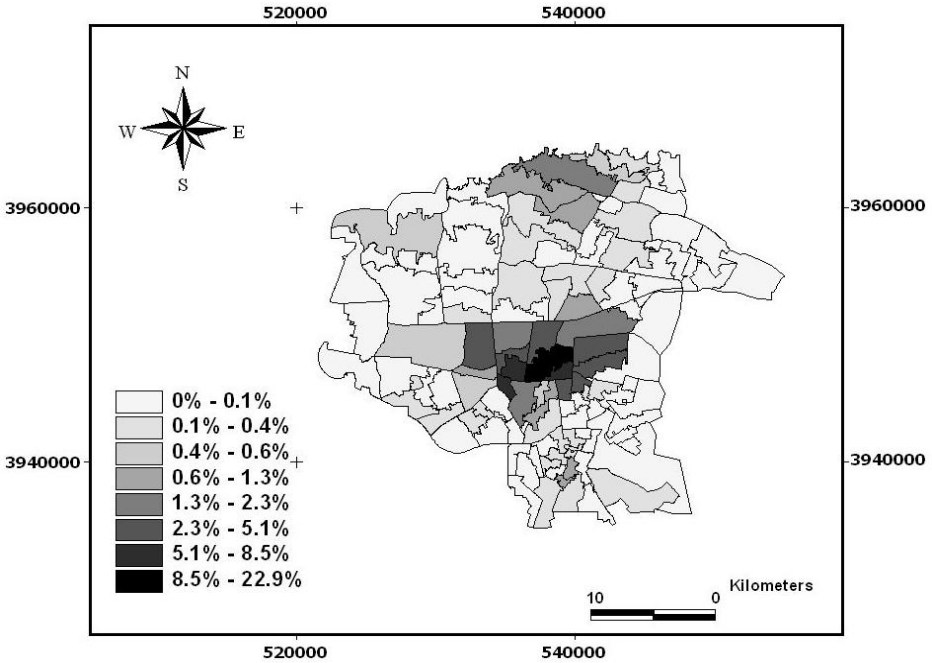

Figure 3-17 The distribution of *Sun Dried Brick* structures in the initial inventory as a percentage of total number of buildings in that structural type

REFERENCES

Athanassopoulos, A.D. 1998. Decision support for target-based resource allocation of public services in multiunit and multilevel systems, Management Science, 44(2), 173-187.

Boiney, L.G. 1995. When efficiency is insufficient: Fairness in decisions affecting a group, Management Science, 41(9), 1523-1537.

Bolin, R. and Stanford, L.1998. The Northridge earthquake vulnerability and disaster, Routledge, New York.

Davidson, R. A., Nozick, L. K., Dodo, A., and Xu, N. 2005. Equity in regional earthquake mitigation investment, *Symposium on Risk Modeling and Loss Reduction Strategies for Natural and Technological Hazards, Part of Ninth International Conference on Structural Safety and Reliability ICOSSAR\'05,* Rome, Italy, June 19-23.

Fields, G.S. 2001. Distribution and development, a new look at the developing world, The MIT press, Cambridge, Massachusetts.

Lorenz, M.C. 1905. Methods of measuring the concentration of wealth, Publications of The American Statistical Association, 9, 209-219.

Mileti, D.S.1999. Disasters by design: A reassessment of natural hazards in the United States, Joseph Henry Press

Neumayer, E., Plumper, T. 2007. The gendered nature of natural disasters: The impact of catastrophic events on gender gap in life expectancy, 1981-2002, Annuals of the Association of American Geographers, 97(3), 551-566.

Peacock, W.G., Killian, C.D., and Bates, F.L. 1987. The effects of disaster damage and housing aid on household recovery following the 1976 Guatemalan earthquake, International Journal of Mass Emergencies and Disasters, 5(1), 63-88.

Peacock, W.G., Morrow, B.H., and Gladwin, H., eds 1998. Hurricane Andrew: Ethnicity, gender and the sociology of disasters, Routledge, London.

Philips, B.D. 1993. Cultural diversity in disasters: Sheltering, housing, and long term recovery, International Journal of Mass Emergencies and Disasters, 11(1),99-110.

Savas, E.S. 1978. On equity in providing public services, Management Science, 24(8), 800-808.